UNIVERSIDAD NACIONAL AUTÓNOMA DE MÉXICO

POSGRADO EN CIENCIAS DE LA TIERRA
INSTITUTO DE GEOFÍSICA

Métodos Rápidos en Detección y Estimación Sísmica para Sistemas de Alerta Temprana: Análisis, Propuesta y Evaluación

T E S I S

QUE PARA OPTAR POR EL GRADO DE

D O C T O R E N C I E N C I A S D E L A T I E R R A
(SISMOLOGÍA)

P R E S E N T A

ARMANDO CUÉLLAR MARTÍNEZ

D I R E C T O R

DR. GERARDO SUÁREZ REYNOSO
INSTITUTO DE GEOFÍSICA

M I E M B R O S D E L C O M I T É T U T O R

DR. JORGE AGUIRRE CONZÁLEZ
INSTITUTO DE INGENIERÍA

DR. ARTURO IGLESIAS MENDOZA
INSTITUTO DE GEOFÍSCA

Ciudad Universitaria, Cd. Mx.,.Abril, 2018

AGRADECIMIENTOS

Al posgrado en Ciencias de la Tierra de la UNAM por todas, en verdad todas las facilidades y oportunidades otorgadas.

Al Instituto de Geofísica de la UNAM por darme la oportunidad de aprender y desarrollarme en el campo de la investigación.

A mi tutor Gerardo Suárez Reynoso por su confianza, solidaridad, comprensión, orientación, honestidad, objetividad, ejemplo, dedicación y sobre todo su congruencia.

A Jorge Aguirre González y Arturo Iglesias Mendoza, por todo el apoyo y orientación.

Al Centro de Instrumentación y Registro Sísmico, A. C. por la flexibilidad y apoyo para realizar mi trabajo de investigación.

A Juan Manuel Espinosa Aranda por su amistad, apoyo, confianza, consejos y paciencia.

A Sandra, Guadalupe, Cecilia, Marisela, Raquel, por su amistad, ayuda y grata compañía.

A todos los demás colaboradores de CIRES, muy en especial a Lucio, Martín y Karla.

A mi amiga Cristina por su permanente amistad y apoyo.

A mis padres y hermanos.

Y a lo más importante, mi esposa e hijas por su amor, comprensión y ser mi motivación.

DEDICATORIA

A quienes ayudan de manera desinteresada, como sucedió aquel jueves 19 de septiembre de 1985, poco después de las 07:19 horas de la mañana.

ÍNDICE

RESUMEN

Las alertas tempranas para sismos han tenido un crecimiento notable en lo que va del siglo gracias la tecnología de cómputo y telecomunicaciones que han evolucionado vertiginosamente en las últimas décadas, aunados a los nuevos conocimientos y métodos en sismología. Sin embargo, si bien hay casi una decena de propuestas en el mundo, aún hay pocos sistemas implementados.

El Sistema de Alerta Sísmica de México (SASMEX) fue el primer sistema de alerta en el mundo, nació en 1991 con el fin de avisar a la ciudad de México previo a un sismo potencialmente destructivo. Hasta 2018, SASMEX dispone de 97 sensores que cubren la costa del Océano Pacífico desde Jalisco hasta Oaxaca, además cubre el sur del eje Neo-volcánico transversal en los estados de Guerrero, Puebla y Oaxaca. La alerta sísmica SASMEX, se difunde principalmente en siete ciudades: Morelia, Puebla, Acapulco, Chilpancingo Oaxaca, Toluca y Ciudad de México con la posibilidad de alertar a más de 25 millones de personas.

La función de alertar en caso de sismo, a diferencia de otros fenómenos naturales presenta un reto enorme tanto desde el punto de vista de la ingeniería como de la sismología. Ya que además de garantizar en la medida de lo posible su disponibilidad,

confiabilidad y rápida diseminación; el diseñar algoritmos para el procesos de detección, pronóstico del rango de magnitud o intensidad y criterios que conlleven a la decisión crucial de emitir una alerta en el menor tiempo posible con la mayor certeza respecto a la dimensión del sismo de manera automática, se han vuelto tópicos de estudio en la actualidad, los cuales se incluyen de manera regular en foros de sismología.

La tesis que desarrollé, presenta trabajos enfocados al análisis, evaluación y nuevas propuestas de algoritmos de detección y estimadores de magnitud sísmica que conlleven a calcular de manera incipiente y en pocos segundos algunos parámetros que permitan estimar el tamaño de un sismo o si éste representa un peligro a la ciudad a alertar. Los algoritmos propuestos hacen rápidas estimaciones de las características de un sismo en progreso con bajo margen de error y con baja incertidumbre para que una alerta sísmica sea efectiva y aplicable para tomar medidas de prevención y respuesta.

El primer capítulo muestra los resultados del SASMEX durante el sismo M_w 7.5 del 20 de marzo de 2012 en Pinotepa y describe a detalle el funcionamiento y desempeño del sistema.

En el capítulo dos se hace una evaluación del algoritmo denominado $2(t_S\text{-}t_P)$, que ha sido utilizado desde el inicio por SASMEX. El análisis principal se basó en sismos $M_w >$ 6 registrados en México desde hace 30 años, con el fin de evaluar posibles escenarios de desempeño. El algoritmo se aplicó también a registros de grandes sismos de los últimos años tales como el de M_w 8.8 de Maule de 2010, y de Tohoku M_w 9.0 en 2011.

Otro capítulo de mi tesis presenta un algoritmo que emplea el lapso $t_S\text{-}t_P$ (esto es el intervalo desde el inicio del arribo de ondas P hasta la detección de las ondas S en el sensor). El algoritmo realiza labores de detección, estimación de magnitud y decisión del alertamiento. El desarrollo se hizo con base en la necesidad de lograr un aviso más rápido para ciudades cercanas a los epicentros de sismos de subducción someros a menos de 40 km de profundidad. Este algoritmo emplea el 50% menos del tiempo de procesamiento comparado con el algoritmo original. Este algoritmo empleó 129

sismos de México desde 1985 a 2016 mayores a 4.5 que constituyeron 400 registros de aceleración que se pudieron utilizar. El modelo se aplicó al sismo de Napa del 24 de agosto de 2014 de magnitud M_w 6. Los resultados muestran que el algoritmo desarrollado en mi tesis tiene resultados más favorables que el sistema de alerta temprana *ShakeAlert* actualmente en desarrollo en los Estados Unidos.

El último capítulo presento un tercer algoritmo que emplea sólo 3 segundos después de la detección de la onda P. Este algoritmo se diseñó para ser utilizado en el procesamiento de sismos a profundidades mayores a 40 km, en la región del *in-slab*. Se procesaron 113 registros de 34 sismos, y con ello se propuso algunos parámetros medidos en el campo cercano y los modelos de estimación de estas propuestas mapean a M_w, para su construcción se utilizaron también métodos con máquinas de aprendizaje. Este artículo presenta tres hipotéticos escenarios con este algoritmo durante los sismos de Tehuacán, Puebla, M_w 7.0 del 15 de junio de 1999, el sismo M_w 6.5 de Zumpango, Guerrero del 10 de diciembre de 2011 y el sismo M_w 7.1 del 19 de septiembre de 2017 en Morelos que ha sido el que más daños causó después de los sismos de septiembre de 1985.

INTRODUCCIÓN

El daño sufrido en varias ciudades y principalmente en la ciudad de México tras el terremoto M_w 8.1 del 19 de septiembre de 1985 (*e.g.*, Rosenblueth, 1986; Esteva, 1988) y recientemente por los sismos M_w 8.2 en Tehuantepec del 7 de septiembre de 2017 y el sismo M_w 7.1 de Morelos del 19 de septiembre de 2017, nos ha demostrado, lo frágil y vulnerable que puede ser un crecimiento urbano sin el conocimiento, monitoreo, comunicación, capacidad de respuesta y fundamentalmente su preparación ante esta amenaza. Sin embargo, esta fragilidad no es exclusiva de México, sino de todas las grandes urbes del mundo próximas a regiones sísmicas activas (Kanamori, *et al*. 1997).

Si bien la idea de sistemas de alerta temprana se remonta a mediados del siglo XIX (Cooper, 1868); México y Japón fueron los primeros en desarrollar sistemas de alerta temprana, (Espinosa-Aranda, *et al*. 1992; 1995; Nakamura 1989; 1996;), a México le corresponde ser el primero en alertar a la población desde 1993 para la Ciudad de México y 2003 para la Ciudad de Oaxaca. El avance en sistemas de alerta temprana para sismos incluyen países como Taiwán, Rumania, Turquía, con desarrollos para propósitos específicos (Wu, *et al.* 1998; Wenzel, *et al*, 1999; Erdik, *et al*. 2003), pero

fue hasta 2007 que Japón inició su servicio de alertamiento público a nivel nacional (Hoshiba, *et al*. 2008).

En Estados Unidos, Italia, China, entre otros países de Asia y Europa (Allen, *et al*. 2009), comenzaron en este siglo el desarrollo de sus sistemas de alerta temprana, enfocados en los procesos de detección, cálculo de parámetros y pronóstico para activar o no una alerta sísmica (Allen and Kanamori 2003; Gasparini *et al*. 2007). También se ha puesto en manifiesto la necesidad de disponer de información rápida más allá de una alerta temprana con bajo índice de error en sus pronósticos.

El Sistema de Alerta Sísmica (SAS) inició su servicio en 1991 en la Ciudad de México cubriendo con 12 sensores la región sísmica de la "Brecha de Guerrero" (Espinosa-Aranda, *et al*. 1995). Los sismos de 1999 en Tehuacán, Puebla M_w 7.0 el 15 de junio de 1999 y Puerto Escondido, Oaxaca M_w 7.5 el 30 de septiembre, detonaron el desarrollo en 2003 del Sistema de Alerta Sísmica de Oaxaca (SASO) que cuenta con 39 sensores (Espinosa-Aranda, *et al*. 2009; 2011). A partir de la ampliación de la cobertura del SAS y la integración del SASO en 2012, se conforma el Sistema de Alerta Sísmica Mexicano (SASMEX) que dispone de 97 sensores sísmicos que cubren la región de subducción de la placas de Cocos y Norte-América a lo largo de las costa del Pacífico en los estados de Jalisco, Colima, Michoacán, Guerrero y Oaxaca y las regiones sísmicas del *inslab* en Puebla, norte de Guerrero y norte de Oaxaca. Esta evolución del sistema conlleva a plantearse nuevos retos para un mensaje anticipado de alerta para ciudades vulnerables próximas a las regiones sísmicas, con relativa excepción la que posee la Ciudad de México.

La efectividad de una alerta temprana recae principalmente en el tiempo de anticipación previo al arribo de las ondas sísmicas que pueden generar daños a las ciudades vulnerables, este tiempo de anticipación de alerta está ligado a la distancia entre el epicentro y la ciudad a alertar. Por otro lado, el buscar el menor índice de errores en sus estimaciones, promueve una adecuada capacidad de respuesta (United Nations, 2006).

El enfoque de este trabajo se centra en el análisis, la evaluación y la propuesta de algoritmos de detección y pronóstico para sistemas de alerta temprana de acuerdo con el contexto sísmico mexicano para brindar en la medida de lo posible una rápida y correcta activación de alerta sísmica.

Se emplearon principalmente los catálogos sísmicos del Servicio Sismológico Nacional y el *Global Centroid Moment Tensor* (http://www.globalcmt.org) para obtener la información de los sismos al sur de México desde 1985 a 2017 acontecidos en la Placa de Cocos y Norte-América mayores a M_w 4.5. Inicialmente se generó una colección de más de 230 sismos y 1600 registros de aceleración obtenidos del Instituto de Ingeniería, UNAM y de la red del SASMEX. Sin embargo, durante el trabajo se realizaron una serie de procesos para seleccionar aquellos registros de aceleración que permitieran ser analizados, evaluados y con la posibilidad de construir modelos en el contexto de un sistema de alerta sísmica, que al final se logró obtener poco más de 160 sismos y 500 registros.

El escaso número de sismos fuertes que pudieran ser aprovechados para la construcción de modelos que estimen en pocos segundos de manera rápida y con un bajo índice de error el tamaño de un gran sismo en desarrollo y los pocos registros de aceleración completos, esto es donde se observen los inicios de las ondas P y ondas S con sus respectivas codas, le agregan una mayor complejidad a cualquier propuesta para obtener un modelo de regresión o clasificación que estime con cierta precisión la magnitud, intensidad u otro parámetro que permita determinar si amerita o no el emitir una alerta sísmica a la población.

Si bien la capacidad de cómputo en la actualidad es una magnífica herramienta de procesamiento para observar, medir y calcular de manera incipiente un sismo en desarrollo; aún está acotado primero, en no poder realizar procedimientos o métodos que consuman un tiempo suficientemente largos para tener mayor certeza en una medición, que de hacerlo, podrían comprometer el tiempo de anticipación con el que dispone la población para realizar con eficacia algún proceso de prevención; y segundo, las condiciones de ingeniería y tecnología de sistemas de cómputo y

comunicaciones de alto desempeño y bajo consumo de energía, aún no son tan confiables, aunado a la incertidumbre por la situación de seguridad en los lugares destinados para el monitoreo.

La presente tesis parte en exponer cómo es y cómo funciona el sistema de alerta temprana en México SASMEX, de acuerdo con el resultado del sismo M_w 7.5 del 20 de marzo de 2012, que generó aviso de alerta a varias ciudades del país y describe cada detalle en sus procesos, especialmente en el monitoreo, comunicación, diseminación y capacidad de respuesta; posteriormente, realiza un análisis y evaluación en su algoritmo llamado $2(t_S\text{-}t_P)$ para la detección y pronóstico de magnitud, este algoritmo es sometido a un conjunto de pruebas que nos muestren qué tan confiable puede ser para sismos fuertes; luego se propone un algoritmo más rápido que el original al que hemos llamado $t_S\text{-}t_P$ que podría ser aprovechado en sensores ubicados relativamente próximos a los epicentros de sismos someros. El método utiliza máquinas de aprendizaje para reducir los márgenes de error en la estimación de magnitud. Finalmente, se presenta otra propuesta de algoritmo rápido de tan solo 3 segundos de procesamiento, llamado $t_P\text{+}3$, que propone un nuevo parámetro, para otro tipo de escenario sísmico donde si bien los sensores están relativamente próximos a los epicentros, los sismos son profundos y por consiguiente los focos sísmicos están lejos de los sensores sísmicos.

El Capítulo I presenta el desempeño del SASMEX durante el sismo M_w 7.5 del 20 de marzo de 2012; el sistema en ese entonces en su fase final de integración entre el SAS y SASO, emitió una alerta con más de 70 segundos de anticipación para la Ciudad de México, se explica cómo es la cobertura y los dos tipos de rango de alerta Preventiva y Pública a la población y se revisan los diversos tiempos de anticipación de la alerta en otras ciudades donde se difunde ésta, tales como Acapulco, Chilpancingo, Toluca y Oaxaca. Además se detalla cómo operó este sistema segundo a segundo durante el proceso de detección, pronóstico y diseminación de la alerta de acuerdo a las aceleraciones de los sensores más próximos de la red. Finalmente, expone algunos

ejemplos de la capacidad de respuesta y cómo es aprovechado el tiempo de anticipación para llevar a cabo acciones de preparación.

El Capítulo II presenta un análisis y evaluación del algoritmo del SASMEX llamado $2(t_S\text{-}t_P)$, este algoritmo fue desarrollado al inicio del sistema, cuando sólo cubría la región de la Brecha de Guerrero y se emitía avisos de alerta a la Ciudad de México. El algoritmo invierte en su procesamiento precisamente dos veces el intervalo de tiempo entre la detección de las ondas P y las ondas S. El capítulo expone a detalle el proceso de detección y presenta decenas de ejemplos de estos resultados en sismos $M_w > 6$. El trabajo describe el proceso de estimación, el cual utiliza un modelo de clasificación basado en dos parámetros obtenidos de la sumas cuadráticas de aceleración longitudinal, transversal y vertical; cuyo criterio para alertar requiere las estimaciones de magnitud de dos sensores que de acuerdo a la distancia de estos sensores a la ciudad a alertar se decide emitir o no alguna alerta. El trabajo presenta en primera instancia, una revisión de los sismos que han emitido alerta por el SASMEX y se revisan sus parámetros, luego se lleva a cabo una evaluación de acuerdo a los sismos $M_w > 6$ desde 1985 a la fecha en la región de subducción de la zona costera del Océano Pacífico en México para observar el porcentaje de aciertos de este algoritmo. Este algoritmo se sometió también a los dos grandes sismos ocurridos en los años recientes uno ocurrido en Maule, Chile en 2010 de magnitud M_w 8.8 y otro en Tohoku, Japón en 2011 de magnitud M_w 9.0. Los resultados muestran que el algoritmo obtiene estimaciones correctas en el 92% de casos de registros de sismos si el margen de error es de ±1.0 y del 83% para ±0.5 de unidad de magnitud; por otro lado, en sismos $M_w > 6$ de los 61 sismos procesados, se muestra que en todos los casos el algoritmo habría emitido una alerta Pública. En el caso de los sismos grandes de Chile y Japón se habría estimado como mayor de 6. Sin embargo, en estos dos casos, el tiempo de procesamiento quizás no habría generado tiempos de anticipación efectivos para alerta temprana.

El Capítulo III presenta una propuesta de algoritmo rápido para regiones sísmicas de subducción cuyos focos sísmicos estén a profundidades menores de 40 km, como

ocurre principalmente en la costa de México del Océano Pacífico. Esta propuesta utiliza el 50% de tiempo de procesamiento respecto al algoritmo original $2(t_S-t_P)$. Este algoritmo denominado t_S-t_P sólo emplea el intervalo de tiempo entre las detecciones de los inicios de las ondas *P* y *S* e inicia su proceso desde la detección de las ondas *P*. Adicionalmente, sólo utiliza las aceleraciones de las ondas *P* del componente vertical de los acelerómetros triaxiales. El algoritmo t_S-t_P, utiliza un modelo de regresión basado en los parámetros de la suma cuadrática de las aceleraciones y la aceleración cuadrática máxima de la componente vertical. Los parámetros se analizan para observar qué tanto pueden correlacionarse con la magnitud M_w y con ello se propone un modelo de regresión por medio de mínimos cuadrados que para su construcción utilizó máquinas de aprendizaje con supervisión y emplea un estrategia de segmentar por niveles los valores que se obtienen de la suma de aceleraciones cuadráticas, y aceleraciones máximas respecto a M_w.

Los datos que se utilizaron fueron de sismos someros a menos de 40 km de profundidad de la región de subducción a lo largo de la costa de México en el Océano Pacífico. Después de un proceso de depuración y selección, se eligieron 400 registros de 129 sismos de magnitud $4.7 \leq M_w \leq 8.1$ desde 1985 hasta 2017. Los resultados obtenidos muestran un 85% para márgenes de error de ±0.5 y 90% para un error de ±1.0; se sometió el algoritmo t_S-t_P al contexto de un sistema de alerta temprana que contemple la confirmación de dos sensores como ocurre en el SASMEX pero considerado sólo un rango de alerta que establecimos para sismos $M_w > 5.8$, así se pudo observar para 109 sismos, que habrían sido resueltos 98 correctamente, 7 habrían sido sobreestimados y sólo 4 subestimados. Finalmente el algoritmo t_S-t_P se prueba para el sismo de Napa, California de magnitud M_w 6.0 en 2014 cuyo escenario es ideal para este tipo de algoritmos, el resultado muestra que las estimaciones del algoritmo t_S-t_P habrían estimado magnitudes mayores a 6 en 2 segundos de procesamiento y por consiguiente, se habría podido emitir una alerta pública; de acuerdo al proyecto de sistema de alerta sísmica temprana para California, conocido como *ShakeAlert* (Kuyuk, *et al*. 2013) su sistema para la ciudad de Berkeley hubiera

logrado un tiempo de anticipación de 5 segundos (Allen, *et al*., 2014). Sin embargo, con la propuesta del algoritmo t_S-t_P se hubiera generado un tiempo de 10 segundos.

Finalmente, el Capítulo IV propone un algoritmo para regiones sísmicas del *in-slab*, cuyos focos ocurren generalmente a profundidades mayores a 40 km, por lo que no hay manera de aproximarse más para así reducir los tiempos de procesamiento con los algoritmos expuestos en los capítulos anteriores. El algoritmo que se propone denominado t_P*+3* utiliza los primeros tres segundos de medición de las aceleraciones del componente vertical de las ondas *P*. Este algoritmo emplea un modelo de regresión basado en dos parámetros que mapean a M_w. Los parámetros son la suma de las aceleraciones cuadráticas y el otro parámetro consiste en el ángulo de inflexión medio de la curva de la suma acumulada de aceleraciones cuadráticas obtenido de dos pendientes de dicha curva. El modelo de regresión del algoritmo t_P*+3* se construyó de manera similar al algoritmo t_S-t_P expuesto en el Capítulo III; es decir, utilizando una máquina de aprendizaje que parametriza los valores de la suma de aceleraciones cuadráticas de Ondas P de la componente vertical obtenidas en el intervalo de 3 segundos. Los parámetros que emplea el modelo son sometidos a un análisis de correlación respecto a M_w utilizando 113 registros de 34 sismos a profundidades mayores de 40 km en la región sísmica del *in-slab* de México. Al evaluar el modelo en el contexto de alerta temprana del SASMEX y al considerar el criterio de confirmación de dos estaciones en donde se propone un umbral de activación de alerta si las estimaciones de magnitud mayores o iguales a 5.8, se obtuvo para 24 sismos, una subestimación, cuatro sobreestimaciones y las 19 restantes fueron correctas. Para poder comprender las ventajas de emplear el algoritmo t_P*+3* en este escenario sísmico, se muestran los posibles desempeños para tres sismos: el de Tehuacán Puebla del 15 de junio de 1999 de magnitud M_w 7.0, el de Zumpango del Río, Guerrero del 10 de diciembre de 2011 de magnitud M_w 6.5 y el de Morelos del 19 de septiembre de 2017 de magnitud M_w 7.1 en donde se observan notables ventajas en el tiempo de anticipación en comparación con el algoritmo original *2(*t_S-t_P*)* y t_S-t_P de haberse activado una alerta pública.

REFERENCIAS

Allen, R. and Kanamori H., (2003) The potential for Earthquake early warning in South California, Science 300, 786-789

Allen, R. M., Gasparini, P., Kamigaichi, O., & Böse, M. (2009). The status of earthquake early warning around the world: An introductory overview. Seismological Research Letters, 80(5), 682-693.

Allen, R. V., D. Given, T. Heaton, H. and J. Vidale, (2014). Successful ShakeAlert Performance for the Napa Quake. 2014 AGU Fall Meeting. San Francisco, CA (S44D-01).

Cooper, M. D. (1868) Editorial in San Francisco Daily Evening Bulletin, November 3.

Erdik, M., Fahjan, Y., Ozel, O., Alcik, H., Mert, A., & Gul, M. (2003). Istanbul earthquake rapid response and the early warning system. Bulletin of earthquake engineering, 1(1), 157-163.

Espinosa-Aranda, J. M., Jimenez A., Contreras O., Ibarrola G., and Ortega R. (1992) Mexico City Seismic Alert System, International Symposium on Earthquake Disaster Prevention 18-21 may 1992, Mexico, Proceedings Centro Nacional de Prevención de Desastres and Japan International Cooperation Agency CENAPRED-JICA. Mexico I: 1992. p. 315–24,

Espinosa-Aranda, J. E., Jimenez, A., Ibarrola, G., Alcantar, F., Aguilar, A., Inostroza, M., & Maldonado, S. (1995). Mexico City seismic alert system. Seismological Research Letters, 66(6), 42-53.

Espinosa-Aranda, J. M., Cuellar, A., Garcia, A., Ibarrola, G., Islas, R., Maldonado, S., & Rodriguez, F. H. (2009). Evolution of the Mexican seismic alert system (SASMEX). Seismological Research Letters, 80(5), 694-706.

Espinosa-Aranda, J. M., Cuéllar, A., Rodríguez, F. H., Frontana, B., Ibarrola, G., Islas, R., & García, A. (2011). The seismic alert system of Mexico (SASMEX): Progress and its current applications. Soil Dynamics and Earthquake Engineering, 31(2), 154-162.

Esteva, L. (1988). The Mexico earthquake of September 19, 1985-Consequences, lessons and impact on research and practice, Earthquake Spectra, 4(3), 413-426.

Gasparini, P., Manfredi, G., & Zschau, J. (2007). Earthquake early warning systems (p. 350). Berlin: Springer.

Hoshiba, M., Kamigaichi, O., Saito, M., Tsukada, S. Y., & Hamada, N. (2008). Earthquake early warning starts nationwide in Japan. EOS, Transactions American geophysical union, 89(8), 73-74.

Iglesias, A., S. K. Singh, M. Ordaz, M. A. Santoyo and J. Pacheco (2007). The seismic alert system for Mexico City: an evaluation of its performance and a strategy for its improvement, Bull. Seismol. Soc. Am., 97(5), 1718-1729.

Kanamori, H., Hauksson, E., & Heaton, T. (1997). Real-time seismology and earthquake hazard mitigation. Nature, 390(6659), 461-464.

Kuyuk, H. S., Allen, R. M., Brown, H., Hellweg, M., Henson, I., & Neuhauser, D. (2013). Designing a network-based earthquake early warning algorithm for California: ElarmS-2. Bulletin of the Seismological Society of America.

Nakamura Y. (1989) Earthquake alarm system for Japan Railways, Japanese Railway Engineering 28, 4, 3-7

Nakamura, Y. (1996). Real-time information systems for seismic hazards mitigation UrEDAS, HERAS and PIC. QUARTERLY REPORT-RTRI, 37, 112-127.

Suárez, G., Novelo, D. and Mansilla, E. (2009). Performance evaluation of the seismic alert system (SAS) in Mexico City: a seismological and a social perspective. Seismol. Res. Lett., 80(5), 707-716.

United Nations (2006). Global Survey of Early Warning Systems An assessment of capacities, gaps and opportunities towards building a comprehensive global early warning system for all natural hazards. United Nations Inter–Agency Secretariat of the International Strategy for Disaster Reduction (UN/ISDR)) Final Version.

Wu, Y. M., Shin, T. C., & Tsai, Y. B. (1998). Quick and reliable determination of magnitude for seismic early warning. Bulletin of the Seismological Society of America, 88(5), 1254-1259.

Rosenblueth, E. (1986). The 1985 earthquake: causes and effects in Mexico City, J. Am. Concrete Institute, 8.5, 23-24.

Wenzel F. Onescu, M. C. Baur, M., Friedrich F. (1999) An early warning system for Bucharest Seism. Res. Lett. 70, 2, 161-169.

CAPÍTULO I

The Mexican Seismic Alert System (SASMEX): Its Alert Signals, Broadcast Results and Performance During the M7.4 Punta Maldonado Earthquake of March 20th, 2012

[**Cuéllar, A.**, Espinosa-Aranda, J. M., Suárez, G., Ibarrola, G., Uribe, A., Rodríguez, F. H., …& Frontana, B. (2014). The Mexican Seismic Alert System (SASMEX): Its alert signals, broadcast results and performance during the M 7.4 Punta Maldonado earthquake of March 20th, 2012. In *Early Warning for Geological Disasters* (pp. 71-87). Springer Berlin Heidelberg.]

Chapter 4
The Mexican Seismic Alert System (SASMEX): Its Alert Signals, Broadcast Results and Performance During the M7.4 Punta Maldonado Earthquake of March 20th, 2012

A. Cuéllar, J. M. Espinosa-Aranda, G. Suárez, G. Ibarrola, A. Uribe, F.H. Rodríguez, R. Islas, G. M. Rodríguez, A. García and B. Frontana

Abstract The Mexican Seismic Alert System (SASMEX) compromises the Seismic Alert System of Mexico City (SAS), in continuous operation since 1991, and the Seismic Alert System of Oaxaca City (SASO) that started its services in 2003. The SAS generates automatic broadcasts of Public and Preventive Alert Signals to the cities of Mexico, Toluca, Acapulco and Chilpancingo, and SASO by now only to Oaxaca City. Historically in Mexico City, due to their great distance to the coast of Guerrero, the SAS has issued its Alert Signals with an opportunity average of 60 s. In Oaxaca City the SASO gives 30 s time opportunity, if the earthquake detected is occurring in the Oaxaca coast region, or less time, if the seismic event hits near this town. The paper reviews both systems, its performance characteristics and its recent test by the Ometepec M 7.4 earthquake of March 20, 2012.

4.1 Introduction

The Seismic Alert System of Mexico City (SAS) generates automatic broadcast of Public and Preventive Alert Signals to the cities of Mexico, Toluca, Acapulco and Chilpancingo, and the Seismic Alert System of Oaxaca City (SASO) by now only to Oaxaca City. Two types of SASMEX Seismic Alert Signals ranges were determined in accordance with each local Civil Protection Authorities: Public Alert if they

A. Cuéllar (✉) • J. M. Espinosa-Aranda • G. Ibarrola • A. Uribe • R. Islas • A. García
Centro de Instrumentación y Registro Sísmico, A. C., Anaxágoras 814 Narvarte,
03020 México, D. F., México
e-mail: acuellarmtz@yahoo.com.mx

F. H. Rodríguez • G. M. Rodríguez • B. Frontana
Facultad de Ingeniería, Universidad Nacional Autónoma de México,
México, D. F., México

A. Cuéllar • G. Suárez
Instituto de Geofísica, Universidad Nacional Autónoma de México,
México, D. F., México

F. Wenzel and J. Zschau (eds.) *Early Warning for Geological Disasters*,
Advanced Technologies in Earth Sciencies, DOI: 10.1007/978-3-642-12233-0_4,

expect strong earthquake effects and Preventive Alert Signal, for moderated ones. SAS originally had 12 field sensor stations covering partial segment of the Guerrero coast, nowadays covers additionally Michoacan, Jalisco Colima and Guerrero coast completely with 36 field sensor stations supported by the Mexico City Government; the SASO has 37 field sensor stations operating in the coast, central and north of the Oaxaca, covering their seismic danger territory. Since 1993, the SAS is pioneer in the automatic public alerts broadcast services, thanks to the support of the *Asociación de Radiodifusores del Valle de México, A.C.* (ARVM). Historically in Mexico City, due to their great distance to the coast of Guerrero, the SAS has issued its Alert Signals with an opportunity average of 60 s. In Oaxaca City the SASO gives 30 s time opportunity, if the earthquake detected is occurring in the Oaxaca coast region, or less time, if the seismic event hits near this town. Also the SASO has been supported since its implementation for local commercial radio stations. To this day the SAS and SASO have generated respectively 14 and 20 Public Alert Signals, also 59 and 13 Preventive Alerts of more than 2200 earthquakes detected by their sensing field stations. Additionally the federal government is promoting to increase the observation capacity of the seismic danger in Mexico City and the other cities located in seismic regions, to detect and warn any strong seismic effect.

To reach better efficiency in the seismic warning delivery, the Government of the Federal District through the Authority of the Historical Center in 2008, to innovate the SAS, installing VHF radio transmitters, similar to the communication technology like the National Weather Radio (NWR) and Specific Area Message Encoding (SAME) called NWR-SAME, following the code standards of the National Oceanographic and Atmospheric Administration (NOAA) and the Emergency Alert Systems (EAS) of United States; adding a new code (SARMEX) with the capabilities like fast response (2 s or less) to emit the earthquake early warning signal in order to enhance the effectiveness in the Seismic Alert Signals required. This technology also will be implemented in the SASO, and recently the federal authorities have decided to support the coverage with NWR-SAME-SARMEX receivers in other populated cities or urban areas located in seismic regions of Mexico.

On March 20, 2012, during the occurrence of earthquake M 7.4 Ometepec Gro., close to Punta Maldonado, the SASMEX warned Public Alert in the cities of Acapulco and Chilpancingo, Gro., and Oaxaca, Oax., and warned Preventive Alert in the metropolitan area of the valley of Mexico. The time of opportunity was between 80 and 40 s, due to the distance between 175 and 360 km from epicenter to cities where the SASMEX broadcasted their public earthquake early warnings.

After experiencing the serious seismic disaster generated by the "Caleta de Campos" M8.1 Michoacán earthquake in 1985, Mexico City Authorities have been promoting since 1989 the design and evolution of *Sistema de Alerta Sísmica* (*SAS*), with the aim to mitigate possible future earthquake damage produced by such as the latent "Guerrero Gap" seismic danger (Espinosa-Aranda et al. 1992).

The original *SAS* idea was developed by *Centro de Instrumentación y Registro Sísmico* (CIRES) Civil Association. This technological resource started its experimental operation in August 1991 and has been available and evaluated as a public service since 1993. To date it is applied and evaluated in more than 80 elementary

schools, both private and public, located in urban regions prone to seismic risk and where early warning of seismic alert signals from *SAS* has been useful, as well as in the Mexico City subway rail transport (METRO). Recently has started the installation of more than 40,000 NWR-SAME-SARMEX receivers for elementary public schools of Mexico City.

SAS disseminates public seismic alert in the valleys of Mexico and Toluca, this one located about 50 km NW of Mexico City. In addition, it also alerts on a contract basis to more than 280 miscellaneous institutions comprising schools, public buildings and emergency organizations. The implementation of *SAS* in the Mexico Valley has made possible to anticipate the arrival of the effects of S-waves with an average of 60 s, time enough to allow execution of safety of automatic system procedures for the protection of equipment or systems susceptible to undergo damage, such as power plants, computer systems and telecommunication networks (Kanamori 2003). On May 14, 1993, after *SAS* identified an earthquake M6.0 and anticipated with 65 s the imminent arrival of its effect in Mexico City, the local authorities decided to disclose early warning notices publicly. The alert signal broadcast was possible thanks to the support from most of the commercial radio and television networks grouped in the *Asociación de Radiodifusores del Valle de Mexico* (ARVM), Civil Association, which agreed to contribute as a social service for their audience since August 1993. *SAS*, has high availability and reliability of their four basic sub-systems: Seismic Detection, Communication, Warning Dissemination and Central Control and Recording, to guarantee the effective earthquake alert public service (Espinosa-Aranda et al. 1995).

On September 14, 1995 at 8:04 AM in Mexico City, having elapsed almost ten years after the tragic earthquake of 1985 (Espinosa-Aranda et al. 1995), *SAS* anticipated with 72 s the arrival of the effect of an M 7.3 earthquake occurred near the town of Copala, Guerrero, This earthquake proved the adequacy of the processes of response and evacuation of schools, where the *SAS* early warnings were received, since the population performed these activities successfully (Goltz and Flores 1997).

On June 15th 1999, a damaging M6.7 earthquake induced the Department of Civil Protection of Oaxaca to request CIRES the design, construction and installation of the *Sistema de Alerta Sísmica de Oaxaca* (*SASO*). A better time-efficiency criteria to define the seismic range of the *SASO* warnings emerged in a technological evolution from the original algorithm used by *SAS*, designed back in 1989 (Espinosa-Aranda et al. 1992), to fulfill the requirements demanded by this application.

Thanks to the Oaxaca Authorities initiative, the Mexico City Mayor, with the participation of the Mexican Secretariat of the Interior, it has been agreed a *SASO* and *SAS* function integration to constitute them as a single entity, the so-called *Sistema de Alerta Sísmica Mexicano* (*SASMEX*). And recently has been decided to increase as necessary the number of seismic sensors to provide an effective warning of impending regional seismic risk disseminating notices of seismic alert in vulnerable cities (Fig. 4.1). With the service rendered by EA*SAS* systems in each sensible region, it will be possible to prevent in advance the seismic effects on the site as well as define the most suitable alert warning for each particular risk condition, and to review these factors systematically (Espinosa-Aranda et al. 2009).

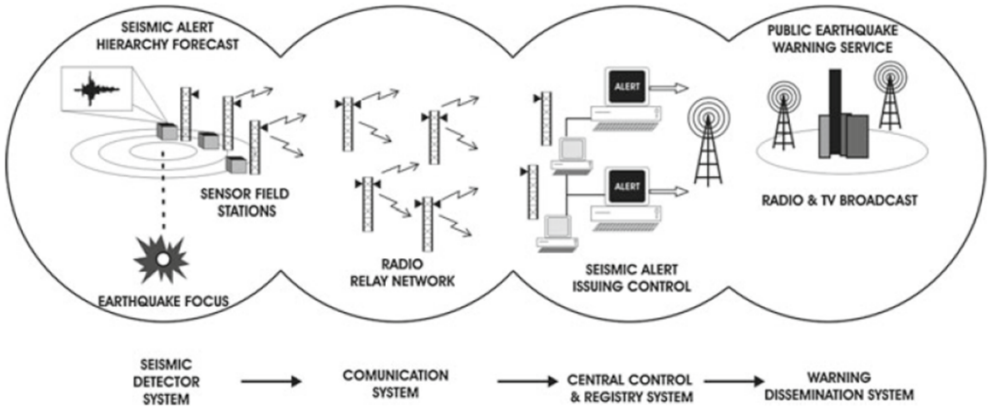

Fig. 4.1 The Mexican Seismic Alert System

In 2007, to support the activities of Civil Protection of the coastal state of Guerrero, Mexico City Authorities authorized the installation of Alternate Emitters for the warning issued by the *SAS* (EA*SAS*) in the cities of Acapulco and Chilpancingo. The EA*SAS* of Guerrero provide public automatic alert services controlling the transmissions of the local commercial broadcasting stations covering the demand of private seismic alert services offered to 102 institutional users.

In order to improve the efficiency in the dissemination of the warning provided by *SAS* initially in schools, recently *La Autoridad del Centro Histórico* in Mexico City sponsored the installation of three dedicated VHF radio transmitters, thus benefiting by the use of commercially available low-cost receivers carrying the Public Alert^{TM} logo, that meet technical standards of NOAA Weather Radio (NWR) Specific Area Message Encoding (SAME) protocols and the Emergency Alert System (EAS) event codes, such as those in use to warn against diverse natural hazards in the USA. The Mexico City application require the NOAA-SAME-EAS protocols, an enhancement in order to include a new code to operate earthquake early warning signals, without delay, omitting the normal two tones previous to signal advise (Espinosa-Aranda et al. 2009).

The Consumer Electronics Association Standards of United States (CEA), approved the Mexican Risks Advisory System (SARMEX) standard that uses all characteristics of the NWR-SAME protocols in March 2011, but enhances the response time when the Earthquake Early Warning codes are emitted, additionally, the Mexican earthquake early warning sound is included to distinguish it from others messages.

4.2 SASMEX Achievements

The SASMEX part for the Mexico City (called SAS) has been regarded as the first system in the world for earthquake early warning that disseminates its notices to the public (Lee and Espinosa-Aranda 1998). The Prevention Time is close to 60 s. This is because the major seismic effects threatening the Valley of Mexico are originated at

the coastal region of the Pacific Ocean at a distance of at least 320 km and since their strongest components travel at 4 km per second, taking 80 s to arrive, whereas notices broadcasted by radio from the epicenter area can be transmitted instantaneously anticipating the seismic effects.

The SASMEX forecast begins calculating parameters measured in the Field Stations, FS, when an earthquake is detected, SASMEX in the Mexican Pacific Coast from Colima to Oaxaca, uses the acceleration data of the vertical, longitudinal and transversal components to calculate the Acceleration Quadratic Integration and the rate of this integration, both measured during the 2*(S-P) lapse, that is, the first P wave arrives until the S wave begins. In north and center of Oaxaca it uses the dominant period, measured in the vertical component during the first three seconds after de P wave begins; in case of the S-P is less than 3 s, then the FS uses two additional parameters: the Maximum Acceleration and the Acceleration Quadratic Integration, from the vertical component too (Espinosa-Aranda et al. 2010).

The parameters are sent automatically to determine the alert range, this forecast is used to define the seismic warning range of the impending occurrence of a dangerous earthquake detected by the first two FS (Espinosa-Aranda and Rodriguez 2003). The first FS message defines the warning range, either strong or moderate, and with the second one, triggers the Type of Warning process respectively as "Public Alert" or "Preventive Alert". However the range of Public and Preventive in Oaxaca, Chilpancingo and Acapulco is less than Mexico City, in order to be more sensible due to minor distance from these cities to the danger seismic area in contrast with Mexico City. The Prevention Time is defined as the time elapsed between the beginning of the warning signal and the beginning of the S phase, related to the region where it is intended to mitigate the risk (Espinosa-Aranda et al. 2009).

SASMEX for Mexico City (SAS) since its experimental operational stage in 1991, *SAS* has detected more than 2300 seismic events with magnitudes from M3.0 to M 7.4 and it has emitted 14 earthquakes warnings as "Public Alerts" and 59 as "Preventive Alerts (Table 4.1). The *SAS* performance showed in the Table 4.1 is accounted by the number of FS's that registered each warned earthquake (# SENS. OP.), the Forecast (MAGNITUDE), the Type of Warning emitted (ALERT RANGE) and Prevention Time. The DISTANCE in Table 4.1 is measured from the epicenter to the first FS which detected the earthquake.

SASMEX for Oaxaca (called *SASO)* constitutes a technological development evolved from *SAS*; *SASO* has 36 FS and 11 radio relay stations to link its coastal, central, and northern included isthmus regions (Fig. 4.2). Since its commissioning, *SASO* has issued 20 Public Alert and 13 Preventive Alert warnings from the detection and analysis of more than 230 sensed earthquakes (Table 4.2 similar to Table 4.1).

From April 2012, *SASMEX* identifies the strong earthquakes along the coast of the State of Guerrero, Michoacán, Jalisco and Colima with a linear layout of 36 of SAS and 11 of SASO FS spaced approximately every 25 km to be able to perform an efficient survey because many seismic foci of this region occur at similar depths (Fig. 4.2).

Table 4.1 SAS Performance of earthquake early warnings since 1991–2012

		NACIONAL SEISMIC SERVICE (SSN), UNAM				SAS FORECAST RESULT		
#	Region	Local date-time	Latitude	Longitude	Depth (km)	Sens. Op.	Alert range	Prevention time (s)
72	Oaxaca	02/04/2012 12:36	16.27	−98.47	10	6	Preventive	80
71	Oaxaca	20/03/2012 12:03	16.42	−498.36	15	7	Preventive	80
70	Guerrero	10/12/2011 19:48	17.84	−99.98	58	10	Preventive	16
69	Guerrero Coast	18/06/2011 17:55	16.92	−99.60	26	5	Preventive	
68	Guerrero Coast	05/05/2011 08:24	16.61	−98.91	11	6	Public	65
67	Guerrero Coast	25/05/2010 18:36	17.11	−101.2	15	8	Preventive	63
66	Guerrero Coast	27/04/2009 16:46	16.90	−99.58	7	4	Preventive	57
65	Guerrero	27/03/2009 02:48	17.35	−100.82	30	7	Preventive	58
64	Guerrero	11/11/2008 05:02	16.62	−100.8	15	4	Preventive	
63	Guerrero	06/11/2007 00:35	17.08	−100.14	9	9	Public	68
62	Guerrero	28/04/2007 08:56	16.94	−99.82	9	6	Preventive	
61	Guerrero	13/04/2007 03:43	17.27	−100.27	51	8	Preventive	56
60	Guerrero	13/04/2007 00:42	17.09	−100.44	41	6	Public	58
59	Guerrero	31/03/2007 00:18	17.00	−99.79	34	5	Preventive	
58	Guerrero	18/09/2005 06:25	17.05	−100.02	8	3	Preventive	
57	Guerrero Coast	09/01/2003 20:08	16.97	−100.3	30	7	Preventive	58
56	Guerrero	27/09/2002 02:04	17.16	−100.59	37	4	Preventive	58
55	Guerrero Coast	25/09/2002 13:14	16.86	−100.12	5	4	Preventive	57
C	Guerrero Coast	18/04/2002 12:02	16.42	−101.1	15	0	Fail	
54	Guerrero Coast	16/02/2002 22:10	16.94	−99.93	37	6	Preventive	
53	Guerrero Coast	07/10/2001 22:39	16.94	−100.14	4	8	Public	65
52	Guerrero	06/03/2001 15:57	17.14	−100.1	32	9	Preventive	63
51	Guerrero Coast	05/03/2001 04:17	17.13	−100.06	32	8	Preventive	66
50	Guerrero Coast	14/04/2000 20:45	16.88	−100.35	9	5	Preventive	66

(continued)

Table 4.1 Continued

#	Region	NACIONAL SEISMIC SERVICE (SSN), UNAM				SAS FORECAST RESULT		
		Local date-time	Latitude	Longitude	Depth (km)	Sens. Op.	Alert range	Prevention time (s)
49	Guerrero	17/03/2000 18:50	17.08	−99.31	31	7	Preventive	68
48	Puebla-Oaxaca Border	15/06/1999 15:42	18.18	−97.51	69	9	Preventive	15
47	Guerrero	30/05/1999 04:58	17.26	−100.79	53	5	Preventive	68
46	Guerrero	24/04/1999 22:08	17.28	−100.8	27	4	Preventive	68
45	Guerrero Coast	07/09/1998 01:53	16.77	−99.67	12	3	Preventive	
44	Guerrero Coast	09/08/1998 11:18	16.87	−100.25	3	3	Preventive	
43	Guerrero Coast	17/07/1998 06:18	16.98	−100.16	27	7	Public	74
42	Guerrero Coast	05/07/1998 14:55	16.83	−100.12	5	6	Public	66
41	Guerrero Coast	09/05/1998 12:03	17.34	−101.41	18	4	Preventive	60
40	Guerrero	11/03/1998 08:13	17.01	−100.11	40	4	Preventive	
39	Guerrero Coast	21/12/1997 23:22	17.14	−101.24	5	5	Public	69
38	Guerrero Coast	26/08/1997 19:13	16.76	−99.00	28	6	Preventive	45
37	Guerrero	19/07/1997 02:34	17.22	−100.56	51	6	Preventive	56
36	Oaxaca-Guerrero Coast	14/07/1997 20:26	16.39	−98.74	11	3	Preventive	
35	Guerrero Coast	11/07/1997 17:23	16.76	−99.7	10	3	Preventive	
34	Low Balsas River	22/05/1997 02:50	18.41	−101.81	59	4	Preventive	
33	Guerrero	08/05/1997 10:58	17.32	−100.44	12	5	Preventive	55
32	Guerrero	23/03/1997 14:23	17.39	−100.88	31	4	Preventive	
31	Guerrero	21/03/1997 21:49	17.04	−99.76	30	7	Preventive	55
30	Michoacan Coast	11/01/1997 14:28	17.91	−103.04	16	7	Preventive	42
29	Guerrero	27/10/1996 03:15	17.11	−100.9	27	3	Preventive	
28	Guerrero	19/07/1996 04:00	17.35	−100.29	20	6	Preventive	
27	Guerrero Coast	15/07/1996 16:23	17.45	−101.16	20	6	Preventive	65
26	Guerrero Coast	13/03/1996 15:04	16.52	−99.08	18	6	Public	74
25	Guerrero Coast	16/09/1995 10:09	16.4	−98.69	10	2	Preventive	
24	Guerrero Coast	15/09/1995 21:20	16.3	−98.62	10	4	Public	

(continued)

Table 4.1 Continued

#	Region	NACIONAL SEISMIC SERVICE (SSN), UNAM				SAS FORECAST RESULT		
		Local date-time	Latitude	Longitude	Depth (km)	Sens. Op.	Alert range	Prevention time (s)
23	Oaxaca-Guerrero Coast	14/09/1995 08:09				5	Preventive	
22	Oaxaca-Guerrero Coast	14/09/1995 08:04	16.31	−98.88	22	9	Public	72
21	Oaxaca Coast	31/05/1995 06:49	15.97	−98.77	14	2	Preventive	
20	Guerrero Coast	14/04/1995 00:01	16.44	−99.09	15	6	Preventive	
19	Low Balsas River	10/12/1994 10:17	18.02	−101.56	78	6	Preventive	34
18	Guerrero Coast	29/10/1994 10:44	16.97	−99.89	24	9	Preventive	58
17	High Balsas River	22/05/1994 19:41	18.03	−100.57	23	8	Preventive	30
B		16/11/1993 19:11				1	Public (Fail)	
A	Guerrero Coast	24/10/1993 01:52				9	(Fail)	
16	Guerrero Coast	10/09/1993 04:50	16.57	−98.94	20	4	Preventive	70
15	Guerrero	29/07/1993 14:17	17.38	−100.65	43	4	Preventive	
14	Oaxaca-Guerrero Coast	15/05/1993 02:26	16.54	−98.65	20	4	Public	
13	Oaxaca-Guerrero Coast	14/05/1993 21:12	16.47	98.72	15	6	Public	73
12	Oaxaca-Guerrero Coast	14/05/1993 21:09	16.43	−98.74	20	6	Public	65
11	Guerrero Coast	31/03/1993 04:18	17.18	−101.02	8	4	Preventive	
10	Guerrero Coast	09/11/1992 20:13	16.89	−100.1	6	3	Public	
9	Guerrero Coast	04/11/1992 22:33	16.83	−99.66	8	2	Preventive	
8	Guerrero Coast	30/10/1992 02:16	17.14	−100.79	21	3	Preventive	
7	Guerrero Coast	16/10/1992 11:28	16.51	−99.17	17.4	5	Preventive	
6	Guerrero	02/08/1992 06:54	17.13	−100.3	25	6	Preventive	
5	Oaxaca-Guerrero Coast	07/06/1992 11:41	16.22	−98.87	5.2	3	Preventive	
4	Oaxaca-Guerrero Coast	07/06/1992 03:01	16.17	−98.9	2	3	Preventive	
3	Guerrero Coast	15/05/1992 02:35	16.83	−99.98	23	3	Preventive	
2	Guerrero Coast	26/04/1992 14:53	16.78	−100.09	15	4	Preventive	
1	Oaxaca-Guerrero Coast	16/10/1991 12:36	16.83	−100.24	5	1	Preventive	

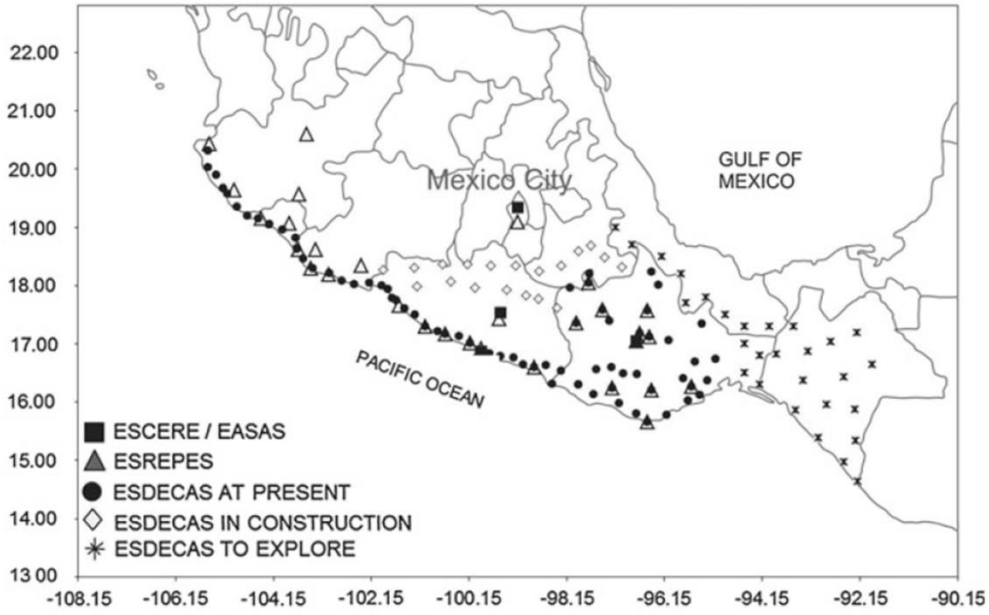

Fig. 4.2 Current topology of SASMEX

4.3 SASMEX Warning Broadcast

After the damages suffered in Mexico City during the 1985 earthquake, the law for Civil Protection and its bylaw were established. Among other requirements, it states that individuals and corporations must design action plans and emergency drills to mitigate vulnerability conditions and reduce the severity of disasters. Each action plan must be registered and certified in presence of municipal or local authorities that also supervise and enforce the regular practice of emergency response procedures (Suárez et al. 2009). The safety and security procedures, as well as the activity of each group in a certain facility, are established accordingly to the display of every building. Distribution of spaces and the identification of the risk and safety zones are considered (Official Gazette of the Federation, 2006; Mexico City Official Gazette 1996).

SASMEX for Mexico City (SAS) has been able to recognize a great number of seismic events, encode their range, and spread warnings as Public or Preventive Alerts. This service operates through three alternative technologies: remotely controlled audio switches installed in radio and TV stations operated by *SAS* that broadcast Public Alert warnings for strong earthquakes; radio receivers that radiate warnings when *SASMEX* emits Preventive and Public Alert signals of strong and moderate earthquakes; and beginning in December of 2008, receivers that include NWR-SAME technology capable of disseminating the Preventive and Public *SAS*'s alerts, as well as other natural disasters' warnings. These warning messages represent a useful service to reduce the vulnerability against a variety of risk conditions. During 2009, in accordance to the Civil Protection of Mexico City Officials

Table 4.2 SASO performance of earthquake early warnings since 2003–2012

#	Region	NACIONAL SEISMIC SERVICE (SSN), UNAM				SASO FORECAST RESULT		
		Local date-time	Latitude	Longitude	Depth (km)	Sens. Op.	Alert range	Prevention time (s)
33	Oaxaca	13/04/2012 08:07	16.22	−98.15	16	12	Public	38
32	Oaxaca	13/04/2012 05:10	16.11	−98.34	14	12	Public	40
31	Oaxaca	02/04/2012 12:36	16.27	−98.47	0	15	Public	40
30	Oaxaca	23/03/2012 19:58	16.26	−98.29	10	5	Preventive	
29	Oaxaca	22/03/2012 17:47	16.48	−98.29	24	13	Public	40
28	Oaxaca	22/03/2012 16:14	16.22	−98.47	9	8	Preventive	
27	Oaxaca	21/03/2012 05:36	16.51	−98.5	20	5	Preventive	
26	Oaxaca	20/03/2012 14:14	16.34	−98.28	15	12	Preventive	
25	Oaxaca	20/03/2012 12:36	16.21	−98.58	14	9	Public	
24	Oaxaca	20/03/2012 12:23	—	—	—	10	Public	
23	Oaxaca	20/03/2012 12:02	16.42	−98.36	15	22	Public	40
22	Oaxaca	04/03/2012 03:58	16.68	−94.4	108	3	Preventive	
21	Oaxaca	11/02/2012 23:56	17.36	−96.51	96	6	Preventive	
20	Oaxaca	15/01/2012 16:49	16.35	−97.83	5	10	Preventive	
19	Oaxaca	30/12/2011 09:47	16.91	−95.37	90	4	Preventive	
18	Oaxaca	16/12/2011 07:02	16.22	−98.3	5	8	Public	
17	Oaxaca	09/07/2011 07:43	15.87	−96.42	22	18	Public	
16	Guerrero	05/05/2011 08:25	16.61	−98.91	11	15	Public	
15	Oaxaca	14/04/2011 11:34	16.7	−95.09	102	5	Public	
14	Veracruz	07/04/2011 08:12	17.2	−94.34	167	23	Public	
13	Oaxaca	05/04/2011 15:18	16.32	−96.15	15	4	Public	
12	Oaxaca	04/02/2011 11:32	17.25	−96.56	76	3	Public	
11	Oaxaca	30/06/2010 02:22	16.22	−98.03	8	22	Public	
10	Oaxaca	16/04/2010 05:01	16.14	−98.41	10	4	Public	

(continued)

Table 4.2 Continued

#	Region	NACIONAL SEISMIC SERVICE (SSN), UNAM				SASO FORECAST RESULT		
		Local date-time	Latitude	Longitude	Depth (km)	Sens. Op.	Alert range	Prevention time (s)
9	Oaxaca	08/02/2010 18:48	15.9	−96.86	37	14	Public	
8	Chiapas	05/07/2007 20:09	16.35	−93.99	113	5	Preventive	40
7	Oaxaca	15/03/2007 07:13	16.08	−97.26	15	6	Preventive	
6	Oaxaca	24/01/2007 22:23	16.21	−97.14	6	2	Preventive	
5	Oaxaca	19/08/2006 00:41	15.91	−97.3	52	8	Public	
4	Oaxaca	15/12/2004 02:05	16.05	−95.43	10	4	Preventive	
B	Oaxaca	18/08/2004 04:03	16.3	−95.12	63	9	(Comx Fail)	
A	Veracruz-Oaxaca	07/08/2004 06:49	17.06	−95.44	112	10	(Fail)	
3	Oaxaca-Guerrero Coast	14/06/2004 17:54	16.31	−98.06	10	6	Public	30
2	Oaxaca Coast	13/01/2004 15:28	16	−97.16	14	10	Public	
1	Oaxaca	13/01/2004 13:50	16.01	−97.16	14	6	Preventive	

(*Secretaría de Protección Civil del GDF*), access to the use of the radio receiver makes mandatory to have an Internal Civil Protection Plan and practice emergency response procedures frequently.

Mexico City since 1992, have pioneered in the use of the *SAS* (Espinosa-Aranda, et al., 1998) beginning with twenty six Elementary Schools of the Ministry of Education of Mexico City (*Secretaría de Educación Pública de la Ciudad de México*). Each facility has an internal plan for civil protection that is systematically practiced and executed whenever *SAS* sends a warning signal to the radio receiver. From 1993 to the date, as stated before, more than 80 elementary, middle, and higher education institutions have been furnished with this equipment.

The Public Electric Transportation System and the METRO have used the *SAS* warnings by means of radio receivers in their control center since 1992, but they do not share the signals with the passengers. In case of a seismic warning, the manager of the control center gives proper instructions for the train operators to stop in the nearest station, or delay their start and keep the doors open for passengers' safety. This is an internal security and emergency procedure that has given great use to the 60 s that *SAS* can offer.

In Mexico, the transmission of radio and TV seismic alert signals began in 1993, through most of the partners of the Association of Broadcasters of the Mexico Valley (*Asociación de Radiodifusores del Valle de México A.C.*) and TV channels 11, 22, 13, and channel 34 in Toluca Valley. To be able of properly disseminate the signals, the broadcasters accepted the use of a remotely controlled switch operated by *SAS*, which substitutes the regular signal for the official alert signal during 60 s in case of a strong earthquake warning. The effectiveness of this resource is optimal in top rating periods because a greater part of the population is warned and can start predefined preventive actions. To date, twenty eight AM, FM and TV channels spread the warnings in Mexico City and Toluca Valley as well as nine radio and two TV stations in Oaxaca City. Also, Emergency Response and Civil Protection Institutions use the radio receiver to prepare emergency vehicles and start the evacuation of their parking lots. There are 13 institutions that use this equipment, including the Red Cross and Firefighters.

Nowadays, *SASMEX for Mexico City (SAS)* serves more than 240 public and private buildings in Mexico City; they receive seismic alert signals through the radio receiver. To guarantee the dissemination of the warning sound, some buildings have displayed loudspeakers arrays where their correct performance should be verified.

In addition to start preventive measures, *SASMEX* signals are used to trigger structural health recording procedures to identify possible damage in buildings.

Since March 27, 2009 at 02:48:32 (local time), when *SAS* emitted a "Preventive Alert" signal, anticipating the effects of the M5.3 earthquake from the coast of Guerrero. Then for the first time *SAS* used the NOAA-SAME technology validating the effective use of this resource. At that time eight monitoring NOAA receivers successfully reacted and provided 58 s of Prevention Time. Nowadays with a technical enhancement to expedite reaction, by reducing receiver's response time, the NWR-SAME with SARMEX protocol helps to mitigate the seismic vulnerability in Mexico.

On April 27, 2009 at 11:46:45 (local time), *SAS* emitted a signal of "Preventive Alert", anticipating the effects of the M5.7 earthquake from the coast of Guerrero. *SAS* confirmed the adequacy to use the NOAA-SAME technology in the city for this purpose. *SASMEX* in Oaxaca has a similar range of users to the one of Mexico City, with the exception of automatic powerful loudspeakers installed in public spaces, which can be heard in the public squares of Oaxaca City. As in Mexico City, Oaxaca and Toluca, in Chilpancingo and Acapulco both Guerrero State cities, received *SAS* warnings in more than 100 users, among radio, TV stations, schools, emergency response institutions and others in 2007. On 20th March 2012, for the earthquake M 7.4 of Oaxaca, SASMEX broadcasted Public Alert Warning to Oaxaca, and Acapulco cities, Chilpancingo and Mexico City, were activated with Preventive Alert Warning range, due to communication issues. On April 13th 2012 SASMEX activated two earthquake early warnings at 05:10:03 08:07:23 (Local Time) for the seismic event M5.2 and 5.1 respectively; with that seismic events, SASMEX for Mexico City worked for first time as an interconnected system.

4.4 The Punta Maldonado Earthquake

The earthquake was located between SAS and SASO seismic station arrays in the Punta Maldonado region with Mw = 7.4, it is noteworthy that on the date of this event, these systems had not yet achieved sensor interface through the link between Mexico City and Oaxaca therefor SAS and SASO's seismic sensor arrays operated in separately way.

The earthquake was detected by 32 seismic stations in Oaxaca and seven in Guerrero. During the first 48 h more than 100 seismic events were recorded under the Llano Grande LG01 seismic station which was closest to the epicenter (Fig. 4.3).

Llano Grande seismic station was the first to detect the earthquake, it is located within 25 km of the hypocenter, the SP time observed was of about 2.6 s. Llano

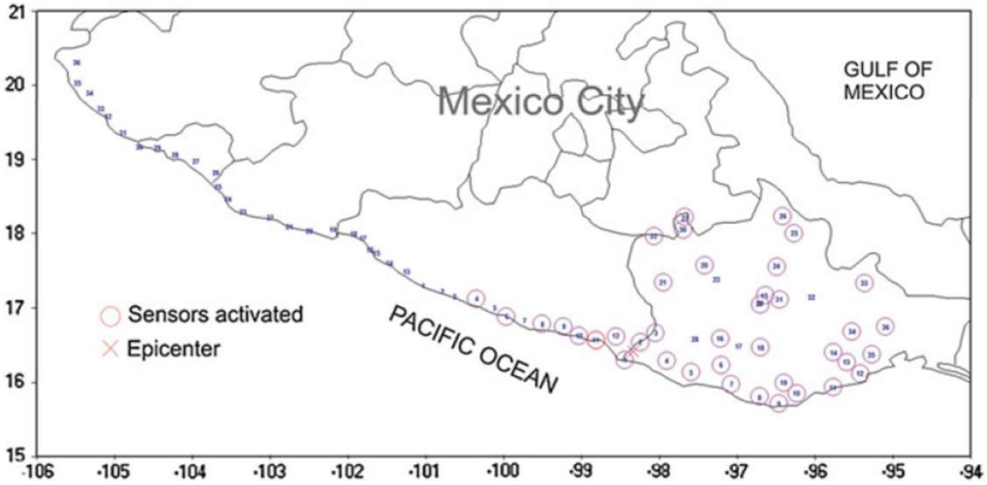

Fig. 4.3 Sensors Activated (*circles*) during the $Mw = 7.4$ earthquake on March 20th, 2012

Table 4.3 Main sequences of SASMEX seismic sensors performance during the Mw = 7.4 earthquake on March 20th, 2012

Local time	Station	Network	Forecast result
12:02:56	LG01	SASO	Strong
12:02:58	MT02	SASO	Strong
12:02:58	Easas Oaxaca	SASO	Public
12:02:59	HU12	SAS	Strong
12:03:03	MA12	SAS	Strong
12:03:03	Easas Acapulco	SAS	Strong
12:03:09	CR10	SAS	Moderate
12:03:09	Easas Chilpancingo	SAS	Preventive
12:03:09	Easas Mexico City	SAS	Preventive
12:03:14	MA11	SAS	Strong
12:03:14	Easas Chilpancingo	SAS	Public

Grande transmitted its power and slope parameters calculated for 2*(S-P) to the city of Oaxaca at 12:02:56, a little more than 5 s after detecting the onset of the P wave, and estimated the event developing as a strong earthquake. The above information began the process of activation of Alert for the city of Oaxaca. MT02-station "Mártires de Tacubaya" confirmed the process, at 12:02:58, 2 s after the previous one, and calculating the parameters of slope and amplitude in the period 2*(S-P) approximately 12 s, conveyed them to the City of Oaxaca, it also predicted strong earthquake, which was the confirmation of the process and prognosis Public Alert activated in Oaxaca.

In Acapulco, the field station HU12-Huehuetán transmitted its parameters with a strong earthquake forecast to 12:02:59. The station was confirmed MA11-Marquelia at 12:03:03 and after calculating the parameters at time 2*(S-P) as HU12, transmitted its parameters a second after the event detected at the beginning of the wave packet P (Table 4.3, Fig. 4.4). This led to the city of Acapulco earthquake also will predict and deliver Strong Public Warning.

Risk parameters and HU12-MA11-Marquelia Huehuetán must be received in Chilpancingo and Mexico City, but due to interference in the stretch of Acapulco and Chilpancingo caused the MA11 data were not recognized. HU12 data were received at 12:02:59 and CR10-"El Carrizo" seismic station transmitted at 12:03:09 parameters once estimated slope parameters and energy in the period 2*(SP) of approximately 16 s (Table 4.2). The station CR10 predicted the earthquake as Moderate. Although, combining strong and moderate earthquake determinations to activate the alert as Preventive, which was issued at Chilpancingo and Mexico City at 12:09:09? During the earthquake, the seismic station Marquelia aired a second time hazard signal, Chilpancingo changed the forecast to Public alert at 12:03:14. The time of opportunity for the city of Acapulco was 25 s, to Oaxaca City 45, to Chilpancingo was estimated to 45 s and finally in Mexico City was of 80 s.

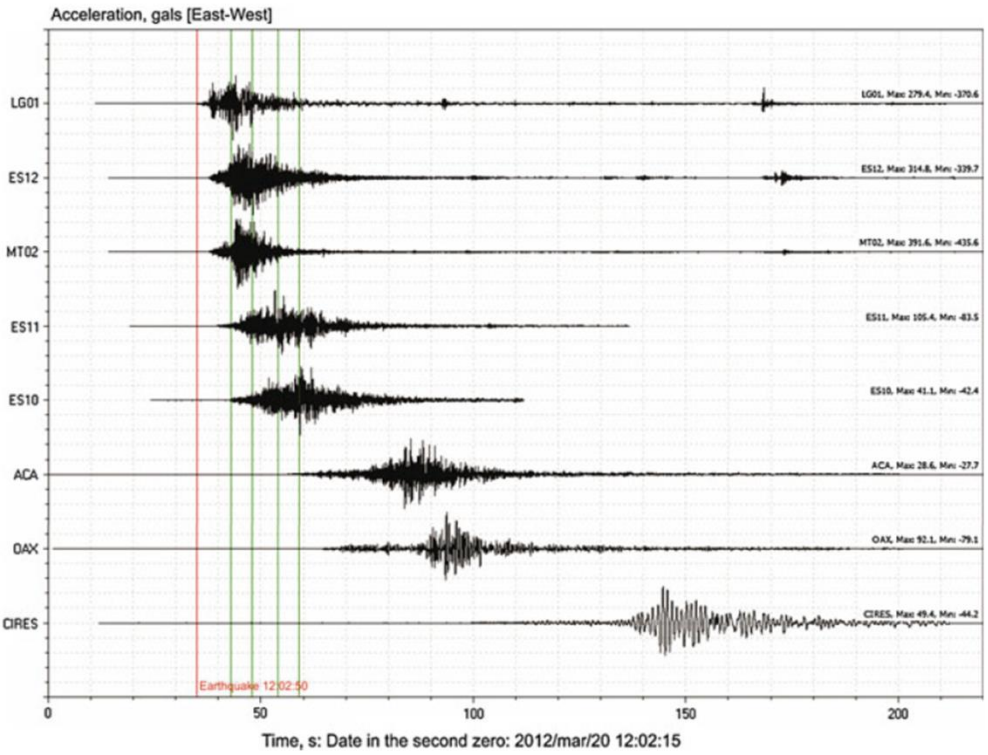

Fig. 4.4 SASMEX performance during the Mw = 7.4 earthquake on March 20th, 2012

4.4.1 Human Response After Activation of the Seismic Alert in Mexico City

During the Preventive Alert warning in Mexico City and given the opportunity time of 80 s civil protection were instrumented procedures and additionally it served to check the effectiveness of the NWR radio receiver SARMEX that had been installed in 640 public schools. Several radio and television broadcasting companies warned their audiences that the alert had been activated and warned with 80 s of opportunity that an earthquake was coming.

In government offices, especially at the House of Representatives, the Federal Electoral Institute documented the reaction of civil defense personnel as well as of the people who were in those buildings; they made use of the seismic alert drills carried out every few months for the case of occurrence of an earthquake.

4.5 Discussion

Since damaging earthquakes are rare, the development of this technological resource has deemed necessary to optimize the reliability and availability indexes of their basic elements in order to guarantee the effective dissemination of alert warnings in the

occurrence of damaging events including forecasting criteria of seismic risk. The *SASMEX* system has its own designs and self-evaluation procedures as well as a continuing technological improvement program aimed to have an assurance of its services. In the design, development and operation of *SAS* and *SASO*, now SASMEX, it is acquired the compromise to improve continuously their subsystems that conform them as well as the processes of detection, computation, communication, forecast and effective broadcast of the warnings in case of earthquake as such as the low-cost NWR-SAME radio receivers with Public alert protocols, SARMEX that includes protocol which improve the activation of NWR receiver for immediately to respond in case of earthquake in order to have the longest time of opportunity possible.

The SASMEX in the process of enlargement and integration envisions a future with federal government support extended to the cities of Chiapas and Veracruz. While Mexico City by soil characteristics and demographics are considered a risk seismic region, there are neighboring cities of seismic hazard zones, which must have notices Seismic Alert System of Mexico. The SASMEX during the earthquake of March 20, 2012, M 7.4 generated earthquake early warnings to Mexico City, Toluca, Acapulco, Chilpancingo and Oaxaca City, giving a time of opportunity at least 25 s in the city of Acapulco, and more than 80 s in Mexico City which warning was disseminated SASPER receptors and SARMEX radio receivers.

Public-oriented discussions together with the proper detection of the earthquake, the reliability of message transmission and the risk evaluation constitute necessary elements in the systems of early warning systems. However, if dissemination and training campaigns launched among the population exposed to natural hazards continue to be insufficiently funded, any early warning system will be exposed to failure to comply with its main objective for which it was designed (United Nations 2006). The technological development of early warning systems applicable to earthquakes is continuously improving and it is convenient to analyze the full spectrum of earthquake early warning. Nevertheless, other high-priority tasks must be reinforced by the authorities, like the diffusion and knowledge of the seismic danger around the city, the continuous program of prevention when the signal of seismic alert is emitted.

Acknowledgments The authors deeply acknowledge the support received from the Mexico City Government Authorities since 1989, originally through its *Secretaría de Obras y Servicios, Comité Directivo del Sistema de Alerta Sísmica,* the *Coordinación General, Secetaría de Educación, Instituto Local de Infraestructura Física Educativa and Secretaría de Protección Civil de la Ciudad de México,* who have decided to apply this technological development, proposed after our 1985 earthquake disaster experience, with the aim to mitigate the seismic vulnerability in the metropolitan population of the Mexico City valley. We are also grateful to *Autoridad del Centro Histórico de la Ciudad de México,* by its valuable sponsorship required to install the radio transmitters system used to disclose via low-cost receivers of the EAS-SAME-Public Alert system the warnings issued by the *SAS* system. We would also like to thank the *Secretaría de Educación Publica* (Public Education Ministry), that supported the *SAS* experimental program since 1992 in some schools of Mexico City; the valuable support from the *Asociación de Radiodifusores del Valle de México*, that since 1993 broadcasts the automatic warnings issued by the *SAS* to the general public; and, the government of Oaxaca, that in 2002, through its *Unidad Estatal de Proteccion Civil*, promoted the *SASO* design and development. Finally but not less, to *Teléfonos de México* (TELMEX) and of *Comisión Federal de Electricidad* (CFE) for their valuable infrastructure support that has expedited the installation

and exploitation of these *SAS* and *SASO* resources. Finally we thank the *Coordinadora Nacional de Protecćión Civil*, *Centro Nacional de Prevención de Desastres (CENAPRED)* and *Secretaría de Seguridad Pública* for its decision and support to coordinate several activities such as to use their telecommunications infrastructure as redundant via to guarantee the SASMEX critical information.

References

Espinosa-Aranda JM, Jimenez A, Contreras O, Ibarrola G, Ortega R (1992) Mexico city seismic alert system. International symposium on earthquake disaster prevention, proceedings CENAPRED-JICA, vol I. Mexico, pp 315–321

Espinosa-Aranda JM, Jimenez A, Ibarrola G, Alcantar F, Aguilar A, Inostroza M, Maldonado S (1995) Mexico city Seismic Alert System. Seismol Res Lett 66(6):42–53

Espinosa-Aranda JM, Rodriguez FH (2003) The Seismic Alert System of Mexico city. International handbook of earthquake and engineering Seismology 81B, International association of Seismology & physics of the earth's interior, committee on education

Espinosa-Aranda JM, Cuellar A, Ibarrola G, Garcia A, Islas R, Maldonado S, Rodriguez FH (2009) Evolution of the Mexican Seismic Alert System (SASMEX). Seismol Res Lett 80(5):694–706

Espinosa-Aranda JM, Cuellar A, Rodríguez FH, Frontana B, Ibarrola G, Islas R, García A (2010) The Seismic Alert System of Mexico (SASMEX): progress and its current applications. Soil Dyn Earthq Eng 31:154–162

Goltz JD, Flores PJ (1997) Real-time earthquake early warning and public policy: a report on Mexico city's Sistema de Alerta Sismica. Seismol Res Lett 68(5):727–733

Kanamori H (2003) Earthquake prediction: an overview. International handbook of earthquake and engineering Seismology 81B, International association of Seismology & physics of the earth's interior, committee on education

Lee WHK, Espinosa-Aranda JM (1998) Earthquake early warning systems: current status and perspectives. International IDNDR-conference on early warning systems for the reduction of natural disasters, Potsdam, Federal Republic of Germany, 7–11 Sept 1998

Mexico City Official Gazette (1996) Reglamento de la Ley de Protección Civil para el Distrito Federal (1996), Gaceta Oficial del Distrito Federal Mexico, 21 Oct 1996

Official Gazette of the Federation (2006) Ley General de Protección Civil (2006) Diario Oficial de la Federación, Mexico, 24 April 2006

Suárez G, Novelo D, Mansilla E (2009) Performance evaluation of the Seismic Alert System (SAS) in Mexico city: a seismological and social perspective. Seismol Res Lett 80(5): 717–726

United Nations (2006). Global Survey of Early Warning Systems An assessment of capacities, gaps and opportunities towards building a comprehensive global early warning system for all natural hazards. United Nations Inter-Agency Secretariat of the International Strategy for Disaster Reduction (UN/ISDR)) Final Version

CAPÍTULO II

Performance Evaluation of the Earthquake Detection and Classification Algorithm $2(t_S - t_P)$ of the Seismic Alert System of Mexico (SASMEX)

[**Cuéllar, A.,** Suárez R. and Espinosa-Aranda J. M.(2017). Performance Evaluation of the Earthquake Detection and Classification Algorithm $2(t_S - t_P)$ of the Seismic Alert System of Mexico (SASMEX). *Bulletin of the Seismological Society of America*, Vol. 107, No. 3, pp. 1451–1463, June 2017, doi: 10.1785/0120150330]

Bulletin of the Seismological Society of America, Vol. 107, No. 3, pp. 1451–1463, June 2017, doi: 10.1785/0120150330

Ⓔ

Performance Evaluation of the Earthquake Detection and Classification Algorithm $2(t_S–t_P)$ of the Seismic Alert System of Mexico (SASMEX)

by Armando Cuéllar,* Gerardo Suárez, and J. M. Espinosa-Aranda

Abstract A performance evaluation of the detection and classification algorithm for earthquake early warning $2(t_S–t_P)$ was conducted to test its reliability and robustness. The Seismic Alert System of Mexico (SASMEX) has used this algorithm since 1991. The algorithm estimates the rate of seismic energy released during two times the $(t_S–t_P)$ period. Based on the energy released, it estimates an empirical magnitude range related to m_b. Depending on the estimated m_b, either preventive or public alerts are issued. In this article, *post facto* tests are presented for 61 earthquakes for which SASMEX issued an alert. The algorithm was also tested on 31 earthquakes ($M_w > 6.0$) that occurred in the Mexican subduction zone from 1985 to 2014. These earthquakes occurred outside the coverage of the SASMEX instruments at the time. This dataset includes the 19 September 1985 M_w 8.1 Michoacán earthquake and the 9 October 1995 M_w 8.0 Colima event. The algorithm was tested also on two great earthquakes: the 22 February 2010 M_w 8.8 Maule, Chile, earthquake and the 11 March 2011 M_w 9.0 Tohoku, Japan, event. The results of the evaluation of 144 acceleration records of the 61 earthquakes detected from the SASMEX network indicate that 92% of the accelerograms of earthquakes with $m_b > 6.0$ have errors in the prediction of magnitude of less than ± 0.5, and 83% for $m_b > 5.5$. Also, the tests conducted on the 59 acceleration records of 31 earthquakes with $M_w \geq 6.0$ indicate that in all cases, with the exception of one strong-motion record, the events are classified as $M_w \geq 6.0$. Thus, the algorithm shows a high level of reliability and robustness. Although the algorithm underestimates the magnitudes of large earthquakes, these events are identified and classified as $M_w \geq 6.0$. Thus, an alert would be issued for these great earthquakes.

Electronic Supplement: Table of earthquake parameters, performance of Seismic Alert System of Mexico (SASMEX), and specific performance evaluation of the $2(t_S–t_P)$ algorithm.

Introduction

Considering the damage suffered by Mexico City after the 19 September 1985 earthquake (e.g., Rosenblueth, 1986; Esteva, 1988), the scientific community proposed in 1986 the creation of a Seismic Alert System for Mexico City (SASMEX; CONACYT-NRC, 1986). The goal was to alert the city of earthquakes originating in the subduction zone along the Pacific coast of Mexico. The possibility of a future great earthquake in the Mexican subduction zone raised local and federal authorities awareness of the need to develop an early warning system. As a result, the Centro de Instrumentación y Registro Sísmico, A.C. (CIRES, Center for Instrumentation and Seismic Recording) initiated the development of the SASMEX in 1989. The objective is to warn the population of the capital city of Mexico about the occurrence of important earthquakes detected by a network of free-field acceleration stations distributed along the coast (Fig. 1).

Mexico City is an ideal location to implement a seismic alert system. The soft clays on which the city is built cause large ground-motion amplifications, as was the case during the 1985 earthquake. This amplification can lead to strong ground motion, even for distant earthquakes for which warning times can be long. SASMEX was conceived to identify future large-magnitude earthquakes along the subduction zone and automatically alert the population of Mexico City prior to the arrival of the incoming seismic waves. The

*Also at Centro de Instrumentación y Registro Sísmico, Anaxágoras 814 Colonia Narvarte, México CDMX 03020.

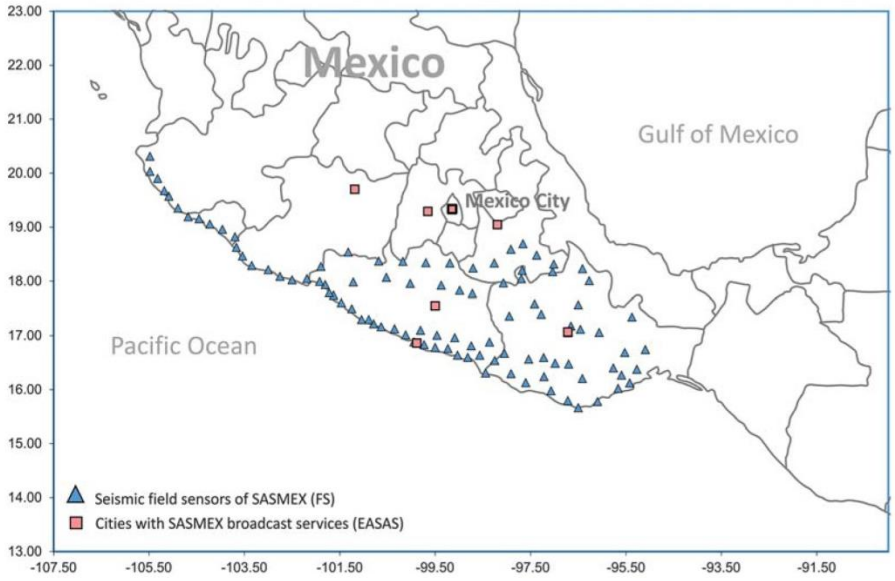

Figure 1. Current distribution of Seismic Alert System of Mexico (SASMEX) strong-motion stations (triangles) and alternate emitters of seismic warnings designed to disseminate the alert in various Mexican cities (squares).

system takes advantage of the slower travel time of seismic waves relative to the rapid transmission of data via radio.

In Mexico City, the warning time allowing the population and authorities to react to the possibility of strong shaking due to earthquakes in the subduction zone, may be as large as 60–90 s. The most recent earthquake with magnitude $M_w > 7.0$ in the subduction zone, immediately to the south of Mexico City, took place in 1911. Therefore, it is generally assumed that an important accumulation of stress probably exists in this segment of the coast of Guerrero, called the Guerrero gap (McCann *et al.*, 1979; Singh *et al.*, 1981). This was the reason why the location of the original seismic coverage of the system was on the Guerrero gap.

This article presents a systematic evaluation of the primary detection and classification algorithm used by SASMEX, called the $2(t_S–t_P)$ algorithm. This algorithm calculates the rate of energy released during twice the elapsed time between the arrival of the *P* and *S* waves. Based on the growth rate of the seismic energy, the algorithm classifies events into three magnitude bins ($m_b < 5.5$, $5.5 \le m_b < 6.0$, and $m_b \ge 6.0$) and makes the decision whether to issue an alert. The algorithm was developed originally using a training set of earthquakes recorded by the strong-motion records of the Guerrero network (Anderson and Quaas, 1988). Although it has been modified slightly over time, the $2(t_S–t_P)$ algorithm remains the basis on which seismic alerts have been issued by SASMEX since 1991.

In this study, we evaluate the $2(t_S–t_P)$ algorithm as it is used today and test it retroactively on the strong-motion database of accelerograms recorded by SASMEX since its inception in 1991. Also, we evaluated its performance for all earthquakes with $M_w \ge 6.0$ that have occurred along the Mexican subduction zone since 1985. These earthquakes lie outside the original coverage of SASMEX. To this end, we use accelerograms recorded by various agencies. Among these events is the 19 September 1985 earthquake, which caused great damage in Mexico City and prompted the effort to develop an early warning system.

In addition, a study was made of the performance of the $2(t_S–t_P)$ algorithm on two great earthquakes: the 2011 M_w 9.0 Tohoku, Japan, and the 2010 M_w 8.8 Maule, Chile, earthquakes. This was done to evaluate the earthquake classification criteria of the $2(t_S–t_P)$ algorithm in the case of a future great magnitude earthquake. Although the epicentral distances of the Tohoku and Maule earthquakes to the closest strong-motion stations are very large and outside of the design parameters of the $2(t_S–t_P)$ algorithm, we use these two earthquakes as extreme tests to verify the robustness and performance of the algorithm in the case of great magnitude earthquakes. The same evaluation criteria are used for the three datasets.

It is important to emphasize that the $2(t_S–t_P)$ algorithm presented here does not estimate a hypocentral location or the source characteristics of the earthquake. It detects the earthquakes in real time and classifies them into three magnitude bins. For this, it requires only two nearby stations confirming the seismic energy growth to issue an alert. Many of the existing seismic early warning systems attempt a more detailed characterization of ongoing earthquakes and require longer times and a larger number of stations to issue a warning. The algorithm Earthquake Alarm Systems (ElarmS), for example, uses at least four stations to confirm an alert (Allen *et al.*, 2009).

The most important conclusion derived from this analysis is that the $2(t_S–t_P)$ algorithm used by SASMEX would

have been able to identify all earthquakes with magnitudes $M_w \geq 6.0$ in the subduction zone of Mexico based only on two strong-motion records near of the epicenter; with only one exception, it would have relayed a warning signal to the population of Mexico City. Similarly, in the case of extreme earthquakes, such as the Chile and Tohoku events ($M_w > 8.5$), the algorithm would have issued a seismic alert, even though the available strong-motion records for these earthquakes are far from the epicenter.

Description of SASMEX

During 2011 and 2012, SASMEX expanded its limited coverage, from the 12 original stations commissioned in 1991 along the southern coast of the state of Guerrero to a network of 97 stations distributed along the Mexican Pacific coast, from the state of Jalisco to the state of Oaxaca (Fig. 1). Also, stations were distributed along 18° N to monitor the seismic activity within the subducted Cocos plate (Fig. 1; Cuéllar *et al.*, 2014). In 2012, SASMEX integrated the Seismic Alert System of the state of Oaxaca that started operating in 2003 (Espinosa-Aranda *et al.*, 2009). Both systems currently constitute the SASMEX (Cuéllar *et al.*, 2014).

In 1991, CIRES was instructed by the authorities to broadcast a preventive alert to owners of dedicated receivers of the system in case of an earthquake with body-wave magnitude $5.0 < m_b < 6.0$. In the case of earthquakes with $m_b \geq 6.0$, SASMEX was instructed to relay a public alert that, in addition to being received by the dedicated receivers, would be broadcast via the radio and television stations that volunteered to disseminate the seismic alert to the public since 1993 (Espinosa-Aranda *et al.*, 1995). Since 2015, the government of Mexico City broadcasts the public alerts through a network of thousands of loudspeakers distributed throughout the city. Today, the alerting policy for the $2(t_S–t_P)$ algorithm is as follows: no alert for earthquakes with $m_b < 5.5$; relay a preventive alert if $5.5 \leq m_b < 6.0$; and issue a public alert when $m_b \geq 6.0$.

The seismic field sensor (FS) stations consist of three-component accelerographs. The broadcast of an alert requires the confirmation of at least two nearby FS stations. In addition to classifying the earthquakes based on the seismic energy released into magnitude ranges or bins, the process of broadcasting the alert takes into account the distance that exists between the first two FS stations detecting the earthquake and the city to be alerted. Today, in addition to Mexico City, the cities of Acapulco, Chilpancingo, Oaxaca, Morelia, Puebla, and Toluca broadcast seismic alerts (Fig. 1).

The Algorithm $2(t_S–t_P)$

Background

The detection and classification algorithm for large earthquakes with which SASMEX has operated since 1991 is known as the $2(t_S–t_P)$ algorithm. It is structured into four modules:

1. *P*- and *S*-phase arrival identification, which in turn determines the $2(t_S–t_P)$ time;
2. estimation of parameters reflecting the seismic energy released in the period $2(t_S–t_P)$;
3. classification of the event into magnitude ranges based on the estimated seismic energy released; and
4. decision-making processes whether or not to issue an alert, be it preventive or public.

P- and *S*-Phase Arrival Identification

The FS stations identify the arrival of the *P* and *S* waves based on two independent approaches: average square input (ASI) and vertical to horizontal (V/H). ASI is based on the sum of quadratic averages of the amplitude of the acceleration records (Espinosa-Aranda, *et al.*, 1995). V/H was used by the Japanese railway earthquake alert system, Urgent Earthquake Detection and Alarm System (Nakamura, 1996). Both methods are described below.

The ASI Method

The original ASI employed by SASMEX (Espinosa-Aranda *et al.*, 1992) processed the sum of the quadratic amplitude of the three strong-motion components of an accelerometer (longitudinal X_l, transverse X_t, and vertical X_v) at a sampling rate of 50 Hz and with a resolution of 10 bits in an average time window of 32 samples. Subsequently, because of increase of the resolution in the FS stations to 12 bits and of the sampling rate to 100 Hz, the average time window was reduced to 16 samples and separately calculates the quadratic amplitude on the horizontal and vertical components (equations 1 and 2). Thus, the average seismic energy growth, expressed as the squared sum of the amplitude of the seismic waves, is estimated as a function of time:

$$\mathrm{ASIH}_{16}(i) = \frac{1}{16}\sum_{i-15}^{i}[X_l^2(i) + X_t^2(i)] \tag{1}$$

$$\mathrm{ASIV}_{16}(i) = \frac{1}{16}\sum_{i-15}^{i} X_v^2(i), \tag{2}$$

in which i is the current sample and X_l, X_t, and X_v are the acceleration amplitudes of the three orthogonal channels: longitudinal, transverse, and vertical.

The V/H Method

The V/H method, defined by equations (3) and (4) (Nakamura, 1996) is used in parallel to confirm the arrival of the *P* and *S* waves:

$$\mathrm{V}(i) = \mathrm{V}(i-1) + X_v^2(i) \tag{3}$$

$$\mathrm{H}(i) = \mathrm{H}(i-1) + X_l^2(i) + X_t^2(i). \tag{4}$$

When the ratio V/H > 1, the *P* wave is predominant, whereas in the case of V/H < 1, the predominant presence of the *S* wave is inferred (Nakamura, 1996). Identification of the *P*- and *S*-phase arrivals is not always stable because of the characteristics of each particular earthquake and the effect of local seismic noise at the site. Therefore, we follow Nakamura (1996) in weighting the vertical and horizontal amplitudes with coefficients α_1, α_2, α_3, β_1, β_2, and β_3. These weighting coefficients range in value from 0 to 1 and are determined empirically for each sensing station based on recorded accelerograms (Nakamura, 1996). The V/H quotients are then estimated as follows:

$$\frac{\alpha_1 \mathrm{V}}{\beta_1 \mathrm{H}} \text{ is calculated from } t_P + 0.5 \text{ s};$$

$$\frac{\alpha_2 \mathrm{V}}{\beta_2 \mathrm{H}} \text{ is calculated from } t_P + 0.5 \text{ to } t_P + 1.0 \text{ s};$$

and

$$\frac{\alpha_3 \mathrm{V}}{\beta_3 \mathrm{H}} \text{ is calculated from } t_P + 1.0 \text{ to } t_P + 24.0 \text{ s}.$$

Then, the arrival of the *P* and *S* waves is defined when all of the following criteria are met:

$$\begin{cases} P: \mathrm{ASIV}_{16} > u_{P1}; V > u_{P2}; \frac{\alpha_1 \mathrm{V}}{\beta_1 \mathrm{H}} > 1; \frac{\alpha_2 \mathrm{V}}{\beta_2 \mathrm{H}} > u_{P3}; T_P > 1 \text{ s} \\ S: \mathrm{ASIV}_{16} > u_{S1}; \frac{\alpha_3 \mathrm{V}}{\beta_3 \mathrm{H}} > u_{S2}; T_S < 24 \text{ s} \end{cases}, \tag{5}$$

in which u_{Pi} and u_{Sk} are the thresholds of the seismic signals estimated dynamically in the following manner:

$$u_{P1} = \frac{1}{100} \sum_{t_P-99}^{t_P} X_v^2(i);$$

$$u_{P2} = \max[\mathrm{V}(i)]_{i=t_P-16}^{t_P};$$

$$u_{P3} = \frac{1}{25} \sum_{i=t_P+50}^{t_P+75} \frac{\mathrm{V}(i)}{\mathrm{H}(i)};$$

$$u_{S1} = 2 \max[\mathrm{ASIH}_{16}(i)]_{i=t_P}^{t_P+200};$$

$$u_{S2} = \min\left[\frac{\mathrm{V}(i)}{\mathrm{H}(i)}\right]_{i=t_P+50}^{t_P+150}.$$

The detection process of the *P* wave starts in the instant t_p, and the identification is based on the following criteria: (1) when ASIV_{16} exceeds the average threshold u_{P1}, dynamically calculated every minute, and reflecting the noise level at the site; (2) when the value of V exceeds the threshold u_{P2} and the parameter $\frac{\alpha_1 \mathrm{V}}{\beta_1 \mathrm{H}}$, proportional to the growth rate of the signal, is larger than 1; and (3) $\frac{\alpha_2 \mathrm{V}}{\beta_2 \mathrm{H}}$ exceeds a threshold u_{P3}. These conditions are expected to occur within an observation window T_p of maximum duration of 1 s.

The detection of the *S* wave is declared when the following conditions are met: (1) ASIV_{16} should exceed the threshold u_{S1}, calculated dynamically, in terms of the maximum peak values generated by the *P* waves. The value u_{S1} is updated every time a new maximum peak value of ASIH_{16} is observed; (2) when $\frac{\alpha_3 \mathrm{V}}{\beta_3 \mathrm{H}} < u_{S2}$. The value of u_{S2} is calculated dynamically based on the minimum V/H after the *P*-wave detection. The algorithm has a maximum observation time of $T_S < 24$ s after the detection of the *P* wave to identify the *S* wave.

Functions ASIV_{16} and ASIH_{16} are shown graphically in Figure 2 and demonstrate the *S* wave identified at the Cacalutla station during the 13 April 2007 M_w 6.0 Atoyac, Guerrero, earthquake (Fig. 2). The epicentral distance of this station is ~40 km from the epicenter.

Evaluation of the *P* and *S* Automatic Arrival-Time Determinations

The sensing stations of SASMEX have no absolute time signals, because they are designed specifically for the purpose of a seismic alert. Furthermore, the other agencies running strong-motion stations in Mexico do not pick *P* and *S* phases on the accelerograms on a routine basis. Thus, to demonstrate the performance of the phase-picking algorithms described above, we present the strong-motion records of selected events and the times in which the arrival of the *P* and *S* phases were automatically selected (Fig. 3).

A more complete set of strong-motion records and the time of the automatic *P*- and *S*-phase picks on several accelerograms used in this analysis are shown also in Ⓔ Figures S1 and S2, available in the electronic supplement to this article. These figures demonstrate that the phase-picking algorithms are robust and effective in identifying the arrival times of the *P* and *S* phases.

Magnitude Estimation

Calculation of Parameters *a* and *m* to Estimate the Magnitude

At time *i*, when the *P* wave is detected, the process initiates the calculation of the two parameters used to estimate the magnitude range of the earthquake. For this purpose, the algorithm uses the sum of ASIV_{16} and ASIH_{16}, which is the cumulative average squared acceleration over the $2(t_S - t_P)$ time window. This function is related to the seismic energy released and is defined as *a* in equation (6).

The second parameter is the derivative *m*, estimated from the beginning of detection of the *P* wave to time $2(t_S - t_P)$ (equation 7) and measured at instant $i = 2(t_S - t_P)$.

$$a = \log_{10}\left[\sum_{i=t_P}^{2(t_S-t_P)} \mathrm{ASIV}_{16}(i) + \mathrm{ASIH}_{16}(i)\right] \tag{6}$$

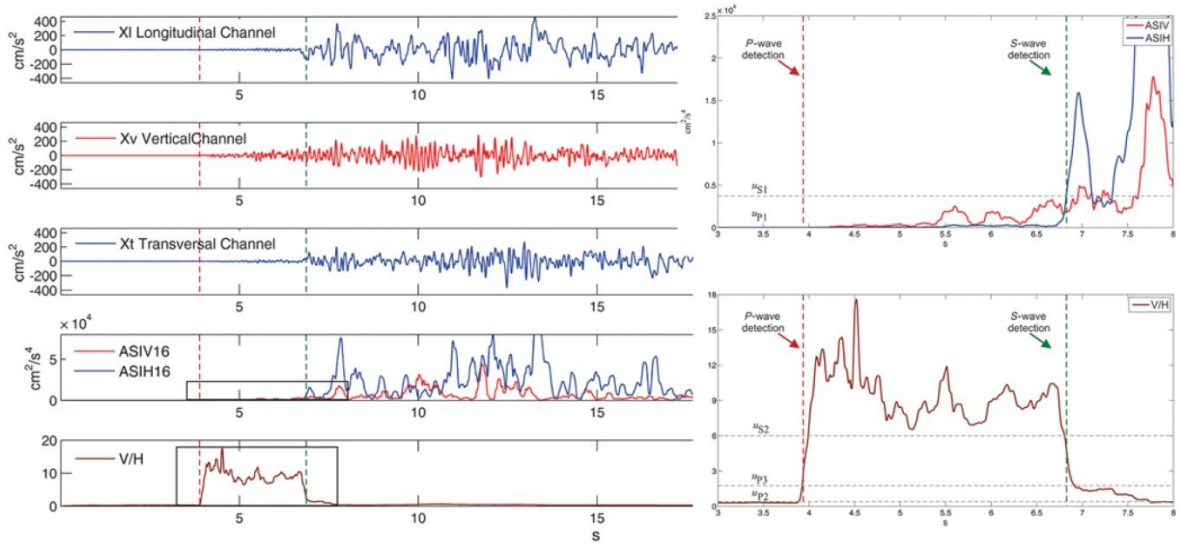

Figure 2. Example of *P*- and *S*-wave detection based on the $2(t_S–t_P)$ algorithm. The first three traces show accelerograms from station Cacalutla for the 13 April 2007 M_w 6.0 Atoyac, Guerrero, Mexico, earthquake. The two lower traces show the characteristic functions used for detecting *P* and *S* waves, which are amplified in the box.

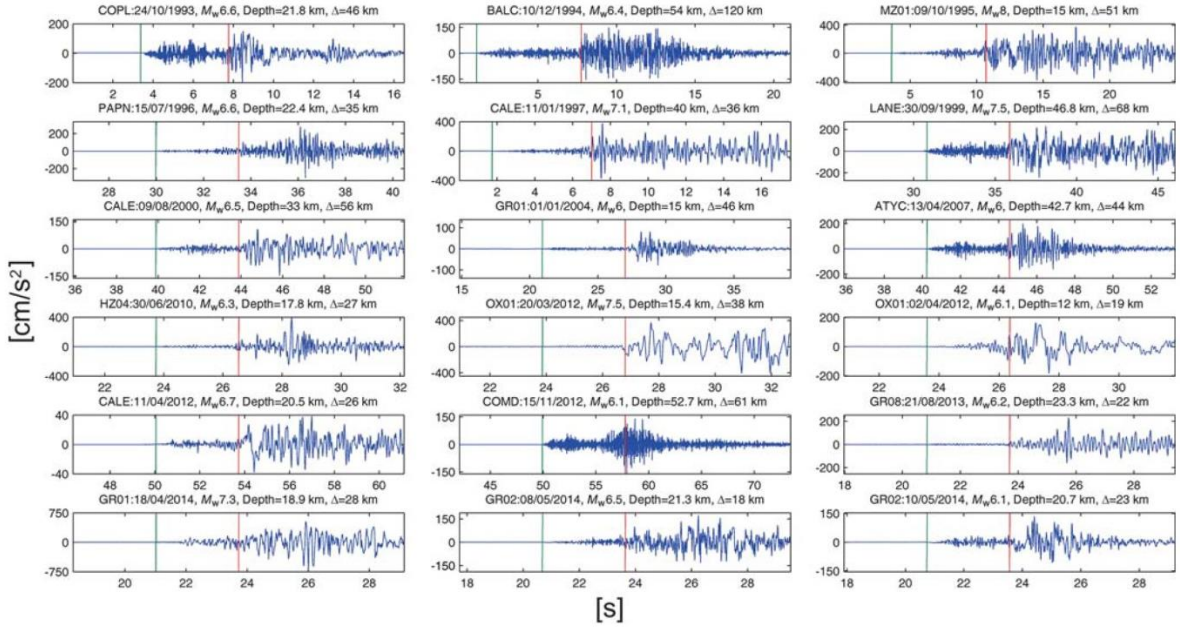

Figure 3. Strong-motion records of selected earthquakes analyzed in this study. The green and red tick marks show the arrival time of the *P* and *S* waves identified by the $2(t_S–t_P)$ algorithm.

$$m = \log_{10}[\mathrm{ASIV}_{16}(2(t_S–t_P)) + \mathrm{ASIH}_{16}(2(t_S–t_P))]. \quad (7)$$

As an example, the energy release parameter a is shown for the 13 April 2007 M_w 6.0 Atoyac earthquake (Fig. 4). The black arrow indicates the time when a and m were obtained.

Criterion for Alert Activation

The activation of the public or preventive alerts requires estimates of magnitude $m_{2(t_S–t_P)}$ in at least two seismic sensing stations close to the epicenter. This criterion prevents false alarms induced by failures in the electronic components

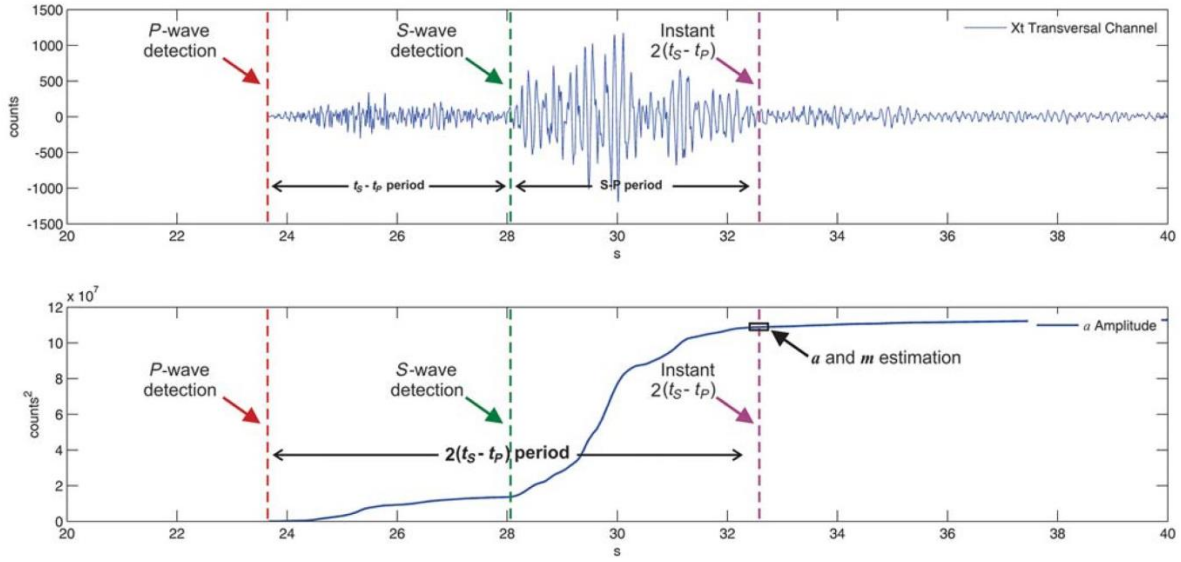

Figure 4. The upper trace shows an accelerogram of the 13 April 2007 M_w 6.0 earthquake. The box below shows the resulting function of the estimated quadratic amplitude a and instant rate of growth m calculated in the time period $2(t_S–t_P)$. The black arrow shows the time $2(t_S–t_P)$ when the parameters are calculated.

or by spurious seismic noise in one of the stations. In addition, it allows simultaneous monitoring of earthquakes in different regions, improving the coherence by geographically delimiting the observation of earthquakes. The algorithm has the additional advantage of requiring only two stations to detect and classify earthquakes. Most other systems make use of a higher number of stations to avoid false alerts.

A shortcoming of this confirmation criterion by more than one sensing station is the need to invest additional time for the activation of the alert. However, considering that today the average spatial separation of SASMEX strong-motion stations in the subduction zone is about 25 km, the time necessary to receive the confirmation of a second station is generally less than 2 or 3 s. During its operational history, SASMEX had only one false alert. It occurred on 16 November 1993, during its early stages of development, when only one FS station was required to activate the alert (Espinosa-Aranda *et al.*, 1995).

The $2(t_S–t_P)$ algorithm assumes that the energy released is empirically associated with the magnitude m_b. The original alerting rules established by the authorities of Mexico City for the design of the system were: not alerting earthquakes with $m_b < 5.0$, relaying a preventive alert if $5.0 \le m_b < 6.0$, and activating a public alert when $m_b \ge 6.0$. The authorities set up this criteria after considering that the earthquakes of $m_b \ge 6.0$ in the Guerrero gap might cause damage and generally would be felt by everyone in Mexico City. On the other hand, earthquakes in the subduction zone of magnitude $5.0 \le m_b < 5.5$ are usually felt only by people in the zones underlain by the soft soils. The motives behind issuing preventive alerts for this magnitude range were to promote the practice of seismic drills in schools. Today, the alerting policy for the $2(t_S–t_P)$ algorithm is as follows: no alert for earthquakes with $m_b < 5.5$; relay a preventive alert if $5.5 \le m_b < 6.0$; and issue a public alert when $m_b \ge 6.0$.

The numerical model to estimate the magnitude is expressed as contours of the parameters a and m as a function of m_b. The contours used by SASMEX and tested in this article were calibrated (Espinosa-Aranda *et al.*, 1992) based on accelerograms of 12 earthquakes that occurred between 1985 and 1989 and recorded by strong-motion stations of the Accelerograph Network of the State of Guerrero (Anderson and Quaas, 1988). Magnitude m_b was used due to the scarce number of earthquakes registered by accelerographs that were operating during the early days of the warning system. Furthermore, m_b was the magnitude normally reported at the time for earthquakes with moderate magnitude by the various agencies responsible (Espinosa-Aranda *et al.*, 1992).

Although the algorithm has been improved, the equations derived from the classification functions to determine the range of magnitude remained unchanged. Equations (8)–(10) define the magnitude range $m_{2(t_S-t_P)}$ as a function of parameters a and m (Fig. 5). As mentioned before, $m_{2(t_S-t_P)}$ is proportional to magnitude m_b.

When the logic function is validated as TRUE by more than one equation, the largest magnitude value is assigned:

$$\text{if } a + m - 7 \ge 0; \text{ is TRUE then } m_{2(t_S-t_P)} \ge 5.0; \quad \text{else } m_{2(t_S-t_P)} < 5.0; \tag{8}$$

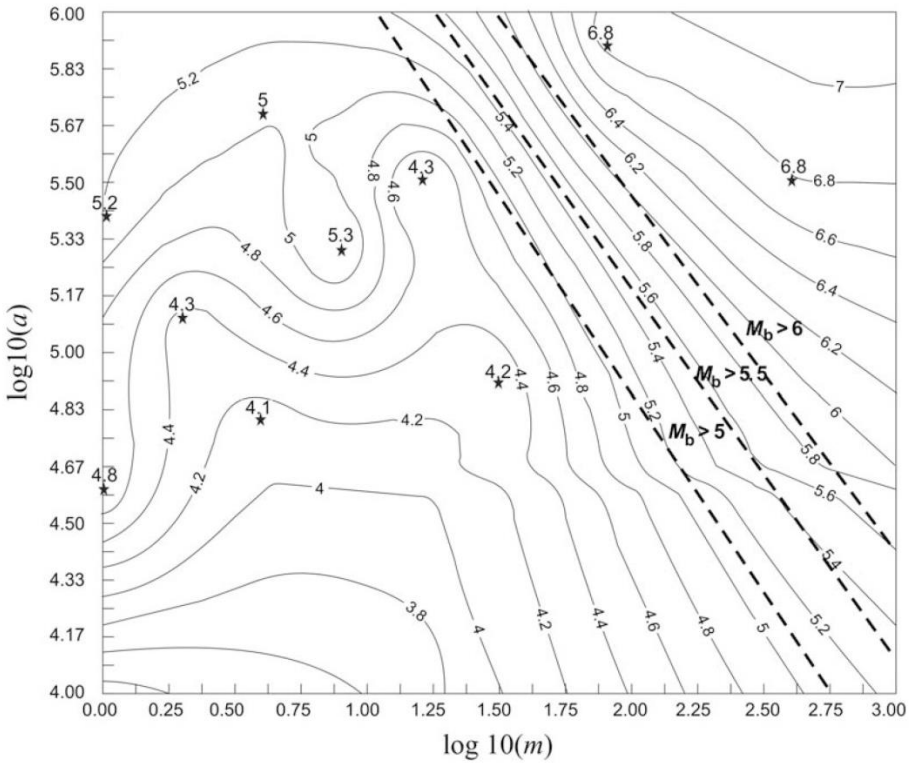

Figure 5. Magnitude m_b contours based on the parameters a and m. The calibration curves were estimated based on the data from 12 earthquakes occurring from 1985 to 1989, for which the epicenter lies at a distance of less than 80 km from the closest seismic sensors of the Guerrero strong-motion network (Anderson and Quaas, 1988).

$$\text{if } a + 0.98m - 7.18 \geq 0; \text{ is TRUE}$$
$$\text{then } m_{2(t_S-t_P)} \geq 5.5; \quad (9)$$

$$\text{if } a + m - 7.6 \geq 0; \text{ is TRUE}$$
$$\text{then } m_{2(t_S-t_P)} \geq 6.0. \quad (10)$$

Evaluation of the Performance of Algorithm $2(t_S–t_P)$

After almost 25 years of operation of SASMEX, it is important to conduct a systematic evaluation of its performance and, in particular, of the $2(t_S–t_P)$ algorithm used for detection and classification of earthquakes. To conduct a fair and objective test, the $2(t_S–t_P)$ algorithm was evaluated based on the same criteria, using the following datasets:

1. All earthquakes recorded by SASMEX strong-motion instruments during its history of operation (Ⓔ Tables S1 and S2).
2. All earthquakes of $M_w \geq 6.0$ which took place in the subduction zone but which were not recorded by the original SASMEX stations. In these cases, the tests were based on accelerograms of other strong-motion networks (Ⓔ Table S3). It should be emphasized that all earthquakes fulfilling these criteria were included without exceptions. This dataset includes the only subduction earthquakes of $M_w > 8.0$ recorded in Mexico by strong-motion instruments: the 9 October 1995 earthquake and the 19 September 1985 great Michoacán earthquake.
3. Also, we tested the robustness of the algorithm for great magnitude earthquakes using records of the 2010 M_w 8.8 Maule, Chile, earthquake and the 2011 M_w 9.0 Tohoku, Japan, earthquake.

Evaluation of the Magnitude Estimates Reported by SASMEX

Iglesias *et al.* (2007) and Suárez *et al.* (2009) argued that SASMEX magnitudes are not always accurate. Although magnitude determination is not the mission of SASMEX, it is important to reevaluate the capability of the algorithm $2(t_S–t_P)$ to classify and discriminate earthquakes in the magnitude bins established.

An analysis is presented of the alerts issued from 1991 to 2014. During that period, the algorithm discriminated over 5400 earthquakes and 8560 acceleration records. The following criteria were considered to develop a consistent database:

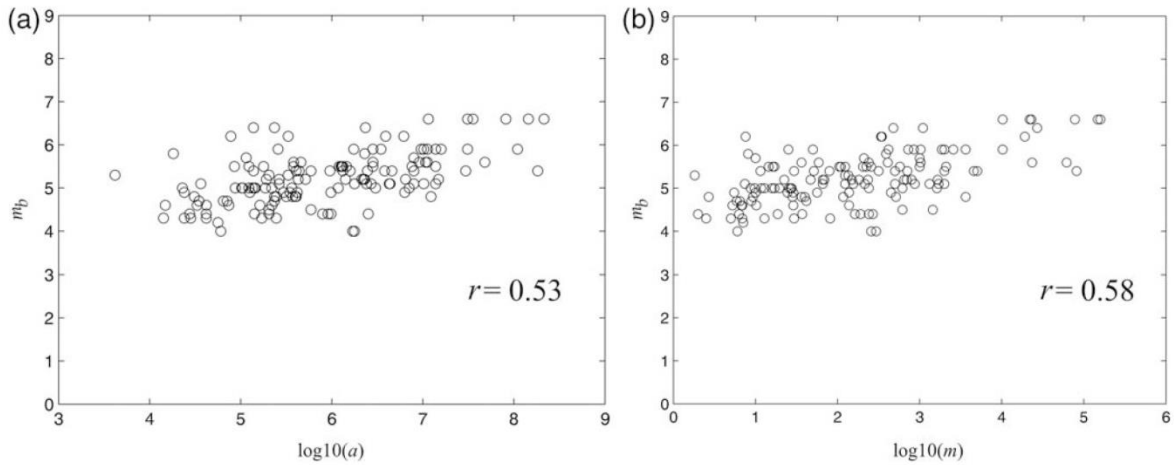

Figure 6. Correlation in a logarithmic scale between parameters based on 144 recordings: (a) m_b versus a and (b) m_b versus m.

1. All earthquakes in the subduction zone are selected that generated either public or preventive alerts in Mexico City and for which an m_b value is available from published seismic catalogs.
2. The accelerograms recorded by two of the early SASMEX stations (GR08 and GR12) are not used in the detection and classification algorithm because they suffer very large amplification effects due to local site conditions.

A total of 61 earthquakes met these criteria and were recorded in 144 strong-motion records (Ⓔ Table S2).

To estimate the correlation of the parameters a and m used as alerting criteria as a function of the observed magnitude m_b, the correlation criterion of Pearson was applied (Pearson, 1896). The correlation between parameters a and m observed in the 144 acceleration records used in the analysis (Ⓔ Table S2) shows a coefficient of $r = 0.53$, whereas the correlation of parameters m and m_b is equal to $r = 0.58$ (Fig. 6). These results show an acceptable degree of correlation between the parameters employed by the $2(t_S–t_P)$ algorithm and magnitude m_b. It should be noted that the correlation between parameters a and m is $r = 0.88$. The significant linear relationship between these two variables indicates that they are potentially redundant.

For the 61 earthquakes analyzed, a comparison is made between the magnitude m_b reported by the Servicio Sismológico Nacional (SSN) and other international agencies and the estimated magnitude range $m_{2(t_S-t_P)}$ (Ⓔ Table S2). Our results show that for the acceleration records of earthquakes with $m_b < 5.0$, 65% of the magnitudes predicted by the algorithm fall within ± 0.5 units of the reported catalog magnitude. When the same evaluation is done for acceleration records of earthquakes with $m_b \geq 6.0$ and $m_b \geq 5.5$, the success rate increases to 92% and 83%.

The earthquake early warning system in Japan tolerates errors of ± 1.0 in magnitude estimation (Hoshiba *et al.*, 2008). Assuming this same magnitude tolerance, the algorithm $2(t_S–t_P)$ has a success rate of 92% and 87% for $m_b \geq 6.0$ and $m_b > 5.5$, respectively. Thus, for the magnitude ranges used in the decision-making process of whether to issue public or preventive alerts, the $2(t_S–t_P)$ algorithm demonstrates that it is a robust and reliable tool to rapidly classify earthquakes into magnitude ranges and to issue alerts with a high degree of confidence.

Evaluation of Mexican Subduction Earthquakes with $M_w \geq 6.0$ since 1985

In the first 24 years of operation, the coverage of SASMEX was limited to 12 strong-motion sensors located to the southeast of Acapulco (Espinosa-Aranda *et al.*, 1995). Many subduction earthquakes of $M_w \geq 6.0$ took place outside the zone originally covered by SASMEX. To test the performance of the algorithm on these earthquakes, we obtained and processed the acceleration records of these earthquakes recorded by other strong-motion networks.

According to the centroid moment tensor catalog (Dziewonski *et al.*, 1981, 1999; Ekström *et al.*, 2012), 41 earthquakes ($M_w \geq 6.0$) took place from 1985 to 2014 along the Mexican subduction zone. Out of these 41 earthquakes, 31 of them were recorded on 59 acceleration records (Fig. 7 and Ⓔ Table S3). The earthquakes to be evaluated were chosen based on the following criteria:

1. earthquakes of $M_w \geq 6.0$ occurring since September 1985 along the Mexican subduction zone;
2. earthquakes for which the distance between the epicenter and Mexico City is less than 600 km; and
3. earthquakes for which two seismic stations are located close to the epicenter, within a maximum distance of 120 km and for which the acceleration recordings show both the P and S waves.

The two stations closest to the epicenter were selected whenever $t_S–t_P$ times were available. Most of the records are from

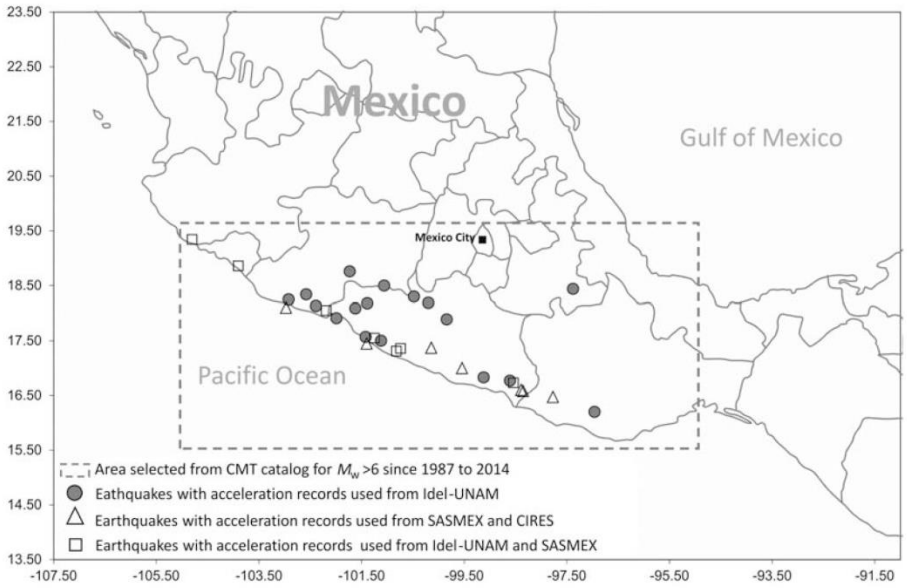

Figure 7. Location of the earthquakes with $M_w \geq 6.0$ used in the analysis, which have occurred in southern Mexico since 1985.

the strong-motion networks operated by the Instituto de Ingeniería, Universidad Nacional Autónoma de México (Pérez-Yáñez *et al.*, 2014) and by the SASMEX network managed by CIRES. The majority of these earthquakes are located at distances of less than 50 km from the closest strong-motion station (Ⓔ Table S3). Among these earthquakes, there are seven earthquakes of $M_w \geq 7.0$, all strongly felt in Mexico City. The summarized results obtained with algorithm $2(t_S–t_P)$ are shown in Figure 8.

For both the great 19 September 1985 M_w 8.1 Michoacán earthquake and the 9 October 1995 M_w 8.0 Colima earthquake, the algorithm $2(t_S–t_P)$ determined a magnitude range of $m_{2(t_S–t_P)} > 6.0$, even though the strong-motion stations were few and located far from the epicenter. Although the magnitude of these two large events based only on the existing accelerograms is severely underestimated, the $2(t_S–t_P)$ algorithm would have triggered a public alert, had it been operating at the time. Even under these unfavorable conditions, the warning time in Mexico City for these two earthquakes would have been 90–110 s.

In the case of the 19 September 1985 event, acceleration records exist for stations CALE and ZACA. These stations are located at a distance of 40 and 57 km, respectively. CALE was the only station for which both *P* and *S* waves were recorded. In ZACA, the station triggered after the arrival of the *P* wave. The low accelerations observed in CALE were attributed to the fact that the nucleation of the 1985 earthquake was located beneath station CALE (Mendez and Anderson, 1991); the value of parameter *a* for the 1985 event is smaller than that observed for 21 September (M_w 7.6) (Fig. 8). Similarly, a slow growth in seismic energy was observed in stations located close to the hypocenter of other large earthquakes such as the 20 March 2012 (M_w 7.4) event recorded by station OX01 at a distance of 42 km from the epicenter (Fig. 8).

The results of the evaluation of the $2(t_S–t_P)$ algorithm performed on earthquakes of $M_w \geq 6.0$ (Ⓔ Table S3) show that the magnitudes were classified consistently by the algorithm as $m_{2(t_S–t_P)} \geq 6.0$. The only exception is the earthquake of 9 August 2000 (M_w 6.5) in the state of Michoacán, where the algorithm $2(t_S–t_P)$ estimated a magnitude $m_{2(t_S–t_P)} \geq 5.5$ in one of the two acceleration records used (Fig. 8). This result is probably due to the fact that the second closest station to the epicenter (UNIO station) is located 90 km from the epicenter.

The results obtained demonstrate that the algorithm is robust and correctly identifies and classifies large-magnitude earthquakes. Our results show also that more accurate magnitudes are obtained for earthquakes with $M_w \geq 6.0$, when there are stations located close to the epicenter. The current average separation of SASMEX sensing stations along the subduction zone is ~25 km. This spacing gives confidence that future large-magnitude earthquakes will be properly identified and discriminated to issue a public alert.

Performance of the Magnitude Classification Algorithm for Earthquakes with $M_w \geq 6$

The tests described above confirm the robustness of the algorithm to identify large earthquakes ($M_w \geq 6$). However, it is important to test whether it is effective also in classifying small-magnitude earthquakes in the subduction zone. To this end, it is worth mentioning that from 1991 to 2014, the SASMEX network detected ~5400 earthquakes; the majority of

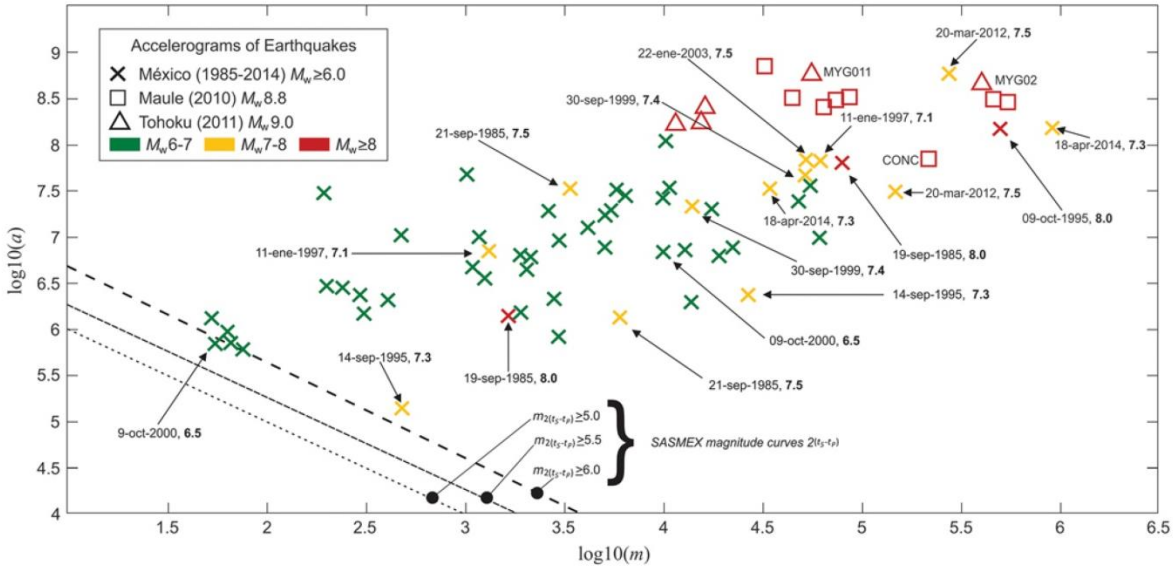

Figure 8. Magnitude estimated based on the $2(t_S–t_P)$ algorithm based on the accelerograms of earthquakes $M_w \geq 6.0$, which occurred in Mexico from 1985 to 2014, as well as for the 2010 M_w 8.8 Chile earthquake and the 2011 M_w 9.0 Tohoku event.

which are $M_w < 5$. Out of these 5400 earthquakes, SASMEX issued only 92 alerts based on the $2(t_S–t_P)$ algorithm (see Data and Resources). These results indicate that it correctly discriminates small earthquakes of $M_w < 5$ and does not emit an alert to the population.

As mentioned before, the coverage of the SASMEX system was considerably expanded and improved in 2013, and the alerting criteria were modified at the same time. The system now covers the whole Mexican subduction zone (Fig. 1). To further illustrate the ability of the $2(t_S–t_P)$ algorithm to discriminate the prescribed magnitude bins, the earthquakes recorded by SASMEX from 2013 to August 2016 are classified by year and magnitude range (Table 1). The magnitude values used are those reported by the SSN. The dataset covers 710 earthquakes recorded in the last four years. These data are detected based on the current distribution of SASMEX stations and the alerting criteria used today. This allows a fair and homogeneous comparison of the performance of the algorithm (Table 1).

To facilitate the analysis, a confusion matrix was constructed to compare the various alerts issued during this same period (Table 2). The elements along the diagonal of the matrix reflect earthquakes which were correctly classified. Out of the 710 events detected within this period, 701 were correctly screened out as earthquakes for which no alert was issued. Also, the five earthquakes with $M_w \geq 6$, which occurred during this period, were correctly identified as deserving public alerts. The elements off the diagonal of the matrix are those earthquakes incorrectly classified. In all cases, the events misclassified are in the magnitude bin $5.5 \leq M_w < 6.0$, in which preventive alerts should be issued. In the case of two events in this magnitude range, the algorithm incorrectly issued a public alert. In two other cases, no alert was issued when a preventive alert should have been emitted.

Table 1
Alerts Issued by the $2(t_S–t_P)$ Algorithm in the Mexican Subduction Zone by Alert Category and Magnitude

M_w	2013		2014		2015		2016	
≥6.0	Public	1	Public	3	Public		Public	1
	Preventive		Preventive		Preventive		Preventive	
	No alert		No alert		No alert		No alert	
$5.5 \leq M_w < 6.0$	Public		Public		Public	1	Public	1
	Preventive		Preventive		Preventive		Preventive	
	No alert		No alert	2	No alert		No alert	
<5.5	Public		Public		Public		Public	
	Preventive		Preventive		Preventive		Preventive	
	No alert	275	No alert	169	No alert	140	No alert	117

Table 2
Alerts Issued by the $2(t_S-t_P)$ Algorithm from January 2013 to August 2016

SASMEX Warning	$M_w < 5.5$	$5.5 \le M_w < 6.0$	$M_w \ge 6.0$
No alert	701	2	0
Preventive	0	0	0
Public	0	2	5

SASMEX, Seismic Alert System of Mexico.

These errors reflect the difficulties of the algorithm to correctly classify earthquakes within this very narrow magnitude range. In fact, a discussion is taking place as to whether preventive alerts should continue to be emitted based on this narrow magnitude range, or whether SASMEX should only issue public alerts for events $m_b < 5.5$, eliminating preventive alerts. Regardless, the results of the past four years show that the $2(t_S-t_P)$ algorithm is a reliable tool that correctly classifies earthquakes to issue alerts of large incoming earthquakes.

Evaluation of the 2010 M_w 8.8 Maule Earthquake

The 27 February 2010 M_w 8.8 Chile earthquake occurred in the Maule region in central Chile (e.g., Delouis *et al.*, 2010). With the idea of testing the $2(t_S-t_P)$ algorithm for great earthquakes, we obtained and processed eight acceleration records observed along the coast of Chile (Ⓔ Table S4; Boroschek *et al.*, 2012). The acceleration recording stations closest to the epicenter are in the cities of Concepción (CONC) and Constitución (CONT), at epicentral distances of 108 and 78 km, respectively (Ⓔ Fig. S3 and Ⓔ Table S4). *P* waves are not identifiable on most of these accelerograms. Furthermore, the distances between the epicenter and the closest stations fall outside the design parameters of the $2(t_S-t_P)$ algorithm.

Despite these unfavorable conditions, the algorithm classified the Maule earthquake as magnitude $m_{2(t_S-t_P)} \ge 6.0$, even at strong-motion stations located at distances of 270 km from the epicenter (Ⓔ Fig. S3 and Ⓔ Table S4). If SASMEX had been in operation at that time, even with this unfavorable station distribution, a public alert would have been issued for the Maule earthquake.

Evaluation of the 2011 M_w 9.0 Tohoku Earthquake

On 11 March 2011, the region of Tohoku, Japan, along the coast of Honshu suffered an earthquake of M_w 9.0 (e.g., Mori *et al.*, 2011). The fault was located up-dip of the subduction zone, close to the trench. Because of this, the distance between the strong-motion stations on land and the rupture zone is very large. Thus, this earthquake represents an extreme test for the robustness of the algorithm. Five acceleration records were obtained from the stations closest to the epicenter. These strong-motion stations are part of Japan's earthquake early warning system (Hoshiba *et al.*, 2011).

The closest accelerographs are located at distances of more than 100 km from the epicenter (Ⓔ Fig. S4 and Ⓔ Table S5). Consequently, the (t_S-t_P) time is ~20 s. Despite this disadvantageous situation, the magnitude was classified as $m_{2(t_S-t_P)} \ge 6.0$ at all stations (Ⓔ Table S5). Although the magnitude is again severely underestimated, the algorithm would have been able to discriminate the Tohoku event as a very large earthquake and would have issued a public alert. Evidently, because of the large distances between the epicentral area and the closest seismic sensing stations on land, the warning time for Tokyo and neighboring cities would have been only a few seconds.

Summary and Conclusions

Since the beginning of operations in 1991, SASMEX has used an algorithm which, based on the quadratic sum of the amplitude of the acceleration of the three orthogonal components in the period $2(t_S-t_P)$, discriminates and classifies the magnitude based on two parameters: the amplitude a and the instantaneous rate of growth of the energy m. Originally, these parameters are used to classify the earthquakes into magnitude ranges: $m_b < 5.0$, $5.0 \le m_b < 6.0$, and $m_b \ge 6.0$. No alert is issued in the first case and either a preventive or a public alert is issued for the two last instances, respectively. Today, the ranges for $2(t_S-t_P)$ algorithm are modified as $m_b < 5.5$, $5.5 \le m_b < 6.0$, and $m_b \ge 6.0$ considering the distance of 450 km or more of Mexico City.

The results presented here show that parameters a and m provide the basis for an adequate estimate of magnitude ranges for the alerting criteria used by SASMEX. Nevertheless, it should be mentioned that there is a high linear dependence between these parameters. This may be the reason for the less successful discrimination of earthquakes in a magnitude range $m_b < 6.0$. The performance analysis of magnitude estimation based on the $2(t_S-t_P)$ algorithm, accepting an error of ± 0.5, shows a success rate of 92% for magnitude range $m_b > 6.0$ and 83% for magnitude range $m_b > 5.5$ for the acceleration records analyzed. In the case of an error tolerance of ± 1.0 in magnitude, the estimation success rate reaches almost 92% and 87% for magnitude range $m_b > 6.0$ and $m_b > 5.5$, respectively.

A performance test was conducted based on 52 acceleration recordings corresponding to all earthquakes with $M_w \ge 6.0$ located along the Mexican subduction zone (Fig. 8 and Ⓔ Table S3). When executing the alerting algorithm $2(t_S-t_P)$ retroactively on these strong-motion records, all earthquakes, with a single exception in one acceleration record, were classified as being in the magnitude range of $m_{2(t_S-t_P)} \ge 6.0$. The only accelerogram not properly classified ($m_{2(t_S-t_P)} \ge 5.5$) has a very large epicentral distance to the closest strong-motion station. In the case of some large earthquakes, magnitudes are underestimated due to the greater magnitude range of the algorithm, precisely $m_{2(t_S-t_P)} \ge 6.0$.

Also, *post facto* performance tests were conducted using the $2(t_S-t_P)$ algorithm for the great Chile (M_w 8.8) and Tohoku (M_w 9.0) earthquakes. These performance tests represent extreme examples due to the very large distances between the strong-motion stations and the epicenters. Nonetheless, both earthquakes were classified in the magnitude range $m_{2(t_S-t_P)} > 6.0$ (Fig. 8; Ⓔ Tables S4 and S5). These results suggest that, even under quite unfavorable conditions, the method is robust enough to identify great earthquakes and issue a public alert. It should be stressed, however, that in these two scenarios, in which the earthquake occurs far from the seismic sensing stations, the algorithm $2(t_S-t_P)$ would not be suitable to issue a timely alert. We are currently working on faster algorithms for events in which t_S-t_P is large.

The most important conclusion of this performance evaluation is that for the station versus epicentral distances found in the Mexican subduction zone, the $2(t_S-t_P)$ algorithm is robust and reliable. There are two main reasons behind this: first, the short distance between the hypocenters of large subduction earthquakes and the seismic sensing stations installed along the coast results in t_S-t_P times that are usually less than 3–4 s. Second, the distance between the subduction zone and Mexico City allows ample warning time to issue an alert prior to the initiation of strong shaking. Finally, it is worth mentioning that the current station distribution of SASMEX records an average of 500 earthquakes per year in the subduction zone. Out of this large number of earthquakes, only a handful of seismic alerts are issued.

Data and Resources

Accelerograms from the Seismic Alert System of Mexico (SASMEX) stations were provided by the Centro de Instrumentación y Registro Sísmico (CIRES) with the authorization of the Instituto para la Seguridad en las Construcciones del Distrito Federal in Mexico City and the Coordinación Estatal de Protección Civil de Oaxaca in Oaxaca state. Strong-motion data for the Mexican subduction earthquakes are from the web page of the Instituto de Ingeniería of the Universidad Nacional Autónoma de México (UNAM) https://aplicaciones.iingen.unam.mx/AcelerogramasRSM/Default.aspx (last accessed December 2016). The National Accelerograph Network and the Seismological Service of the Universidad de Chile provided the strong-motion data for the Chilean earthquake. The Japanese accelerograms are from the National Research Institute for Earth Sciences and Disaster Prevention, Japan. Data from the Global Centroid Moment Tensor Project are from http://www.globalcmt.org/CMTsearch.html (last accessed December 2016). SASMEX historical catalog of alerts is available at http://www.cires.org.mx/sasmex_historico_es.php (last accessed December 2016).

Acknowledgments

The authors express their gratitude to the institutions that provided the strong-motion data: the Mexico City and Oaxaca governments (who allowed us to use the waveform database of the Seismic Alert System of Mexico [SASMEX]), the Instituto de Ingeniería of the National University of Mexico (UNAM), the Japan Meteorological Agency (JMA), and the National Research Institute for Earth Science and Disaster Prevention of Japan (NIED). The authors thank S. Barrientos for data from the National Accelerograph Network of the Department of Civil Engineering (RENADIC) and the Seismological Service at the Department of Geophysics (GUC), both of the Universidad de Santiago, Chile. G. S. acknowledges the Consejo Nacional de Ciencia y Tecnología (CONACYT) Grant 082821. A. C. acknowledges support of Centro de Instrumentación y Registro Sísmico (CIRES). The authors appreciate the comments and suggestions made by the anonymous reviewers, which helped improve the quality of this article.

References

Allen, R. M., H. Brown, M. Hellweg, O. Khainovski, P. Lombard, and D. Neuhauser (2009). Real-time earthquake detection and hazard assessment by ElarmS across California, *Geophys. Res. Lett.* **36,** no. 5, doi: 10.1029/2008GL036766.

Anderson, J. G., and R. Quaas (1988). The Mexico earthquake of September 19, 1985—Effect of magnitude on the character of strong ground motion: An example from the Guerrero, Mexico strong motion network, *Earthq. Spectra* **4,** no. 3, 635–646.

Boroschek, R. L., V. Contreras, D. Y. Kwak, and J. P. Stewart (2012). Strong ground motion attributes of the 2010 M_w 8.8 Maule, Chile, earthquake, *Earthq. Spectra* **28,** no. S1, S19–S38.

CONACYT-NRC (1986). Investigación para aprender de los sismos de septiembre 1985 en México, *Informe técnico preparado por comités conjuntos del Consejo Nacional de Ciencia y Tecnología (México) y el National Research Council (EUA)*, México (in Spanish).

Cuéllar, A., J. M. Espinosa-Aranda, G. Suárez, G. Ibarrola, A. Uribe, F. H. Rodríguez, and B. Frontana (2014). The Mexican Seismic Alert System (SASMEX): Its alert signals, broadcast results and performance during the *M* 7.4 Punta Maldonado earthquake of March 20th, 2012, in *Early Warning for Geological Disasters*, F. Wenzel and J. Zschau (Editors), Springer, Berlin, Germany, 71–87 pp.

Delouis, B., J. M. Nocquet, and M. Vallée (2010). Slip distribution of the February 27, 2010 $M_w = 8.8$ Maule earthquake, central Chile, from static and high-rate GPS, InSAR, and broadband teleseismic data, *Geophys. Res. Lett.* **37,** no. 17, doi: 10.1029/2010GL043899.

Dziewonski, A. M., T.-A. Chou, and J. H. Woodhouse (1981). Determination of earthquake source parameters from waveform data for studies of global and regional seismicity, *J. Geophys. Res.* **86,** 2825–2852, doi: 10.1029/JB086iB04p02825.

Dziewonski, A. M., G. Ekström, and N. N. Maternovskaya (1999). Centroid-moment tensor solutions for April–June, 1998, *Phys. Earth Planet. In.* **112,** no. 1, 11–19.

Ekström, G., M. Nettles, and A. M. Dziewonski (2012). The global CMT project 2004–2010: Centroid-moment tensors for 13,017 earthquakes, *Phys. Earth Planet. In.* **200/201,** 1–9, doi: 10.1016/j.pepi.2012.04.002.

Espinosa-Aranda, J. M., A. Cuellar, A. Garcia, G. Ibarrola, R. Islas, S. Maldonado, and F. H. Rodriguez (2009). Evolution of the Mexican seismic alert system (SASMEX), *Seismol. Res. Lett.* **80,** no. 5, 694–706.

Espinosa-Aranda, J. M., A. Jimenez, O. Contreras, G. Ibarrola, and R. Ortega (1992). Mexico City Seismic Alert System, International Symposium on Earthquake Disaster Prevention 18–21 May 1992, Mexico, *Proc. Centro Nacional de Prevención de Desastres and Japan International Cooperation Agency (CENAPRED-JICA)*, Mexico, Vol. I, 315–324.

Espinosa-Aranda, J. M., A. Jimenez, G. Ibarrola, F. Alcantar, A. Aguilar, M. Inostroza, and S. Maldonado (1995). Mexico City seismic alert system, *Seismol. Res. Lett.* **66,** no. 6, 42–53.

Esteva, L. (1988). The Mexico earthquake of September 19, 1985—Consequences, lessons and impact on research and practice, *Earthq. Spectra* **4,** no. 3, 413–426.

Hoshiba, M., K. Iwakiri, N. Hayashimoto, T. Shimoyama, K. Hirano, Y. Yamada, and H. Kikuta (2011). Outline of the 2011 off the Pacific coast

of Tohoku Earthquake (M_w 9.0)—Earthquake early warning and observed seismic intensity, *Earth Planets Space* **63,** no. 7, 547–551.

Hoshiba, M., O. Kamigaichi, M. Saito, S. Y. Tsukada, and N. Hamada (2008). Earthquake early warning starts nationwide in Japan, *Eos Trans. AGU* **89,** no. 8, 73–74.

Iglesias, A., S. K. Singh, M. Ordaz, M. A. Santoyo, and J. Pacheco (2007). The seismic alert system for Mexico City: An evaluation of its performance and a strategy for its improvement, *Bull. Seismol. Soc. Am.* **97,** no. 5, 1718–1729.

McCann, W. R., S. P. Nishenko, L. R. Sykes, and J. Krause (1979). Seismic gaps and plate tectonics: Seismic potential for major boundaries, *Pure Appl. Geophys.* **117,** no. 6, 1082–1147.

Mendez, A. J., and J. G. Anderson (1991). The temporal and spatial evolution of the 19 September 1985 Michoacan earthquake as inferred from near-source ground-motion records, *Bull. Seismol. Soc. Am.* **81,** no. 3, 844–861.

Mori, N., T. Takahashi, T. Yasuda, and H. Yanagisawa (2011). Survey of 2011 Tohoku earthquake tsunami inundation and run-up, *Geophys. Res. Lett.* **38,** no. 7, doi: 10.1029/2011GL049210.

Nakamura, Y. (1996). Real-time information systems for seismic hazards mitigation UrEDAS, HERAS and PIC, *Quarterly Report-RTRI*, Vol. 37, 112–127.

Pearson, K. (1896). Mathematical contributions to the theory of evolution. III. Regression, heredity and panmixia, *Phil. Trans. Roy. Soc. London* **187,** 253–318.

Pérez-Yañez, C., L. Ramirez-Guzman, A. L. Ruiz, R. Delgado, M. A. Macías, H. Sandoval, L. Alcantara, and A. Quiroz (2014). Strong ground motion database system for the Mexican seismic network, presented at the *AGU Fall Meeting*, 14–19 December, San Francisco, California.

Rosenblueth, E. (1986). The 1985 earthquake: Causes and effects in Mexico City, *J. Am. Concr. Inst.* **8,** no. 5, 23–24.

Singh, S. K., L. Astiz, and J. Havskov (1981). Seismic gaps and recurrence periods of large earthquakes along the Mexican subduction zone: A reexamination, *Bull. Seismol. Soc. Am.* **71,** no. 3, 827–843.

Suárez, G., D. Novelo, and E. Mansilla (2009). Performance evaluation of the seismic alert system (SAS) in Mexico City: A seismological and a social perspective, *Seismol. Res. Lett.* **80,** no. 5, 707–716.

Instituto de Geofísica
Universidad Nacional Autónoma de México
Ciudad Universitaria
Mexico CDMX 04510
cuellara@cires.org.mx
gerardo@geofisica.unam.mx
(A.C., G.S.)

Centro de Instrumentación y Registro Sísmico
Anaxágoras 814
Colonia Narvarte
México CDMX 03020
espinosajm@cires.org.mx
(J.M.E.-A.)

Manuscript received 23 November 2015;
Published Online 7 March 2017

Electronic Supplement

This electronic supplement contains four figures and five tables. **Figures S1** and **S2** show the arrival times determined automatically by the algorithm of the *P* and *S* waves on strong-motion recordings of Mexican earthquakes. **Figures S3** and **S4** show the location of the strong-motion stations relative to the epicenter of the 2010 Chile and 2011 Tohoku earthquakes, respectively.

Table S1 shows the hypocentral data of the earthquakes recorded by Seismic Alert System of Mexico (SASMEX) for which an alert was issued from 1991 to 2014, making use of the algorithm 2(t_S–t_P). **Table S2** includes the focal parameters of earthquakes along the Mexican subduction zone that propitiated an early warning alert in Mexico City, together with the (t_S–t_P) time, parameters *a* and *m*, and a comparison between the magnitude obtained from the algorithm ($m_{2(tS-tP)}$) and the magnitude reported by official agencies. **Table S3** shows the list of subduction earthquakes with M_w>6.0 recorded by other networks, which occurred from 1985 to 2014. **Table S3** also shows the results of the performance test of the algorithm 2(t_S–t_P) for these earthquakes. **Tables S4** and **S5** show the strong-motion stations and the results of the performance test of the 2010 M_w 8.8 Maule, Chile, and the 2011 M_w 9.0 Tohoku, Japan, earthquakes, respectively.

Table S1. List of earthquakes used in the performance tests of the Seismic Alert System of Mexico (*SASMEX*) from 1991-2014 with data recorded by *SASMEX* sensors. Hypocentral information is from the Mexican Seismological Service (SSN) and the Global Centroid-Moment-Tensor (CMT).

SASMEX		Data from the Mexican Seismological Service (SSN)									Data from the CMT Catalog				
No.	Type of Warning	GMT Date	GMT Origin Time	Latº	Lonº	Depth (km)	m_b	M_s	M_c*	m_{pre}*	Latº	Lonº	Depth (km)	M_w	M_s
92	Preventive	2014/05/24	08:24:45.0	16.21	-98.42	18.0				5.7	16.52	-98.25	14.1	5.7	5.6
91	Public	2014/05/10	07:36:01.0	17.16	-100.95	12.0				6.1	17.30	-100.73	20.9	6.1	6.0
90	Public	2014/05/08	17:00:16.0	17.11	-100.87	17.0				6.4	17.30	-100.69	23.2	6.5	6.4
89	Public	2014/04/18	14:27:23.0	17.18	-101.19	10.0				7.2	17.45	-101.23	21.0	7.2	7.2
88	Preventive	2013/10/06	15:10:56.0	16.81	-100.11	10.0				5.0	17.05	-99.97	20.6	5.1	4.9
87	Preventive	2013/08/26	12:54:01.0	16.65	-99.60	10.0				4.8					
86	Public	2013/08/21	12:38:30.0	16.79	-99.56	20.0				6.0	16.97	-99.50	24.4	6.2	6.2
85	Preventive	2013/08/16	15:32:59.0	16.54	-98.59	20.0				5.1	16.77	-98.43	27.0	5.3	5.2
84	Public	2013/08/06	20:17:30.0	16.49	-98.58	16.0				4.9					
83	Public	2013/06/16	05:19:03.0	18.04	-99.25	60.0				5.8	18.25	-99.18	49.6	5.9	5.8
82	Preventive	2013/05/09	19:30:10.0	16.51	-98.16	32.0				4.6					
81	Public	2013/04/21	01:16:34.0	17.87	-102.19	10.0				5.8	18.05	-102.19	26.6	6.1	6.0
80	Preventive	2013/04/12	03:45:09.0	17.78	-101.58	35.0				5.2	17.95	-101.47	35.8	5.3	5.2
79	Preventive	2013/03/26	07:04:45.0	15.78	-98.61	10.0				5.4	16.28	-98.22	12.3	5.4	5.5
78	Preventive	2013/03/16	04:25:23.0	16.67	-98.65	22.0				4.6					
77	Public	2012/11/15	03:20:22.0	18.17	-100.52	40.0				6.1	18.30	-100.48	52.7	6.1	6.1
76	Public	2012/09/22	07:29:57.0	16.23	-98.30	2.0				5.4	16.55	-98.10	19.5	5.5	5.4
75	Preventive	2012/04/13	08:06:28.0	16.22	-98.15	16.0				5.0	16.38	-98.17	12.2	5.0	4.7
74	Preventive	2012/04/13	05:10:03.0	16.11	-98.34	14.0				5.2	16.35	-98.23	13.9	5.3	5.2
73	Preventive	2012/04/02	12:36:42.0	16.27	-98.47	10.0				6.0	16.58	-98.35	12.0	6.1	6.0
72	Preventive	2012/03/20	17:02:47.0	16.25	-98.52	16.0				7.4	16.60	-98.39	15.4	7.5	7.6
71	Preventive	2011/12/11	01:47:25.0	17.84	-99.98	58.0				6.5	17.89	-99.84	55.3	6.5	6.5
70	Preventive	2011/06/18	23:54:44.0	16.92	-99.60	26.0				5.2					
69	Public	2011/05/05	13:24:07.0	16.61	-98.91	11.0				5.5	16.85	-98.72	30.7	5.7	5.7
68	Preventive	2011/04/26	05:07:28.0	16.71	-99.69	7.0				5.5	16.91	-99.45	22.9	5.4	5.5
67	Preventive	2010/05/25	23:36:15.0	17.11	-101.20	15.0				5.0	17.39	-100.96	23.6	5.1	5.0
66	Preventive	2009/04/27	16:46:27.0	16.90	-99.58	7.0				5.7	17.06	-99.41	32.2	5.8	5.8
65	Preventive	2009/03/27	08:48:16.0	17.35	-100.82	30.0				5.3	17.42	-100.60	38.7	5.3	5.3
64	Preventive	2008/11/11	11:02:06.0	16.62	-100.80	15.0				4.7	16.94	-99.81	28.0	4.9	4.7

63	Public	2007/11/06	06:35:42.0	17.08	-100.14	9.0				5.6	17.14	-99.91	18.4	5.4	4.9
62	Preventive	2007/04/28	13:54:35.0	16.94	-99.82	9.0				5.0	17.04	-99.64	29.9	5.1	5.0
61	Preventive	2007/04/13	08:43:50.0	17.27	-100.27	51.0				5.4	17.40	-100.23	66.8	5.3	
60	Public	2007/04/13	05:42:22.0	17.09	-100.44	41.0				6.3	17.37	-100.14	42.7	6.0	6.0
59	Preventive	2007/03/31	05:18:56.0	17.00	-99.79	34.0				4.7	14.31	-93.32	12.0	5.1	
58	Preventive	2005/09/18	11:25:53.0	17.05	-100.02	9.0				4.4					
57	Preventive	2003/01/10	02:08:02.0	16.97	-100.30	30.0	5.1	4.5	4.9		16.88	-99.85	44.7	5.2	4.5
56	Preventive	2002/09/27	07:04:58.0	17.16	-100.59	36.0	5.2	4.6	4.9		17.44	-100.10	36.4	5.1	4.6
55	Preventive	2002/09/25	18:14:48.0	16.86	-100.12	5.0	5.2	4.7	5.3		16.86	-99.79	19.0	5.3	4.7
54	Preventive	2002/02/17	04:10:20.0	16.94	-99.93	37.0	4.4		4.7						
53	Public	2001/10/08	03:39:19.0	16.94	-100.14	4.0	5.6	5.4	5.5						
52	Preventive	2001/03/06	21:57:56.0	17.14	-100.10	32.0	5.1	4.5	5.1						
51	Preventive	2001/03/05	10:17:36.0	17.13	-100.06	32.0	5.0	4.5	4.9						
50	Preventive	2000/04/15	01:45:05.0	16.88	-100.35	9.0	4.0		4.4						
49	Preventive	2000/03/18	00:50:58.0	17.08	-99.31	31.0	4.8	4.3	4.7						
48	Preventive	1999/06/15	20:42:07.1	18.18	-97.51	69.0	6.4	6.5			18.44	-97.38	61.2	6.9	6.5
47	Preventive	1999/05/30	09:58:42.7	17.26	-100.79	53.0	4.4		4.6						
46	Preventive	1999/04/25	03:08:57.7	17.28	-100.80	27.0	4.4		4.6						
45	Preventive	1998/09/07	06:53:17.8	16.77	-99.67	12.0			4.1						
44	Preventive	1998/08/09	16:18:06.6	16.87	-100.25	3.0	4.2		4.5						
43	Public	1998/07/17	11:18:04.0	16.98	-100.16	27.0			4.6						
42	Public	1998/07/05	19:55:07.1	16.83	-100.12	5.0	4.9	4.5	4.9		16.92	-99.73	37.6	5.3	4.5
41	Preventive	1998/05/09	17:03:13.1	17.34	-101.41	18.0	4.8	4.7	4.8		17.31	-101.00	36.2	5.2	4.7
40	Preventive	1998/03/11	14:13:12.1	17.01	-100.11	40.0			4.2						
39	Public	1997/12/22	05:22:07.8	17.14	-101.24	5.0	5.1	5.0	4.6						
38	Preventive	1997/08/27	00:13:26.1	16.76	-99.88	28.0	5.0		4.6						
37	Preventive	1997/07/19	07:34:37.0	17.22	-100.56	51.0	4.6	3.8	4.9						
36	Preventive	1997/07/15	01:26:19.7	16.39	-98.74	11.0	4.0		4.5						
35	Preventive	1997/07/11	22:23:34.4	16.76	-99.70	10.0			4.5						
34	Preventive	1997/05/22	07:50:55.7	18.41	-101.81	59.0	5.9	6.0			18.76	-101.73	55.5	6.5	6.0
33	Preventive	1997/05/08	15:58:29.7	17.32	-100.44	12.0	5.0	4.3	4.8						
32	Preventive	1997/03/23	20:23:16.6	17.39	-100.88	31.0	4.9		4.7						
31	Preventive	1997/03/22	03:49:16.0	17.04	-99.76	30.0	4.7		4.6						
30	Preventive	1997/01/11	20:28:27.2	17.91	-103.04	16.0	6.5	6.9	0.0		18.34	-102.58	40.0	7.1	6.9
29	Preventive	1996/10/27	09:15:38.5	17.11	-100.90	27.0			4.4						

28	Preventive	1996/07/19	09:00:55.2	17.35	-100.29	20.0	4.8	3.9	4.8						
27	Preventive	1996/07/15	21:23:38.5	17.45	-101.16	20.0	5.7	6.5	6.0		17.50	-101.12	22.4	6.6	6.5
26	Public	1996/03/13	21:04:19.8	16.52	-99.08	18.0	5.2	4.4	5.1		16.93	-98.86	29.4	5.1	4.4
25	Preventive	1995/09/16	16:08:57.9	16.40	-98.69	10.0			4.1						
24	Public	1995/09/16	03:20:06.0	16.30	-98.62	10.0	5.1	4.7	5.0						
23	Preventive	1995/09/14		17.00	-99.00										
22	Public	1995/09/14	14:04:30.5	16.31	-98.88	22.0	6.4	7.2	7.3		16.73	-98.54	21.8	7.3	7.2
21	Preventive	1995/05/31	12:49:27.8	15.97	-98.77	14.0	4.1		4.6						
20	Preventive	1995/04/14	06:01:08.3	16.44	-99.09	15.0	4.6		4.8						
19	Preventive	1994/12/10	16:46:46.2	18.02	-101.56	78.0	6.3		6.3		18.18	-101.39	54.0	6.4	
18	Preventive	1994/10/29	16:44:04.3	16.97	-99.89	24.0			5.1						
17	Preventive	1994/05/23	01:41:46.0	18.03	100.57	23.0			5.6		18.19	-100.20	69.2	6.2	
16	Preventive	1993/09/10	10:50:23.7	16.57	-98.94	20.0	4.8		4.8						
15	Preventive	1993/07/29	20:17:01.5	17.38	-100.65	43.0	5.0	4.2	5.0						
14	Public	1993/05/15	08:26:32.0	16.54	-98.65	20.0	4.7		4.8						
13	Public	1993/05/15	03:11:56.0	16.47	-98.72	15.0	5.9	5.9	6.0		16.45	-97.92	38.5	6.0	5.9
12	Public	1993/05/15	08:26:32.0	16.43	-98.74	20.0	5.8	5.8	5.8						
11	Preventive	1993/03/31	10:18:15.5	17.18	-101.02	8.0	5.3	5.0	5.3		17.29	-100.89	26.2	5.5	5.0
10	Public	1992/11/10	02:13:24.7	16.89	-100.10	5.6	4.6	4.2	4.3						
9	Preventive	1992/11/05	04:33:37.0	16.83	-99.66	7.8			3.7						
8	Preventive	1992/10/30	08:24:29.6	17.14	-100.80	20.9	4.7		4.4						
7	Preventive	1992/10/16	17:28:17.3	16.51	-99.17	17.4	4.3	3.8	4.3						
6	Preventive	1992/08/02	12:54:42.3	17.13	-100.30	25.3	4.3		4.3						
5	Preventive	1992/06/07	17.:41:10.7	16.22	-98.87	5.2	5.3	4.8	4.7		16.64	-98.30	15.0	5.2	4.8
4	Preventive	1992/06/07	09:01:43.7	16.17	-98.90	2.2	5.3	5.0	4.6		16.40	-98.28	15.4	5.3	5.0
3	Preventive	1992/05/15	08:35:09.2	16.83	-99.98	22.5	4.2		4.2						
2	Preventive	1992/04/26	20:53:36.9	16.78	-100.09	14.7	4.1		4.3						
1	Preventive	1991/10/16	18:46:38.2	16.83	-100.24	5.0			4.2						

* M_c and m_{pre} are coda wave magnitude and a preliminary magnitude reported by the SSN respectively.

Table S2. Performance of *SASMEX* using *SASMEX* strong motion stations located close to the epicenter with *S-P* time less than 10 s and comparison of seismic magnitudes m_b versus $m_{2(tS\text{-}tP)}$

SASMEX		PARAMETERS FROM THE SSN CATALOG							DATA FROM THE CMT CATALOG				RESULTS OBTAINED FROM THE $2(t_S\text{-}t_P)$ ALGORITHM						M_w and m_b vs. Estimated $m_{2(tS\text{-}tP)}$	
No.	Type of Warning	Local Date	Local Time	Lat°	Lon°	Depth (km)	m_b	m_{pre}*	Lat°	Lon°	Depth (km)	M_w	m_b range	FS Name	$t_S\text{-}t_P$ (s)	a	m	$m_{2(tS\text{-}tP)}$ range	Mag. error ±0.5	Mag. errror ±1.0
92	Preventive	2014/05/24	03:24:45.0	16.2	98.42	18		5.7	16.5	-98.25	14.1	5.7	>5.5	OX04	6.64	6.08	1.77	>6.0	OK	OK
													>5.5	OX05	9.82	4.7	0.96	<5.0		OK
91	Public	2014/05/10	02:36:01.0	17.2	-100.95	12		6.1	17.3	-100.7	20.9	6.1	>6.0	GR02	3.04	6.8	3.28	>6.0	OK	OK
													>6.0	GR01	4.03	6.78	3.33	>6.0	OK	OK
													>6.0	GR03	4.2	6.02	2.62	>6.0	OK	OK
													>6.0	GR13	6.98	5.48	1.21	<5.0		
													>6.0	GR04	7.04	5.56	1.72	>5.5	OK	OK
90	Public	2014/05/08	00:00:16.0	17.1	-100.87	17		6.4	17.3	-100.7	23.2	6.5	>6.0	GR02	2.78	6.89	4.35	>6.0	OK	OK
													>6.0	GR01	4.38	6.96	3.47	>6.0	OK	OK
89	Public	2014/04/18	09:27:23.0	17.2	-101.19	10		7.2	17.5	-124	21..0	7.2	>6.0	GR01	2.5	8.17	5.96	>6.0	OK	OK
													>6.0	GR13	5.47	7.52	4.54	>6.0	OK	OK
													>6.0	GR02	6.01	7.25	3.76	>6.0	OK	OK
													>6.0	GR03	8.75	6.84	3.76	>6.0	OK	OK
													>6.0	GR14	9.08	7.38	3.52	>6.0	OK	OK
88	Preventive	2013/10/06	10:10:56.0	16.8	-100.11	10		5	17.1	-99.97	20.6	5.1	>5.0	GR06	3.29	6.32	2.50	>6.0		OK
													>5.0	GR05	3.8	5.6	2.02	>6.0		OK
													>5.0	GR04	5.69	5.02	1.14	<5.0	OK	OK
86	Public	2013/08/21	07:38:30	16.79	-99.56	20		6.0	16.97	-99.50	24.4	6.2	>6.0	GR08	2.82	6.79	4.28	>6.0	OK	OK
													>6.0	GR06	6.86	6.59	2.54	>6.0	OK	OK
													>6.0	GR31	7.92	4.89	0.88	<5.0		
													>6.0	GR32	9.52	5.52	2.53	>6.0	OK	OK
84	Preventive	2013/08/16	10:32:59	16.54	-98.59	20		5.1	16.8	-98.4	27.0	5.3	>5.5	GR11	3.81	6.08	2.31	>6.0	OK	OK
													>5.5	GR32	4.47	6.11	2.41	>6.0	OK	OK
													>5.5	OX02	4.78	5.58	2.02	>6.0	OK	OK
													>5.5	GR10	6.06	4.93	1.21	<5.0		OK
													>5.5	GR31	8.34	5.25	1.23	<5.0		OK
													>5.5	GR09	8.43	5.09	1.16	<5.0		OK
83	Public	2013/06/16	00:19:03	18.04	-99.25	60		5.8	18.25	-99.18	49.6	5.9	>5.5	GR25	6.1	6.98	3.27	>6.0	OK	OK
													>5.5	GR24	6.82	7.01	3.01	>6.0	OK	OK
													>5.5	GR27	7.45	6.24	1.70	>6.0	OK	OK
													>5.5	GR26	8.83	5.41	1.40	<5.0		OK
81	Public	2013/04/21	20:16:34	17.87	-102.19	10		5.8	18.05	-102.19	26.6	6.1	>5.5	GR02	4.95	7.68	3.01	>6.0	OK	OK
													>5.5	GR01	5.63	6.45	2.38	>6.0	OK	OK
													>5.5	GR17	6.55	6.96	2.61	>6.0	OK	OK
													>5.5	GR16	7.65	5.66	1.56	>5.0	OK	OK
													>5.5	GR15	8.45	5.58	1.77	>5.5	OK	OK
80	Preventive	2013/04/11	22:45:09	17.78	-101.58	35		5.2	17.95	-101.47	35.8	5.3	>5.0	GR16	4.8	6.15	1.82	>6.0		OK
													>5.0	GR14	5.29	5.28	1.84	>5.0	OK	OK
													>5.0	GR17	5.69	6.36	2.17	>6.0		OK
													>5.0	GR28	6.24	5.71	2.26	>6.0		OK
													>5.0	GR18	6.73	5.42	1.35	<5.0	OK	OK
79	Preventive	2013/03/26	07:04:45	15.78	-98.61	10		5.4	16.3	-98.2	12.3	5.4	>5.5	OX01	4.45	6.10	2.76	>6.0	OK	OK
76	Public	2012/09/22	07:29:57	16.23	-98.30	2		5.4	16.55	-98.10	19.5	5.5	>5.0	LG01	3.39	6.58	3.66	>6.0		OK
													>5.0	T02	3.65	5.98	2.50	>6.0		OK
													>5.0	HZ04	5.11	6.12	2.50	>6.0		OK
													>5.0	LA03	5.94	6.20	2.50	>6.0		OK
													>5.0	TU05	8.85	5.14	1.06	<5.0	OK	OK
75	Preventive	2012/04/13	08:06:28	16.22	-98.15	16		5.0	16.38	-98.17	12.2	5.0	>5.0	LG01	3.6	6.07	3.21	>6.0		OK
													>5.0	T02	5.94	5.16	1.07	<5.0	OK	OK
													>5.0	HZ04	6.5	5.34	1.43	<5.0	OK	OK
													>5.0	LA03	7.98	5.27	1.29	<5.0	OK	OK
74	Preventive	2012/04/13	05:10:03	16.11	-98.34	14		5.2	16.35	-98.23	13.9	5.3	>5.0	LG01	3.16	6.66	3.30	>6.0		OK
													>5.0	T02	6.07	5.61	1.71	>5.5	OK	OK
													>5.0	HZ04	6.57	5.64	1.90	>5.5	OK	OK
													>5.0	LA03	8.47	5.77	1.47	>5.0	OK	OK
73	Preventive	2012/04/02	12:36:42	16.27	-98.47	10		6.0	16.58	-98.35	12.0	6.1	>5.5	LA03	7.1	4.26	0.91	<5.0		OK
													>5.5	HA04	7.92	6.36	2.59	>6.0	OK	OK
72	Preventive	2012/03/20	12:02:47	16.25	-98.52	16		7.4	16.60	-98.39	15.4	7.5	>6.0	LG01	2.84	7.49	5.17	>6.0	OK	OK

													>6.0	T02	5.47	8.16	5.20	>6.0	OK	OK
													>6.0	Q11	5.6	7.55	4.89	>6.0	OK	OK
													>6.0	CR10	7.88	7.06	4.01	>6.0	OK	OK
													>6.0	LA03	7.97	8.33	4.34	>6.0	OK	OK
													>6.0	HZ04	8.14	7.91	4.36	>6.0	OK	OK
68	Preventive	2011/04/26	06:07:28	16.71	-99.69	7		5.5	16.91	-99.45	22.9	5.4	>5.0	CT08	3.04	5.52	2.09	>6.0		OK
67	Preventive	2010/05/25	18:36:15	17.11	-101.20	15		5.0	17.39	-100.96	23.6	5.1	<5.0	CT08	4.44	7.09	3.56	>6.0		
66	Preventive	2009/04/27	11:46:27	16.90	-99.58	7		5.7	17.06	-99.41	32.2	5.8	>5.5	CT08	5.5	6.90	3.00	>6.0	OK	OK
65	Preventive	2009/03/27	02:48:16	17.35	-100.82	30		5.3	17.42	-100.60	38.7	5.3	>5.0	VN02	4.47	6.90	2.70	>6.0		OK
													>5.0	PN01	5.27	6.39	2.85	>6.0		OK
64	Preventive	2008/11/11	05:02:06	16.62	-100.80	15		4.7	16.94	-99.81	28.0	4.9	<5.0	JD06	3.21	5.77	3.16	>6.0		
													<5.0	PJ05	3.44	5.31	2.79	>6.0		
63	Public	2007/11/06	00:35:42	17.08	-100.14	9		5.6	17.14	-99.91	18.4	5.4	>5.0	PJ05	2.03	8.26	4.91	>6.0		OK
													>5.0	JD06	3.98	7.47	3.70	>6.0		OK
62	Preventive	2007/04/28	08:54:35	16.94	-99.82	9		5.0	17.04	-99.64	29.9	5.1	<5.0	JD06	4.3	6.80	2.65	>6.0		
61	Public	2007/04/13	00:42:22	17.09	-100.44	41		6.3	17.37	-100.14	42.7	6.0	>5.5	CA04	4.45	8.04	4.01	>6.0	OK	OK
													>5.5	TT03	5.76	7.20	3.56	>6.0	OK	OK
													>5.5	PJ05	6.24	7.49	3.41	>6.0	OK	OK
													>5.5	VN02	7.29	7.05	3.30	>6.0	OK	OK
													>5.5	JD06	8.71	7.14	2.62	>6.0	OK	OK
60	Preventive	2007/04/13	03:43:50	17.27	-100.27	51		5.4	17.40	-100.23	66.8	5.3	>5.5	CA04	4.13	7.14	3.32	>6.0	OK	OK
													>5.5	PJ05	5.26	6.88	3.00	>6.0	OK	OK
													>5.5	TT03	6.14	6.16	2.35	>6.0	OK	OK
													>5.5	JD06	7.3	6.45	2.04	>6.0	OK	OK
													>5.5	VN02	7.63	6.12	2.09	>6.0	OK	OK
59	Preventive	2007/03/31	00:18:56	17.00	-99.79	34		4.7	14.31	-93.32	12.0	5.1	<5.0	PJ05	5.35	5.99	1.75	>6.0		
													<5.0	CT08	6.46	5.47	1.00	<5.0	OK	OK
													<5.0	CA04	7.58	5.62	1.46	>5.0	OK	OK
57	Preventive	2003/01/09	20:08:42	16.97	-100.30	30	5.1		16.88	-99.85	44.7	5.2	>5.0	CA04	3.8	7.14	3.12	>6.0		OK
													>5.0	PJ05	4.65	7.01	3.30	>6.0		OK
													>5.0	TT03	5.45	6.25	2.09	>6.0		OK
													>5.0	JD06	6.37	6.43	1.82	>6.0		OK
56	Preventive	2002/09/27	02:04:58	17.16	-100.59	36	5.2		17.44	-100.10	36.4	5.1	>5.0	TT03	4.47	6.35	2.84	>6.0		OK
													>5.0	CA04	5.19	6.81	2.90	>6.0		OK
													>5.0	PJ05	7.4	6.35	2.37	>6.0		OK
55	Preventive	2002/09/25	13:14:48	16.86	-100.12	5	5.2		16.86	-99.79	19.0	5.3	>5.0	JD06	3.13	7.17	3.22	>6.0		OK
													>5.0	PJ05	3.35	6.33	2.81	>6.0		OK
													>5.0	CA04	5.65	5.63	1.67	>5.5	OK	OK
54	Preventive	2002/02/16	22:10:19	16.94	-99.93	37	4.4						<5.0	PJ05	4.53	5.90	2.43	>6.0		
													<5.0	JD06	4.59	5.96	2.38	>6.0		
													<5.0	CA04	6.44	5.31	1.27	<5.0	OK	OK
53	Public	2001/10/07	21:39:20	16.94	-100.14	4	5.6						>5.5	JD06	2.27	7.03	4.79	>6.0	OK	OK
													>5.5	CA04	4.11	7.05	4.37	>6.0	OK	OK
52	Preventive	2001/03/06	15:57:56	17.14	-100.10	32	5.1						>5.0	PJ05	4.6	6.90	3.23	>6.0		OK
													>5.0	CA04	5.45	6.38	2.70	>6.0		OK
													>5.0	JD06	5.8	6.63	2.33	>6.0		OK
51	Preventive	2001/03/05	04:17:30	17.13	-100.06	32	5.0						>5.0	PJ05	4.54	6.85	2.79	>6.0		OK
													>5.0	CA04	5.29	5.56	1.44	>5.0	OK	OK
													>5.0	JD06	5.52	6.48	2.38	>6.0		OK
50	Preventive	2000/04/14	20:45:05	16.88	-100.35	9	4.0						<5.0	CA04	3.69	6.25	2.41	>6.0		
													<5.0	PJ05	4.14	6.23	2.47	>6.0		
49	Preventive	2000/03/17	18:50:58	17.08	-99.31	31	4.8						<5.0	CT08	7.27	5.61	1.56	>5.0	OK	OK
47	Preventive	1999/05/30	04:58:42	17.26	-100.79	53	4.4						<5.0	VN02	4.98	6.40	2.28	>6.0		
													<5.0	TT03	5.18	4.62	0.80	<5.0	OK	OK
46	Preventive	1999/04/24	22:08:57	17.28	-100.80	27	4.4						<5.0	VN02	4.32	5.99	2.21	>6.0		
													<5.0	TT03	4.75	4.44	0.30	<5.0	OK	OK
													<5.0	CA04	7.17	5.15	1.57	<5.0	OK	OK
44	Preventive	1998/08/09	11:18:07	16.87	-100.25	3	4.2						<5.0	PJ05	3.34	4.75	0.85	<5.0	OK	OK
42	Public	1998/07/05	14:55:07	16.83	-100.12	5	4.9		16.92	-99.73	37.6	5.3	<5.0	PJ05	3.54	5.10	2.14	>5.0	OK	OK
41	Preventive	1998/05/09	12:03:13	17.34	-101.41	18	4.8		17.31	-101.00	36.2	5.2	<5.0	PN01	4.47	5.60	2.71	>6.0		
39	Public	1997/12/21	23:22:00	17.14	-101.24	5	5.1						>5.0	PN01	2.77	6.64	2.94	>6.0		OK
													>5.0	VN02	4.8	5.42	2.19	>6.0		OK
38	Preventive	1997/08/26	19:13:17	16.76	-99.88	28	5.0						>5.0	JD06	3.36	5.15	1.44	<5.0	OK	OK
													>5.0	PJ05	4.52	4.36	1.41	<5.0	OK	OK
37	Preventive	1997/07/19	02:34:37	17.22	-100.56	51	4.6						<5.0	CA04	5.08	5.34	1.01	<5.0	OK	OK
													<5.0	TT03	5.61	4.62	0.84	<5.0	OK	OK
													<5.0	VN02	6.05	4.87	0.83	<5.0	OK	OK
36	Preventive	1997/07/14	20:26:18	16.39	-98.74	11	4.0						<5.0	Q11	3.63	4.78	0.78	<5.0	OK	OK
33	Preventive	1997/05/08	10:58:30	17.32	-100.44	12	5.0						>5.0	TT03	5.47	4.94	1.11	<5.0	OK	OK
													>5.0	VN02	6.36	5.13	1.20	<5.0	OK	OK
													>5.0	PJ05	6.7	5.09	1.23	<5.0	OK	OK
32	Preventive	1997/03/23	14:23:16	17.39	-100.88	31	4.9						<5.0	PN01	5.28	5.54	1.39	<5.0	OK	OK
													<5.0	TT03	5.96	4.38	0.74	<5.0	OK	OK
31	Preventive	1997/03/21	21:49:16	17.04	-99.76	30	4.7						<5.0	JD06	5.23	4.81	0.77	<5.0	OK	OK

													<5.0	PJ05	5.85	4.85	0.81	<5.0	OK	OK
28	Preventive	1996/07/19	04:00:54	17.35	-100.29	20	4.8						<5.0	CA04	5.42	5.37	0.97	<5.0	OK	OK
													<5.0	TT03	6.1	4.49	0.43	<5.0	OK	OK
27	Preventive	1996/07/15	16:23:39	17.45	-101.16	20	5.7		17.50	-101.12	22.4	6.6	>5.5	VN02	5.85	5.06	2.32	>5.5	OK	OK
													>5.5	PJ05	6.41	5.06	1.00	<5.0		OK
24	Public	1995/09/15	21:20:05	16.30	-98.62	10	5.1						>5.0	Q11	4.43	4.56	0.87	<5.0	OK	OK
22	Public	1995/09/14	08:04:35	16.31	-98.88	22	6.4		16.73	-98.54	21.8	7.3	>6.0	Q11	2.12	6.37	4.43	>6.0	OK	OK
													>6.0	CR10	3.55	5.14	2.68	>6.0	OK	OK
													>6.0	VI09	5.69	5.37	3.04	>6.0	OK	OK
21	Preventive	1995/05/31	06:49:28	15.97	-98.77	14	4.1		17.3	-100.9	26.2	5.5	>5.0	Q11	3.63	3.62	0.26	<5.0	OK	OK
20	Preventive	1995/04/14	12:01:08	16.44	-99.09	15	4.6						<5.0	CR10	2.24	5.21	1.46	<5.0	OK	OK
													<5.0	Q11	3.52	4.17	0.72	<5.0	OK	OK
													<5.0	VI09	3.74	4.52	2.14	<5.0	OK	OK
16	Preventive	1993/09/10	04:50:24	16.57	-98.94	20	4.8						<5.0	CR10	3.41	5.39	1.45	<5.0	OK	OK
													<5.0	Q11	4	5.50	1.60	>5.0	OK	OK
													<5.0	VI09	4.93	5.57	2.07	>6.0		
15	Preventive	1993/07/29	14:17:01	17.38	-100.65	43	5.0						>5.0	TT03	4.84	5.02	0.94	<5.0	OK	OK
													>5.0	CA04	6.41	5.01	0.99	<5.0	OK	OK
13	Public	1993/05/14	21:12:00	16.47	-98.72	15	5.9						>5.5	Q11	3	6.54	2.93	>6.0	OK	OK
12	Public	1993/05/14	21:09:39	16.43	-98.74	20	5.8		16.45	-97.92	38.5	6.0	>5.5	Q11	3.02	6.45	2.86	>6.0	OK	OK
11	Preventive	1993/03/31	04:18:15	17.18	-101.02	8	5.3						>5.0	VN02	4.18	5.31	2.13	>5.5	OK	OK
8	Preventive	1992/10/30	02:16:00	17.14	-100.80	20.9	4.7						<5.0	VN02	2.92	5.37	1.62	<5.0	OK	OK
													<5.0	TT03	3.33	4.54	0.95	<5.0	OK	OK
7	Preventive	1992/10/16	11:28:00	16.51	-99.17	17.4	4.3						<5.0	CR10	2.75	4.45	1.11	<5.0	OK	OK
													<5.0	VI09	3.95	5.39	1.91	>5.5		OK
													<5.0	CT08	5.99	4.62	0.70	<5.0	OK	OK
6	Preventive	1992/08/02	06:54:00	17.13	-100.30	25.3	4.3						<5.0	CA04	3.56	5.23	1.47	<5.0	OK	OK
													<5.0	PJ05	4.79	4.38	0.84	<5.0	OK	OK
													<5.0	TT03	5.33	4.15	0.40	<5.0	OK	OK

Table S3. Performance evaluation of the $2(t_S\text{-}t_P)$ algorithm of earthquakes $M_w \geq 6$, located at distances of at least 600 km to Mexico City, which occurred from 1985 to 2004 and were recorded by at least two near field seismic sensors. Hypocentral data are based on the CMT catalogue.

DATA FROM CMT CATALOG								Distance to Mexico City (km)	DATA OF SEISMIC RECORDING STATION					PERFORMANCE OF ALGORITHM $2(t_S\text{-}t_P)$				
Date	Time	Latº	Lonº	Depth km	m_s	M_w	Region		Station	Latº	Lonº	ALT [m]	ELEV (m)	$(t_S\text{-}t_P)$ [s]	a	m	$m_{2(tS\text{-}tP)}$	War-ning
19/09/1985	13:18:25	17.91	-101.99	21.3	8.1	8.0	Michoacán	401	CALE	18.07	-102.75	10	40	3.29	6.14	3.22	>6.0	Public
									ZACA	18.01	-102.18	40	57	10.47	7.8	4.9	>6.0	
21/09/1985	01:37:32	17.57	-101.42	20.8	7.5	7.5	Guerrero	327	AZIH	17.61	-101.47	20	46	4.74	6.12	3.78	>6.0	Public
									PAPN	17.33	-101.04	30	93	10.99	7.52	3.53	>6.0	
30/04/1986	07:07:30	18.25	-102.92	20.7	7.0	6.9	Michoacán	437	CALE	18.07	-102.75	10	54	4.51	6.33	3.45	>6.0	Public
25/04/1989	14:29:06	16.83	-99.12	15.0	6.9	6.9	Guerrero	278	SMR2	16.77	-99.44	83	21	3.28	5.92	3.47	>6.0	Public
									VIGA	16.76	-99.23	35	26	5.03	7.45	3.81	>6.0	
24/10/1993	07:52:23	16.77	-98.61	21.8	6.6	6.6	Guerrero	285	COPL	16.61	-98.98	32	46	4.23	7.24	3.72	>6.0	Public
									VIGA	16.76	-99.23	35	64	5.00	7.45	3.81	>6.0	
23/05/1994	01:46:52	18.19	-100.2	69.6	0	6.2	Guerrero	211	COMD	18.12	-100.52	30	89	6.45	7.51	3.76	>6.0	Public
									PETA	17.54	-101.27	30	144	12.09	6.47	2.3	>6.0	
10/12/1994	16:17:45	18.18	-101.39	54.0	0	6.4	Guerrero	282	BALC	18.01	-101.22	2000	120	6.66	7.54	4.03	>6.0	Public
									PETA	17.54	-101.27	30	100	8.71	7.28	3.42	>6.0	
14/09/1995	14:04:41	16.73	-98.54	21.8	7.2	7.3	Guerrero	280	GR11	16.60	-98.82	28	41	2.12	6.37	4.43	>6.0	Public
									GR10	16.64	-99.03	49	56	3.55	5.14	2.68	>6.0	
09/10/1995	15:36:29	19.34	-104.8	15.0	7.3	8	Colima	561	MZ01	19.07	-104.34	10	51	6.81	8.19	5.7	>6.0	Public
15/07/1996	21:23:42	17.50	-101.12	22.4	6.5	6.6	Guerrero	278	PAPN	17.33	-101.04	30	35	3.45	7.39	4.68	>6.0	Public

									PETA	17.54	-101.27	30	39	4.69	6.89	3.7	>6.0	
11/01/1997	20:28:40	18.34	-102.58	40.0	6.9	7.1	Michoacán	419	CALE	18.07	-102.75	10	36	5.29	7.82	4.79	>6.0	Public
									VILE	18.05	-102.19	81	73	9.16	6.85	3.12	>6.0	
22/05/1997	07:51:00	18.76	-101.73	55.5	6	6.5	Guerrero	291	VILE	18.05	-102.19	81	116	10.21	5.97	1.8	>6.0	Public
									UNIO	17.99	-101.81	56	104	10.54	6.31	2.61	>6.0	
15/06/1999	20:42:13	18.44	-97.38	61.2	6.5	6.9	Puebla	229	CHFL	17.97	-97.87	1694	96	8.18	6.86	4.11	>6.0	Public
									CSER	18.99	-97.38	2656	96	13.66	7.48	2.29	>6.0	
21/06/1999	17:43:09	18.09	-101.62	48.0	5.8	6.3	Guerrero	297	UNIO	17.99	-101.81	56	83	6.3	6.65	3.31	>6.0	Public
									PET2	17.54	-101.26	23	131	9.91	6.17	2.49	>6.0	
30/09/1999	16:31:23	16.20	-96.96	46.8	7.5	7.4	Oaxaca	435	LANE	15.95	-97.19	23	68	5.43	7.67	4.72	>6.0	Public
									TAMA	16.26	-96.58	1699	76	7.86	7.33	4.14	>6.0	
09/08/2000	11:41:53	18.13	-102.39	33.0	6.5	6.5	Michoacán	392	CALE	18.07	-102.75	10	56	4.25	6.84	4	>6.0	Public
									UNIO	17.99	-101.81	56	90	10.69	5.84	1.74	>5.5	
22/01/2003	02:06:49	18.86	-103.9	26.0	7.6	7.5	Colima	550	MZ02	19.07	-104.34	10	48	7.03	7.83	4.72	>6.0	Public
01/01/2004	23:31:53	17.45	-101.4	15.0	5.7	6.0	Guerrero	315	GR01	17.30	-101.04	201	46	6.56	6.67	3.04	>6.0	Public
									COYQ	17.38	-101.06	44	41	6.94	6.37	2.47	>6.0	
11/08/2006	14:30:44	18.50	-101.06	57.8	6.1	6.0	Guerrero	238	CANA	18.57	-101.98	340	116	11.05	5.78	1.88	>6.0	Public
									COMD	18.12	-100.52	306	95	11.94	5.85	1.82	>6.0	
13/04/2007	05:42:26	17.37	-100.14	42.7	6	6.0	Guerrero	255	ATYC	17.21	-100.43	51	44	4.3	7.28	3.74	>6.0	Public
									CA04	17.13	-100.35	28	42	4.45	8.04	4.01	>6.0	
30/06/2010	07:22:33	16.47	-97.77	17.8	6.3	6.3	Oaxaca	353	HZ04	16.30	-97.91	348	27	2.67	7.55	4.74	>6.0	Public
									JAMI	16.28	-97.82	481	24	3.21	7.42	4	>6.0	
11/12/2011	01:47:28	17.89	-99.84	55.3	6.5	6.5	Guerrero	198	TNLP	18.10	-99.56	734	75	8.23	7.02	2.68	>6.0	Public
									COMD	18.12	-100.52	306	88	10.39	7	3.07	>6.0	
20/03/2012	18:02:55	16.60	-98.39	15.4	7.6	7.5	Guerrero	325	OX01	16.31	-98.44	42	38	2.84	7.49	5.17	>6.0	Public
									SJLL	16.66	-98.50	46	40	5.79	8.76	5.44	>6.0	
02/04/2012	17:36:46	16.58	-98.35	12.0	6	6.1	Guerrero	332	OX01	16.31	-98.44	42	19	2	6.99	4.79	>6.0	Public
									SJLL	16.66	-98.50	46	35	4.45	7.3	4.24	>6.0	
11/04/2012	22:55:17	18.10	-102.97	20.5	6.7	6.7	Michoacán	411	CALE	18.08	-102.75	10	26	4.34	6.18	3.28	>6.0	Public
									MC03	18.09	-102.75	132	26	4.67	6.55	3.1	>6.0	
15/11/2012	09:20:23	18.30	-100.48	52.7	6.1	6.1	Guerrero	188	COMD	18.12	-100.52	306	61	5.96	7.1	3.62	>6.0	Public
									TEJU	18.90	-100.16	1340	83	11.33	6.12	1.72	>6.0	
22/04/2013	01:16:35	18.05	-102.19	26.6	6	6.1	Michoacán	364	MC02	18.02	-102.50	47	47	4.95	7.68	3.01	>6.0	Public
									GR18	17.99	-101.92	86	42	5.63	6.45	2.38	>6.0	
21/08/2013	12:38:36	17.00	-99.54	23.3	62	6.2	Guerrero	277	GR08	16.78	-99.50	84	22	2.82	6.79	4.28	>6.0	Public
									VIGA	16.76	99.23	30	40	4.6	6.3	4.14	>6.0	
18/04/2014	14:27:36	17.55	-101.25	18.9	7.2	7.3	Guerrero	294	GR01	17.30	-101.04	181	28	2.5	8.17	5.96	>6.0	Public
									GR13	17.50	-101.25	56	41	5.47	7.52	4.54	>6.0	
08/05/2014	17:00:20	17.36	-100.74	21.3	6.4	6.5	Guerrero	291	GR02	17.22	-100.79	15	18	2.78	6.89	4.35	>6.0	Public
									GR01	17.30	-101.04	181	37	4.38	6.96	3.47	>6.0	
10/05/2014	07:36:05	17.31	-100.82	20.7	6	6.1	Guerrero	297	GR02	17.22	-100.79	15	23	3.04	6.8	3.28	>6.0	Public
									GR01	17.30	-101.04	181	35	4.03	6.78	3.33	>6.0	

Table S4. Performance evaluation of the $2(t_S\text{-}t_P)$ algorithm for the Maule, Chile earthquake (M_w 8.8) on 27 February 2010

STRONG MOTION STATIONS IN CHILE				PERFORMANCE OF SASMEX ALGORITHM $2(t_S\text{-}t_P)$				
Name of FS	**Station Name**	**Latº**	**Lonº**	**Epicentral Distance**	**$t_S\text{-}t_P$ [s]**	***a***	***m***	**Estimated $m_{2(tS\text{-}tP)}$**
CONT	Constitución, Hospital	-35.34	-72.406	78	*12.72	8.50	5.67	>6.0
CONC	Concepción, Colegio Inmaculada Concepción	-36.828	-73.048	108	*6.11	7.86	5.34	>6.0
TAL	Talca, Colegio Integrado San Pío X	-35.43	-71.665	133	*18.95	8.41	4.81	>6.0
HUAL	Hualañe, Hospital	-34.977	-71.805	146	*21.71	8.52	4.94	>6.0
CURI	Curico, Hospital	-34.99	-71.236	194	26.84	8.51	4.65	>6.0
ANGO	Angol, Hospital	-37.795	-72.706	201	21.37	8.85	4.51	>6.0
MAT	Matanzas, Escuela Carlos Ibáñez del Campo	-33.96	-71.873	228	*24.40	8.48	4.87	>6.0
LLO	Llolleo	-33.616	-71.611	273	*22.54	8.46	5.73	>6.0

* Accelerograms without P wave arrivals

Table S5. Performance evaluation of the $2(t_S\text{-}t_P)$ algorithm for the Tohoku, Japan earthquake (M_w 9.0) on 11 March 2011

STRONG MOTION STATIONS IN JAPAN					PERFORMANCE OF SASMEX ALGORITHM $2(t_S\text{-}t_P)$				
Name of FS	**Station Name**	**Latº**	**Lonº**	**Elevation [m]**	**Epicentral Distance**	**$t_S\text{-}t_P$ [s]**	***a***	***m***	**Estimated $m_{2(tS\text{-}tP)}$**
MYG011	OSHIKA	38.3052	141.5044	13	100	19.77	8.75	4.75	M>6.0
MYG002	UTATSU	38.7262	141.5109	79	109	18.69	8.66	5.61	M>6.0
MYG008	KITAKAMI	38.5676	141.4266	26	112	24.61	8.22	4.06	M>6.0
MYGH12	SHIZUGAWA	38.6416	141.4428	18	113	22.44	8.40	4.21	M>6.0
OURI	OURI	38.4573	141.3453	50	118	21.43	8.24	4.19	M>6.0

Figure S1. Mexican strong motion records [1985-2010] of the first and second detections (left and right respectively) analyzed in this study. The green and red tic marks show the arrival time of the P wave and S waves by the $2(t_S-t_P)$ algorithm.

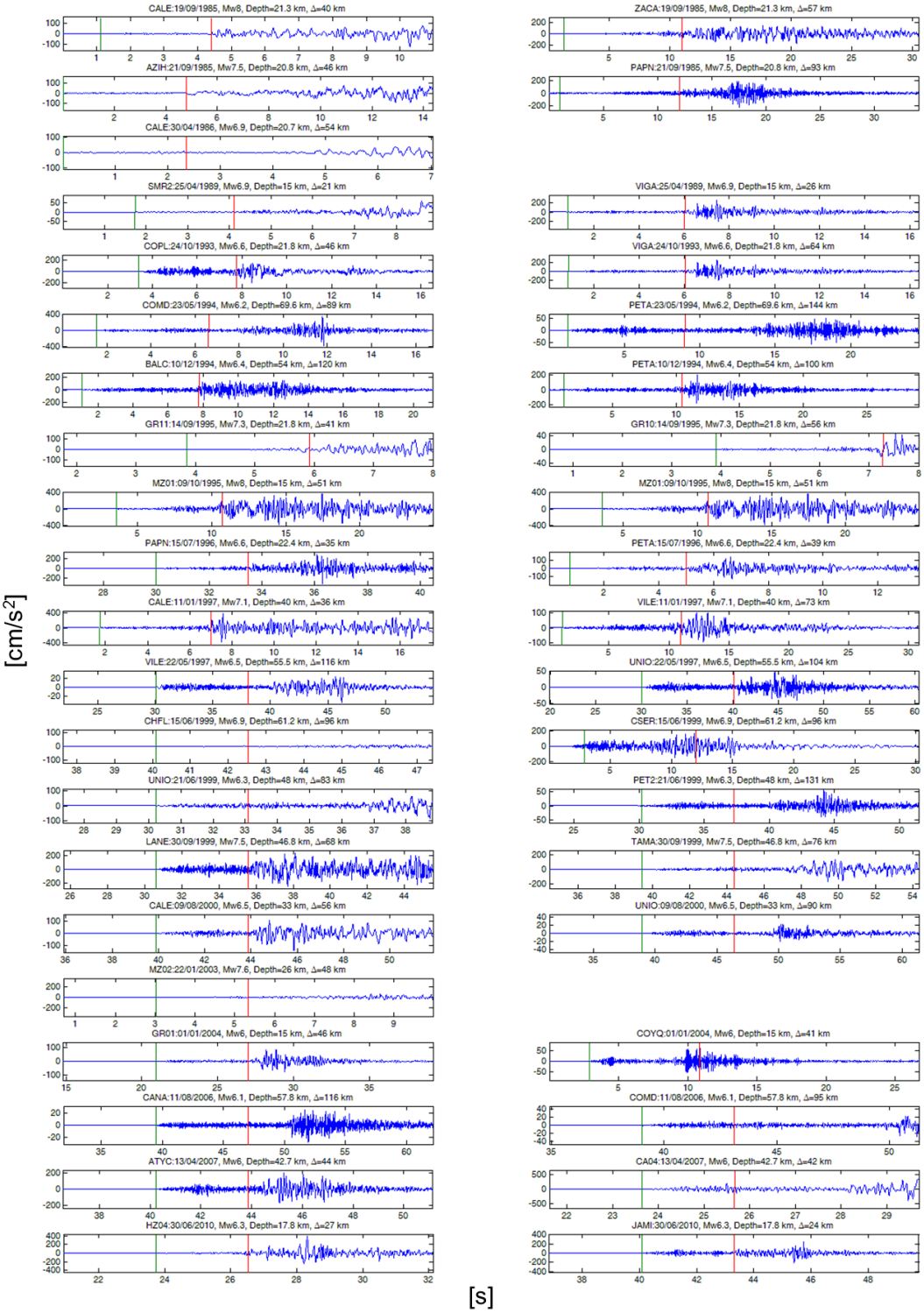

Figure S2. Mexican strong motion records [2011-2014] of the first and second detections (left and right respectively) analyzed in this study. The green and red tic marks show the arrival time of the P wave and S waves by the $2(t_S-t_P)$ algorithm.

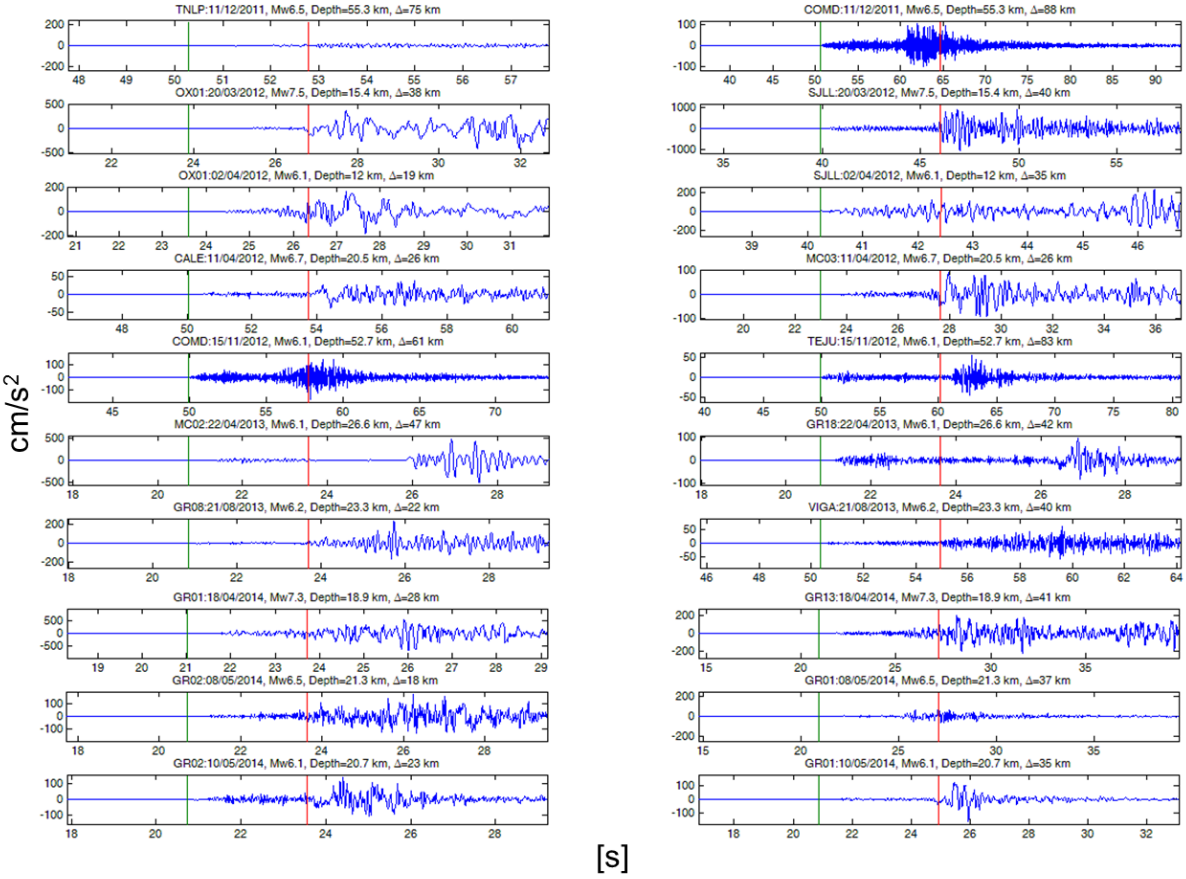

Figure S3. The location of the Maule earthquake of 27 February 2010 in central Chile (M_w 8.8) is shown as a star. The strong motion stations used in the analysis are shown as black squares.

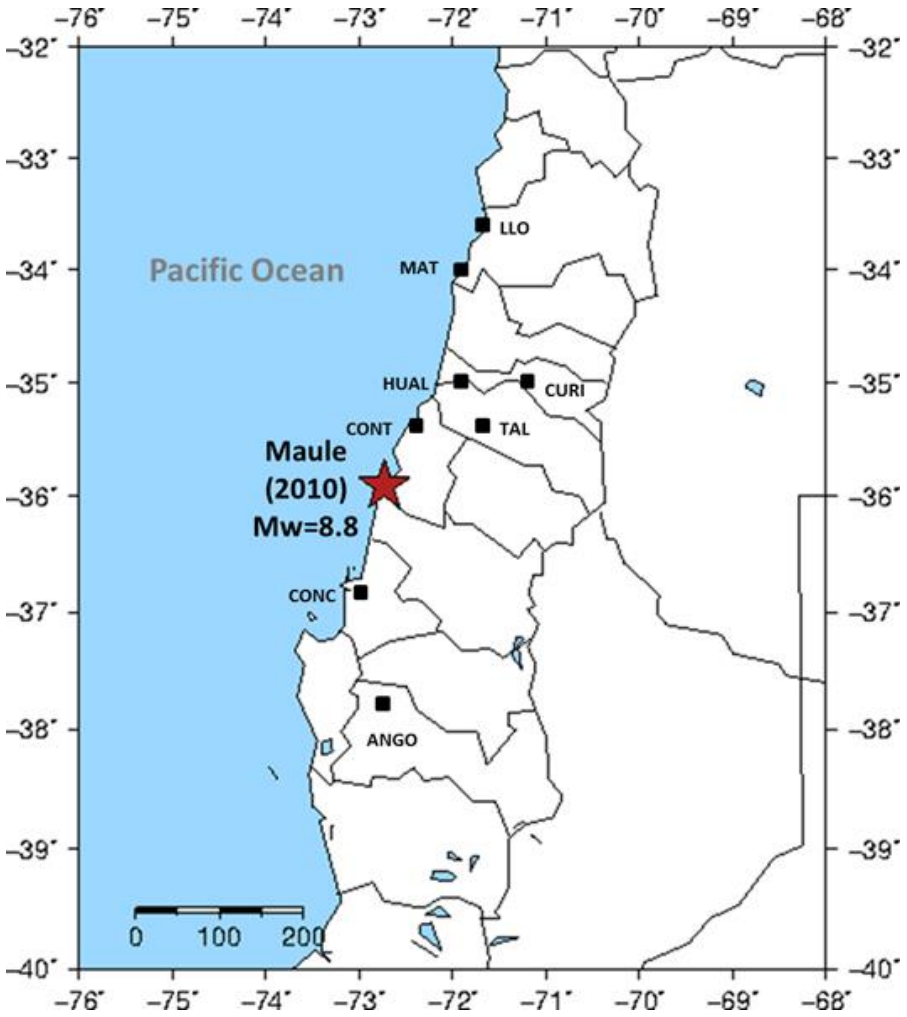

Figure S4. The location of the 11 March 2011 Tohoku, Japan earthquake (M_w 9.0) is shown as a star and squares denote the five seismic sensors used in the analysis.

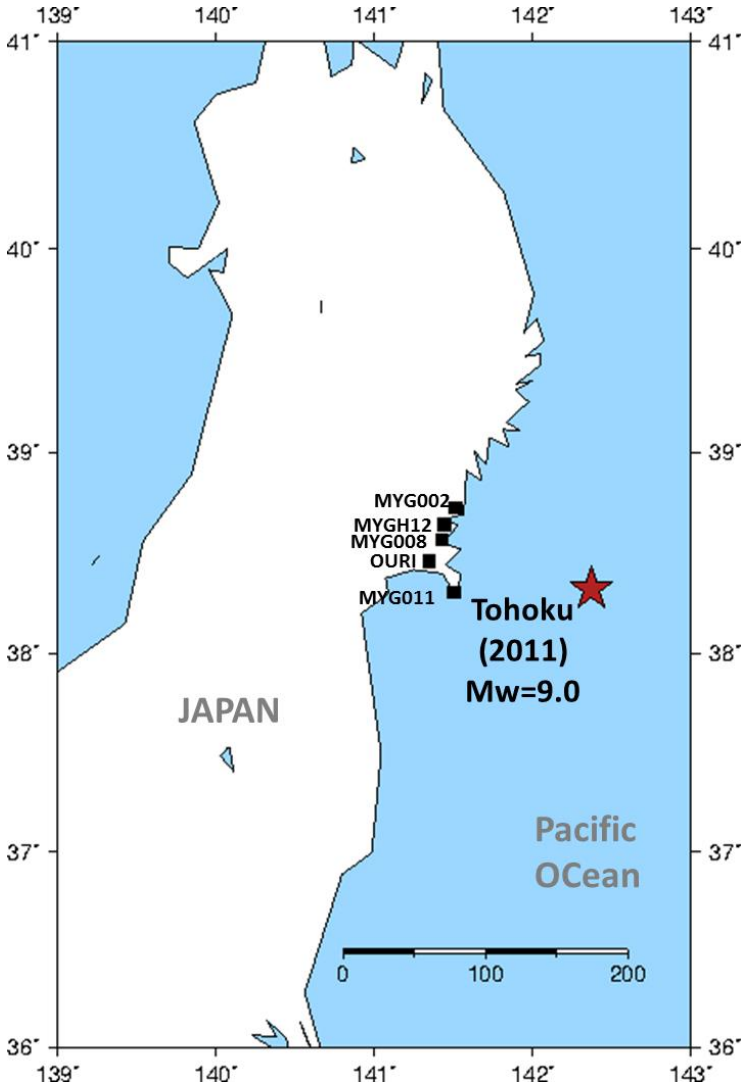

CAPÍTULO III

An Earthquake Early Warning Algorithm Based on the P-Wave Energy Released in the t_S-t_p Interval

[**Cuéllar, A.,** Suárez R. and Espinosa-Aranda J. M.(2017). Performance Evaluation of the Earthquake Detection and Classification Algorithm *2(t_S–t_P)* of the Seismic Alert System of Mexico (SASMEX). *Bulletin of the Seismological Society of America*, Vol. 108, No. 1, pp. 238–247, February 2018, doi: 10.1785/0120170115] (Submitted to *Bulletin of the Seismological Society of America*)

Bulletin of the Seismological Society of America, Vol. 108, No. 1, pp. 238–247, February 2018, doi: 10.1785/0120170115

Ⓔ

An Earthquake Early Warning Algorithm Based on the *P*-Wave Energy Released in the t_S–t_P Interval

by Armando Cuéllar, Gerardo Suárez, and J. M. Espinosa-Aranda

Abstract The t_S–t_P earthquake early warning algorithm measures the energy of the *P*-wave coda on the vertical component in the t_S–t_P period to make a magnitude threshold estimation. The algorithm is based on two parameters: the logarithm of the peak ground acceleration, $\max(a(t_S–t_P))$ and the logarithmic cumulative acceleration $\mathrm{SA}(t_S–t_P)$. The model is built using a learning algorithm that iteratively parameterizes the linear fit of $\max(a(t_S–t_P))$ and $\mathrm{SA}(t_S–t_P)$ to M_w in segments. Training datasets were based on 324 accelerograms from 101 earthquakes ($4.8 \leq M_w \leq 8.1$) in the Mexican subduction zone from 1985 to 2013. The algorithm is supervised to avoid outliers in the data. The process results in a family of linear equations parameterizing the observations to magnitude $m(t_S–t_P)$ calibrated to the observed M_w. The algorithm was successfully tested using a dataset of 28 earthquakes in the Mexican subduction zone, from 2014 to 2017. The performance of t_S–t_P algorithm was tested as a warning tool using 89 earthquakes in the Mexican subduction zone from 1985 to 2017, that met the criterion of having at least two stations within 70 km from the epicenter. The results show that 79 were correctly screened. The magnitude of six events was overestimated and four were underestimated. These earthquakes had an unfavorable station distribution. The M_w 6 South Napa, California, earthquake of 24 August 2014 was used also as a test case. The two closest stations identified it as $M_w \geq 5.8$ within 2 s after the arrival of the *P* phase. This resulted in a lead time of 10 s in Berkeley and 12 s in San Francisco, prior to the arrival of the *S* waves. Thus, the t_S–t_P algorithm proves to be a reliable tool for seismic early warning where hypocenters are close to the target cities.

Electronic Supplement: Earthquake catalog and table showing performance evaluation of the t_S–t_P algorithm.

Introduction

Since its inception in 1991, the Mexican Seismic Alert System (SASMEX) was designed to cover the southeastern Guerrero seismic gap. At the time, the gap was considered potentially capable of generating a great $M_w > 8$ earthquake (McCann *et al.*, 1979; Singh *et al.*, 1981). The original goal of the system was to warn the population of Mexico City of an impending earthquake, similar to the destructive 19 September 1985 earthquake (Espinosa-Armanda *et al.*, 1995). Although the 1985 earthquake took place about 350 km from Mexico City, it produced a large loss of life and unprecedented material damage (e.g., Rosenblueth, 1986; Esteva, 1988). The soft and highly saturated soils, remnant of the pre-Columbian lake on which the city was built, were responsible for the large accelerations and the long duration of the strong motion of the ground. Therefore, Mexico City presented a unique opportunity to develop a seismic early warning system. If earthquakes are correctly identified and their magnitude calibrated, the distance of ~350–400 km from the subduction zone provides an enviable warning time of ~60 s before the strong shaking begins. No other city in the world offers this advantage to implement a seismic early warning system.

SASMEX has grown to 97 dedicated strong-motion stations covering the subduction zone, with an average spacing of ~25km (Fig. 1). Additional seismic stations are located inland to monitor the in-slab earthquakes that occur within the subducted Cocos plate (Cuéllar *et al.*, 2014). The original algorithm used by SASMEX to issue early seismic warnings to Mexico City is based on the growth of seismic energy in twice the observed t_S–t_P time. The $2(t_S–t_P)$ algorithm was

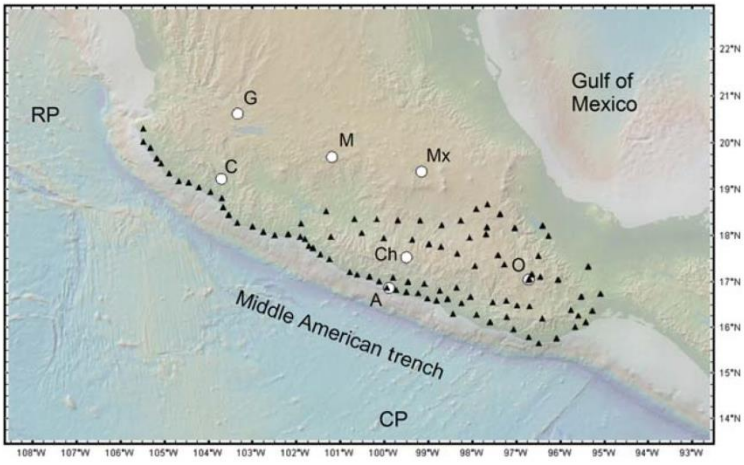

Figure 1. Current distribution of Mexican Seismic Alert System (SASMEX) strong-motion stations (triangles) and cities where the seismic early warning system is now operational (white circles). G, Guadalajara; M, Morelia; Mx, Mexico City; Ch, Chilpancingo; A, Acapulco; O, Oaxaca; RP, Rivera plate; CP, Cocos plate.

thoroughly tested and discussed by Cuéllar *et al.* (2017). Based on the energy released, it estimates an empirical magnitude range related to m_b.

In recent years, other cities were incorporated to SASMEX (Fig. 1). Some of these cities lie close to the subduction zone or to the regions where in-slab earthquakes take place beneath the continent. For this reason, many of these locations do not share Mexico City's advantage of having an almost minute-long warning time; thus, there is a need to develop a faster algorithm to detect earthquakes and to determine a magnitude threshold.

Here, we present an algorithm based on the seismic energy released in the interval t_S–t_P. The algorithm initiates from the detection of the *P* wave and ends with the arrival of the *S* wave. The acceleration of the *P* wave and its coda are measured on the vertical component. We propose a magnitude estimation model $m_{(t_S-t_P)}$ based on two parameters: the logarithm of the maximum quadratic acceleration $\max(a(t_S-t_P))$ and the logarithmic cumulative quadratic acceleration $\mathrm{SA}(t_S-t_P)$ of the *P* wave. The algorithm is calibrated to M_w using a training dataset of 101 earthquakes occurring from 1985 to 2013 in the Mexican subduction zone. Only accelerograms of earthquakes $M_w > 4.7$, located at epicentral distances < 70 km, are used.

The magnitude estimator $m_{(t_S-t_P)}$ is based on a family of logarithmic linear regression models fit in a least-squares sense, iteratively calculated using a machine learning strategy. In contrast to the two-tiered alerting protocol prescribed by the authorities in Mexico City (Cuéllar *et al.*, 2017), here we propose a minimum magnitude cutoff of $m_{(t_S-t_P)} \geq 5.8$ to activate the public earthquake early warning system. The t_S–t_P algorithm neither calculates the location of the earthquake nor estimates potential shaking of the ground. The algorithm waits for the confirmation of two neighboring stations that the magnitude threshold is exceeded to issue an alert.

Description of the t_S–t_P Algorithm

Detection of the *P* and *S* Waves

The detection process of the *P* and *S* phases uses the three orthogonal components of the strong-motion data, running in parallel to the average square input (Allen, 1978) and vertical-to-horizontal (Nakamura, 1996) algorithms. The real-time detection procedure was described in detail for the $2(t_S-t_P)$ algorithm (Cuéllar *et al.*, 2017). The phase detection process takes into account empirical criteria that correct for site effects and for the characteristics of the seismic instrumentation (Cuéllar *et al.*, 2017). In cases where the seismic station detects abnormally high background noise, the algorithm recalibrates its operational parameters. In the case of persistent levels of high noise, the seismic station is temporarily taken out of the detection process until the background seismic noise returns to the predefined level.

Estimation of Parameters $\max(a(t_S-t_P))$ and $\mathrm{SA}(t_S-t_P)$

The algorithm uses the vertical component of three orthogonal component accelerograms. The energy in the t_S–t_P time window is composed essentially of the *P* wave and its coda. The parameter $\max(a(t_S-t_P))$ is the logarithm of the maximum value of the quadratic acceleration of the vertical channel within the t_S–t_P interval (equation 1). The parameter $\mathrm{SA}(t_S-t_P)$ is the sum of the logarithmic cumulative quadratic acceleration of the vertical channel observed within the same interval (equation 2). The algorithm terminates with the detection of the *S* wave and proceeds to estimate the corresponding seismic magnitude threshold.

$$\max(a(t_S-t_P)) = \log_{10}[\max(a(i)^2)]_{i=t_P}^{t_S} \quad (1)$$

$$\mathrm{SA}(t_S-t_P) = \log_{10} \sum_{i=t_P}^{t_S} a(i)^2, \quad (2)$$

in which $a(i)$ are the acceleration values on the vertical channel of the triaxial accelerometer and i is the sample number starting from the *P* wave and ending with the detection of the *S* wave.

Correlation between M_w and $\max(a(t_S-t_P))$ and $\mathrm{SA}(t_S-t_P)$

To explore the correlation between the magnitude M_w of earthquakes in the Mexican subduction zone and parameters

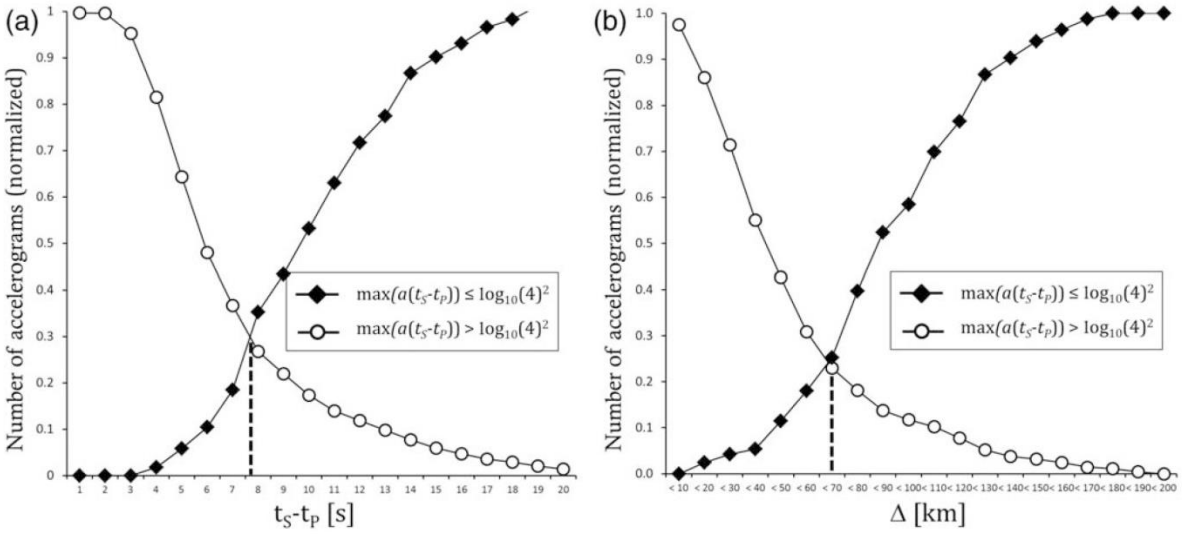

Figure 2. Cumulative distribution of the 1114 acceleration records since 1985–2017 $4.7 > M_w \le 8.1$ grouped into two categories: $\max(a(t_S–t_P)) \le \log_{10}(4^2)$ (open circles) and $\max(a(t_S–t_P)) > \log_{10}(4^2)$ (closed diamonds) plotted with respect to (a) the $t_S–t_P$ time and (b) the epicentral distance Δ.

$\max(a(t_S–t_P))$ and $SA(t_S–t_P)$, data were collected from the following catalogs: the Mexican Seismological Service (SSN), the Global Centroid Moment Tensor (CMT) (Dziewonski *et al.*, 1981, 1999; Ekström *et al.*, 2012), the strong-motion data recorded by the Instituto de Ingeniería, Universidad Nacional Autónoma de México (Pérez-Yañez *et al.*, 2014), and the SASMEX network, operated by the Centro de Instrumentación y Registro Sísmico. A selection criteria were applied as follows:

- A1: earthquakes reported in the Mexican subduction zone in the SSN catalog with focal depths <40 km;
- A2: earthquakes of magnitude $M_w > 4.8$, as reported by the CMT catalog; and
- A3: accelerograms with clear recordings of both *P* and *S* waves.

A total of 1114 acceleration records were selected. In some cases, the accelerograms show very low accelerations that are close to the self-noise of the instruments. The resolution of the majority of the early strong-motion SASMEX instruments was 10 or 12 bits. In those cases, the noise level of the seismic acceleration recordings is at least ±1.0 or ±0.5 cm/s^2, respectively. To be well above the noise level, only acceleration records with values >4 cm/s^2 in the $t_S–t_P$ time window were utilized. This value of acceleration corresponds to $\max(a(t_S–t_P)) > \log_{10}(4^2)$. More recently, the instruments have higher dynamic ranges using 16 or 24 bit digitizers; the threshold criteria would be also acceptable in these cases.

The strong-motion records were grouped in two: one where $\max(a(t_S–t_P)) > \log_{10}(4^2)$ and the other with $\max(a(t_S–t_P)) \le \log_{10}(4^2)$. The cumulative number of these two groups of accelerograms was plotted relative to the epicentral distance and to the $t_S–t_P$ time (Fig. 2). In the case of records with large $t_S–t_P$ times, the cumulative distribution for $\max(a(t_S–t_P)) > \log_{10}(4^2)$ decreases. In contrast, $\max(a(t_S–t_P) \le \log_{10}(4^2)$ increases as a function of time (Fig. 2). We propose using the intersection of these curves to empirically define a criterion of when the acceleration records are above the noise level in the $t_S–t_P$ time. The intersection of these curves corresponds to epicentral distances of ~70 km and $t_S–t_P \sim 7$ s.

Based on these results, the accelerograms selected had to meet the following criteria:

- B1: acceleration values in the vertical channel $a > 4$ cm/s^2 during the $t_S–t_P$ time;
- B2: epicentral distances of <70 km to the strong-motion site; and
- B3: acceleration records with $t_S–t_P < 7$ s.

From the initial dataset of 1114 acceleration records, only 400 accelerograms recorded from 129 earthquakes ranging in magnitude from $4.8 \le M_w \le 8.1$ met these criteria (Fig. 3 and Ⓔ Table S1, available in the electronic supplement to this article). These 400 accelerograms are divided into two sets: the first 324 are used as training data to develop the algorithm, and the other 76 strong-motion records are used as test data.

$\text{Max}(a(t_S–t_P))$ and $SA(t_S–t_P)$ were computed for the selected dataset of 400 acceleration records and plotted against the reported magnitude M_w. The correlation between $\max(a(t_S–t_P))$ and M_w is $r = 0.40$. In the case of the

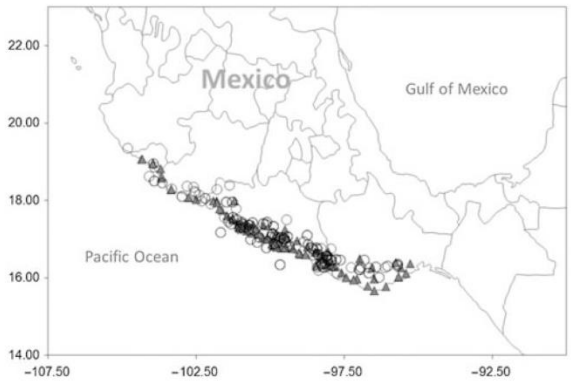

Figure 3. Map showing the 129 selected earthquakes in the Mexican subduction zone from 1985 to 2017 (M_w >4.9; depth <40 km) used as training data (open circles). The seismic field sensors (triangles) are from the networks of the Instituto de Ingeniería, Universidad Nacional Autónoma de México, and SASMEX.

cumulative acceleration SA(t_S–t_P), the correlation coefficient with magnitude is $r = 0.50$ (Fig. 4). The correlation between max($a(t_S$–$t_P)$) and SA(t_S–t_P) is $r = 0.88$, indicating that these two parameters are not completely independent.

Although the plot of max($a(t_S$–$t_P)$) versus M_w indicates that there is a linear correlation between these two parameters, there are several outliers, particularly in the case of large earthquakes $M_w > \sim 7$ (Fig. 4a). The maximum acceleration of the ground observed in the near field in the first few seconds does not reflect necessarily the resulting magnitude of the earthquake. A case in point is the 19 September 1985 earthquake (M_w 8.1) (Fig. 4a and Ⓔ Table S2). The low acceleration observed in station CALE was attributed to the fact that the nucleation of the 1985 earthquake was located immediately beneath that station (Mendez and Anderson, 1991).

The correlation between SA(t_S–t_P) versus M_w shows an asymptotic growth. As in the case of max($a(t_S$–$t_P)$), the cumulative acceleration shows the presence of outliers, corresponding to earthquakes $M_w > \sim 7$. In some cases, outliers are due to earthquakes where the directivity of the seismic energy is radiated away from the recording seismic stations. For example, in the case of the 1995 Copala earthquake (M_w7.3), the seismic energy radiated away from the closest stations (Anderson *et al.*, 1995). As a result, the values of SA(t_S–t_P) and max($a(t_S$–$t_P)$) at stations GR11, COPL, GR10, and GR09 were low at short epicentral distances for this large magnitude earthquake (Fig. 4 and Ⓔ Table S2).

Calibration of Magnitude Based on max($a(t_S$–$t_P)$) and SA(t_S–t_P)

The correlation of parameters max($a(t_S$–$t_P)$) and SA(t_S–t_P) with M_w suggests the possibility to build an algorithm relating the magnitude and the acceleration observed in the *P*-wave coda (Fig. 4). To this end, we use a training set of 324 accelerograms corresponding to 101 earthquakes occurring from 1985 to 2013 that meet the selection criteria described above (Ⓔ Table S1).

The relationships between magnitude and the parameters reflecting the energy released are estimated by a learning machine algorithm exemplified in Figure 5. The input data to the learning machine is vector $[\bar{x}_j, \bar{y}_j]$, in which $\bar{x}_j = (\mathrm{SA}(t_S{-}t_P)_j, \max(a(t_S{-}t_P))_j)$, formed from the 324 acceleration records, and $\bar{y}_j$ is the target data: $\bar{y}_j = M_{w_j}$. Before it is introduced into the learning machine process, the data are ordered so that $\mathrm{SA}(t_S{-}t_P)_j < \mathrm{SA}(t_S{-}t_P)_{j+1}$. The process solves the overdetermined set of equations $\log_{10} M_{w_j} = \alpha \mathrm{SA}(t_S{-}t_P)_j + \beta \max(a(t_S{-}t_P))_j$.

Considering that the cumulative energy released SA(t_S–t_P) behaves in an asymptotic manner, the process is

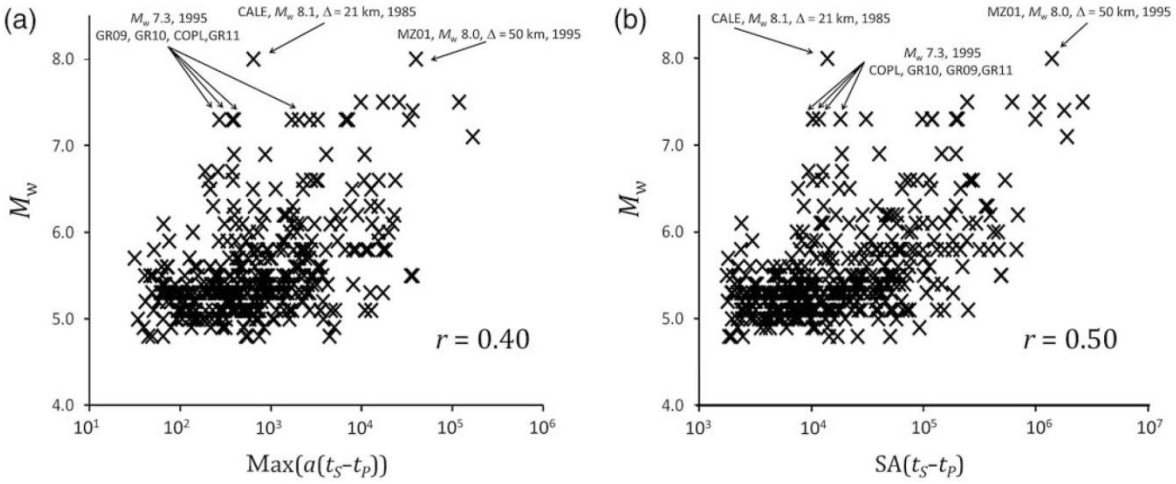

Figure 4. Correlation between parameters (a) max($a(t_S$–$t_P)$) and (b) SA(t_S–t_P) with M_w. The dataset shows the strong-motion records of 324 accelerograms recorded from 1985 to 2013.

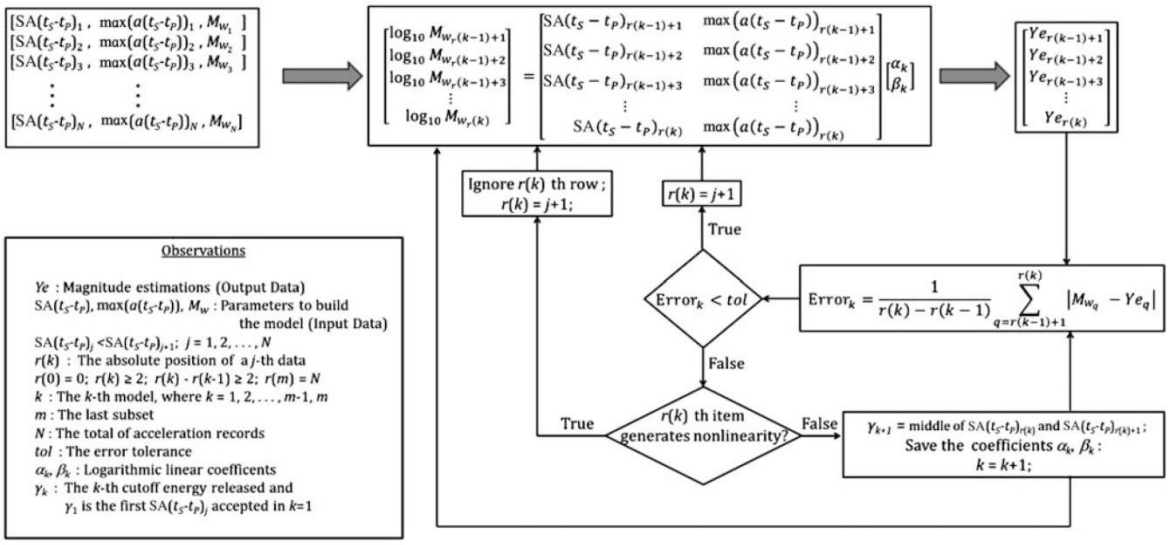

Figure 5. Flow chart showing the process followed by the learning procedure to determine the linear fit in k segments.

linearized in m sections of the curve, in which for each section k, the system of equations is solved with the $(r(k) - r(k-1))$ elements, in which $r(k)$ represents the position of the ordered input data and its value corresponds to $[\bar{x}_j, \bar{y}_j]$ (Fig. 5). The solution to the overdetermined set of equations determines the value of coefficients $[\alpha_k, \beta_k]$ and the error in the linear fit of the kth segment. Error_k is the mean absolute error $|\overline{M_{\text{w}k}} - \overline{Ye}_k|$; in which $\overline{M_{\text{w}k}}$ is the reported magnitude and $\overline{Ye}_k$ is the resulting magnitude of the inversion process in section k.

The process starts by building a solution to the first segment $k = 1$. When the error for that segment is $\text{Error}_k <$ tolerance, the process recycles, adds the next data point $[\bar{x}_{j+1}, \bar{y}_{j+1}]$, and again solves the overdetermined set of equations (Fig. 5). This iterative process continues until $\text{Error}_k >$ tolerance. After several tests, we settled for an error tolerance of 5% in the least-squares fit for each segment. At that point, the algorithm moves on to solve the next section $k+1$ and sets the upper bound γ of section k, as $\gamma_k = \log_{10}(0.5(10^{\text{SA}(t_S-t_P)_j} + 10^{\text{SA}(t_S-t_P)_{j+1}}))$. Thus, the last data point in section k is the jth term $[\bar{x}_j, \bar{y}_j]$. Subsequently, the first data point in section $k+1$ will be the $j+1$th item $[\bar{x}_{j+1}, \bar{y}_{j+1}]$.

The correlations between $\text{SA}(t_S–t_P)$ and $\max(a(t_S–t_P))$ with M_{w} show that the accelerograms of large magnitude earthquakes in the near field often exhibit relatively low values of peak ground acceleration and cumulative energy (Fig. 4). These outliers introduce a nonlinear behavior and increase the value of Error_k. Thus, the inversion process is supervised at each iteration. If a data point $[\bar{x}_j, \bar{y}_j]$ is identified as a clear outlier in model k, the data point is manually eliminated by an active supervision of the learning algorithm (Fig. 5).

The resulting $t_S–t_P$ algorithm, based on the 324 training acceleration records, is defined by nine linear equations that empirically relate $\max(a(t_S–t_P))$ and $\text{SA}(t_S–t_P)$ with $m_{(t_S–t_P)}$ through coefficients α_k and β_k in the m segments of the process. As a result, these nine models are grouped in a family of linear equation parameterized by the γ-values:

$$m_{(t_S-t_P)} = \begin{cases} (10^{\text{SA}(t_S-t_P)})^{\alpha_1} \times (10^{\max(a(t_S-t_P))})^{\beta_1} & \text{if } \text{SA}(t_S-t_P) > \gamma_1 \\ (10^{\text{SA}(t_S-t_P)})^{\alpha_2} \times (10^{\max(a(t_S-t_P))})^{\beta_2} & \text{if } \text{SA}(t_S-t_P) > \gamma_2 \\ (10^{\text{SA}(t_S-t_P)})^{\alpha_3} \times (10^{\max(a(t_S-t_P))})^{\beta_3} & \text{if } \text{SA}(t_S-t_P) > \gamma_3 \\ (10^{\text{SA}(t_S-t_P)})^{\alpha_4} \times (10^{\max(a(t_S-t_P))})^{\beta_4} & \text{if } \text{SA}(t_S-t_P) > \gamma_4 \\ (10^{\text{SA}(t_S-t_P)})^{\alpha_5} \times (10^{\max(a(t_S-t_P))})^{\beta_5} & \text{if } \text{SA}(t_S-t_P) > \gamma_5 \\ (10^{\text{SA}(t_S-t_P)})^{\alpha_6} \times (10^{\max(a(t_S-t_P))})^{\beta_6} & \text{if } \text{SA}(t_S-t_P) > \gamma_6 \\ (10^{\text{SA}(t_S-t_P)})^{\alpha_7} \times (10^{\max(a(t_S-t_P))})^{\beta_7} & \text{if } \text{SA}(t_S-t_P) > \gamma_7 \\ (10^{\text{SA}(t_S-t_P)})^{\alpha_8} \times (10^{\max(a(t_S-t_P))})^{\beta_8} & \text{if } \text{SA}(t_S-t_P) > \gamma_8 \\ (10^{\text{SA}(t_S-t_P)})^{\alpha_9} \times (10^{\max(a(t_S-t_P))})^{\beta_9} & \text{if } \text{SA}(t_S-t_P) > \gamma_9 \end{cases} \quad (3)$$

in which

$$\alpha_1 = 23.570 \times 10^2; \quad \beta_1 = -29.573 \times 10^3; \quad \gamma_1 = 3.230;$$
$$\alpha_2 = 23.556 \times 10^2; \quad \beta_2 = -56.052 \times 10^3; \quad \gamma_2 = 3.380;$$
$$\alpha_3 = 21.214 \times 10^2; \quad \beta_3 = -33.404 \times 10^3; \quad \gamma_3 = 3.690;$$
$$\alpha_4 = 21.214 \times 10^2; \quad \beta_4 = -44.066 \times 10^3; \quad \gamma_4 = 4.016;$$
$$\alpha_5 = 18.176 \times 10^2; \quad \beta_5 = -8.438 \times 10^3; \quad \gamma_5 = 4.149;$$
$$\alpha_6 = 21.492 \times 10^2; \quad \beta_6 = -73.543 \times 10^3; \quad \gamma_6 = 4.278;$$
$$\alpha_7 = 22.792 \times 10^2; \quad \beta_7 = -102.763 \times 10^3; \quad \gamma_7 = 4.637;$$
$$\alpha_8 = 10.767 \times 10^2; \quad \beta_8 = -47.098 \times 10^3; \quad \gamma_8 = 5.394;$$
$$\alpha_9 = 18.747 \times 10^2; \quad \beta_9 = -62.704 \times 10^3; \quad \gamma_9 = 5.609.$$

Based on expressions (4) and (5), described below, the mean absolute error and its standard deviation are estimated:

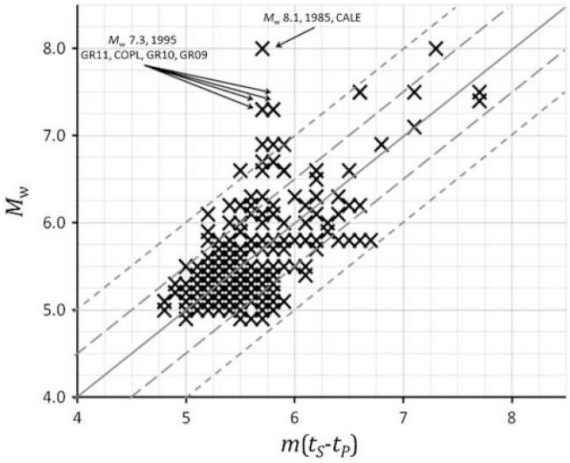

Figure 6. The estimated magnitude $m(t_S–t_P)$ plotted versus the observed M_w of 324 strong-motion records of 101 earthquakes $M_w < 4.8$ recorded from 1985 to 2013 in the Mexican subduction zone.

$$m_{error} = \frac{1}{N}\sum_{j=1}^{N} |M_{w_j} - m(t_S–t_P)_j| \quad (4)$$

$$\sigma_{error} = \left(\frac{1}{N}\sum_{j=1}^{N}(m(t_S–t_P)_j - m_{error})^2\right)^{1/2}. \quad (5)$$

The mean absolute error of the estimated magnitude of the 324 accelerograms corresponding to the training set was $m_{error} = 0.32$, with a standard deviation of $\sigma_{error} = 0.30$. This mean absolute error in magnitude is within the tolerance accepted in the algorithm training process. Assuming an error tolerance in magnitude of ± 0.5 and ± 1.0 as considered in Japan (Hoshiba *et al.*, 2008), the algorithm accurately predicts the magnitude with a success rate of 85% and 96%, respectively. The results of the proposed algorithm, comparing the estimated magnitude $m_{(t_S–t_P)}$ versus the catalog M_w is shown in Figure 6.

Magnitude Estimation $m(t_S–t_P)$ on Independent Test Data from 2014 to 2017

To test the resulting algorithm, a test dataset composed of 76 acceleration records of 28 earthquakes occurring in the Mexican subduction zone from 2014 to 2017 was selected. The magnitude of these 28 earthquakes ranges from $4.8 < M_w < 7.3$. Because of the short time span of the test data available, there are only three earthquakes with $M_w > 6$.

Based on expressions (4) and (5), the mean absolute error of the estimated magnitude was $m_{error} = 0.5$, with a standard deviation $\sigma_{error} = 0.38$. Thus, the resulting algorithm predicted the magnitude $m_{(t_S–t_P)}$ of the test earthquakes within the prescribed error tolerance of ± 0.5. Considering an error tolerance of ± 0.5 and ± 1.0 in the magnitude

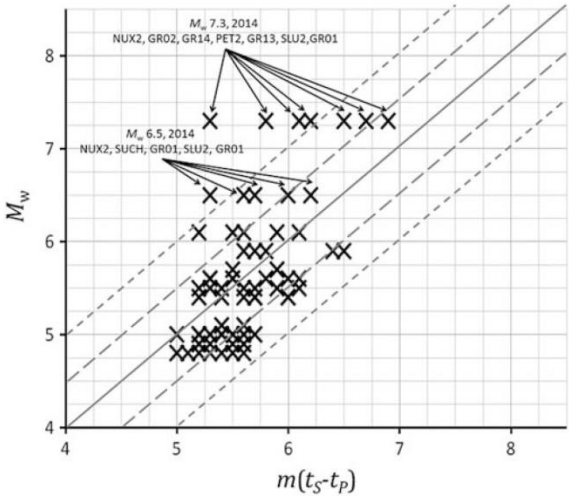

Figure 7. The estimated magnitude $m(t_S–t_P)$ plotted versus the observed M_w for the test data composed of 76 strong-motion records of 28 earthquakes $M_w > 4.8$ recorded from 2014 to 2017 in the Mexican subduction zone.

estimation, the success rate was 70% and 93%, respectively. The magnitude estimated by the $t_S–t_P$ algorithm of the test data is compared with the catalog magnitude in Figure 7 and Ⓔ Table S2.

In the case of the two largest earthquakes in the test dataset, 18 April 2014 (M_w 7.3) and 8 May 2014 (M_w 6.5), the two strong-motion stations closest to the epicenter estimated the magnitude within an error of ± 0.5. The largest errors in magnitude estimation are in stations that are far from the epicenter. However, these other stations, although they are not at an ideal epicentral distance for the algorithm, lie within the established distance range. Thus, they were included for completeness and transparency in the tests.

Performance Evaluation of the $t_S–t_P$ Algorithm on Mexican Subduction Earthquakes $M_w > 4.7$ from 1985 to 2017

Iglesias *et al.* (2007) and Suárez *et al.* (2009) pointed out the difficulties of the $2(t_S–t_P)$ algorithm of correctly identifying the magnitude in the narrow bins prescribed by the Mexico City authorities to issue preventive alerts ($5.5 < M_w < 6$). To avoid this problem of estimating magnitude within very narrow bins, we propose a single earthquake early warning criterion: $M_w \geq 5.8$.

The activation criterion traditionally used by SASMEX to minimize spurious signals (Espinosa-Aranda *et al.*, 1995) requires that two nearby sensors confirm that the magnitude estimate on both is above the prescribed threshold to issue an alert. To test the alerting robustness of the $t_S–t_P$ algorithm using a dataset with a broader range of magnitudes, we use the 89 earthquakes from 1985 to 2017 that meet the criterion of having accelerograms within epicentral distances of

<70 km. (Ⓔ Tables S1 and S2). Therefore, this test evaluates the robustness of the proposed algorithm of discriminating earthquakes above or below the M_w 5.8 threshold, not only the magnitude estimation based on individual accelerograms.

Out of these 89 earthquakes, in 79 cases the seismic alert based on the t_S–t_P algorithm would have been correctly broadcast. In four cases, even though the magnitude of the earthquakes reported in the seismic catalogs was $M_w > 5.8$, the magnitude $m_{(t_S-t_P)}$ was underestimated and no alert would have been issued by the t_S–t_P algorithm. In the case of six events, the algorithm overestimated the magnitude. This means that 89% of the earthquakes would have been correctly classified based on the pre-established warning criteria.

Earthquakes that are larger than the prescribed magnitude threshold, but for which no alert is issued, represent the possibility that an alert may not be issued for a damaging earthquake. Thus, it is worth reviewing the four earthquakes $M_w > 5.8$, for which the magnitude $m_{(t_S-t_P)}$ was underestimated. In the case of the 31 May 1990 earthquake (M_w 5.8), one out of four accelerograms (LLAV) estimated the magnitude as $m_{(t_S-t_P)}$ 6.4. The other three records yield an estimate of $m_{(t_S-t_P)} < 5.8$. The second earthquake is the M_w 6.0 earthquake on 1 January 2004. In this case, the only two stations available estimated $m_{(t_S-t_P)} < 5.8$ (Ⓔ Table S2). Both strong-motion stations lie at the limit of the design criteria of the algorithm, with t_S–t_P times of 5.75 and 6.80 s, respectively. The third case is the 14 June 2004 M_w 5.9 earthquake. It was recorded by five acceleration stations. Station PNTP estimated $m_{(t_S-t_P)}$ 6.3. The next closest station OX04 with t_S–$t_P = 3.01$ s, estimated $m_{(t_S-t_P)}$ 5.5 (Ⓔ Table S2). Finally, the 2 April 2012 M_w 6.0 earthquake, in this case two stations selected estimated $m_{(t_S-t_P)}$ 5.7.

It is worth pointing out that these earthquakes occurred prior to the installation of the new SASMEX stations and, therefore, had a very unfavorable distribution of strong-motion records. Furthermore, they correspond to cases where the reported magnitude is very close to the prescribed threshold of M_w 5.8.

It is also interesting to evaluate the performance of the t_S–t_P algorithm on the eight earthquakes $M_w > 7$ in the dataset (Ⓔ Table S2). Three of these eight earthquakes, the 14 September 1995 Copala (M_w 7.3), the 20 March 2012 (M_w 7.5), and the 18 April 2014 (M_w 7.3), had at least two strong-motion records. Although the true magnitude was underestimated, the t_S–t_P algorithm identified them as large magnitude events and would have issued a correct early warning in all cases (Ⓔ Table S2).

In the case of the other five earthquakes $M_w > 7$, only one accelerogram was available. Thus, we could not evaluate them using the criteria of two confirming stations. Nevertheless, except for the 1985 M_w 8.1 Michoacán earthquake with magnitude estimation $m_{(t_S-t_P)}$ 5.7, the accelerograms of the other four earthquakes were identified as having a magnitude $M_w > 5.8$ and would have had an alert. As mentioned before, in the case of the 1985 Michoacán earthquake, the low acceleration observed at station CALE, located immediately above the hypocenter of the 1985 earthquake, is the result of the nucleation process. From these results, it may be concluded that, even under unfavorable distribution of strong-motion stations, the t_S–t_P algorithm is a reliable tool to issue alerts in a short time span based only on the *P*-wave coda. It is clear that with better seismic coverage, the t_S–t_P algorithm would have a better performance than the one reported here.

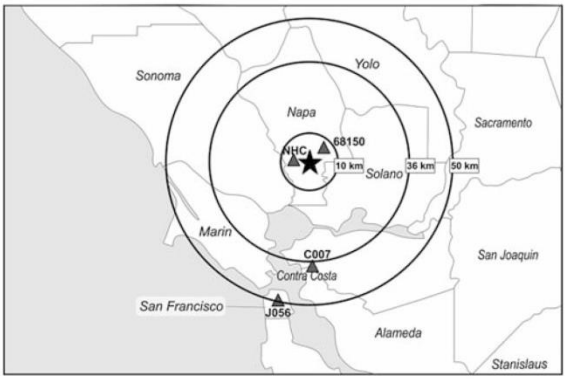

Figure 8. Location of the Napa earthquake of 24 August 2014 (M_w 6) and of the four closest Center for Engineering Strong Motion Data (CESMD) seismic stations. NHC and station 68150 are located at distances of less than 10 km from the epicenter. The stations C007 and JO56, in Berkeley and San Francisco, respectively, are used to determine the arrival of the *S* waves at these locations.

Performance of M_w 6 South Napa Earthquake

The South Napa earthquake is an ideal example of a shallow crustal earthquake that occurs close to important urban areas where the t_S–t_P algorithm can be tested. Several instruments from the Center for Engineering Strong Motion Data (CESMD) recorded the South Napa earthquake of 24 August 2014 (M_w 6) at relatively close distances. The NHC-Huichica Creek and the 68150-Napa College strong-motion stations are the closest to the epicenter and were the first to record the earthquake. They are located 3.9 and 6.4 km away from the epicenter, respectively (Fig. 8).

The application of the t_S–t_P algorithm on the NHC-Huichica Creek seismic record results in a magnitude $m_{(t_S-t_P)}$ 6.2 with a processing time of 2.02 s. The second seismic record in 68150-Napa College processed the algorithm parameters in 2.08 s and estimated a magnitude $m_{(t_S-t_P)}$ 6.5 (Ⓔ Table S3). Based on these two stations, which are the closest to the epicenter, an earthquake early warning would have been broadcast ~2 s after the arrival of the *P* wave (Fig. 9). Considering that the strong shaking coincides generally with the arrival of the *S* waves, the warning time in Berkeley would have been ~10 s, prior to the arrival of the *S* wave, as measured on the C007-Forest Lane strong-motion

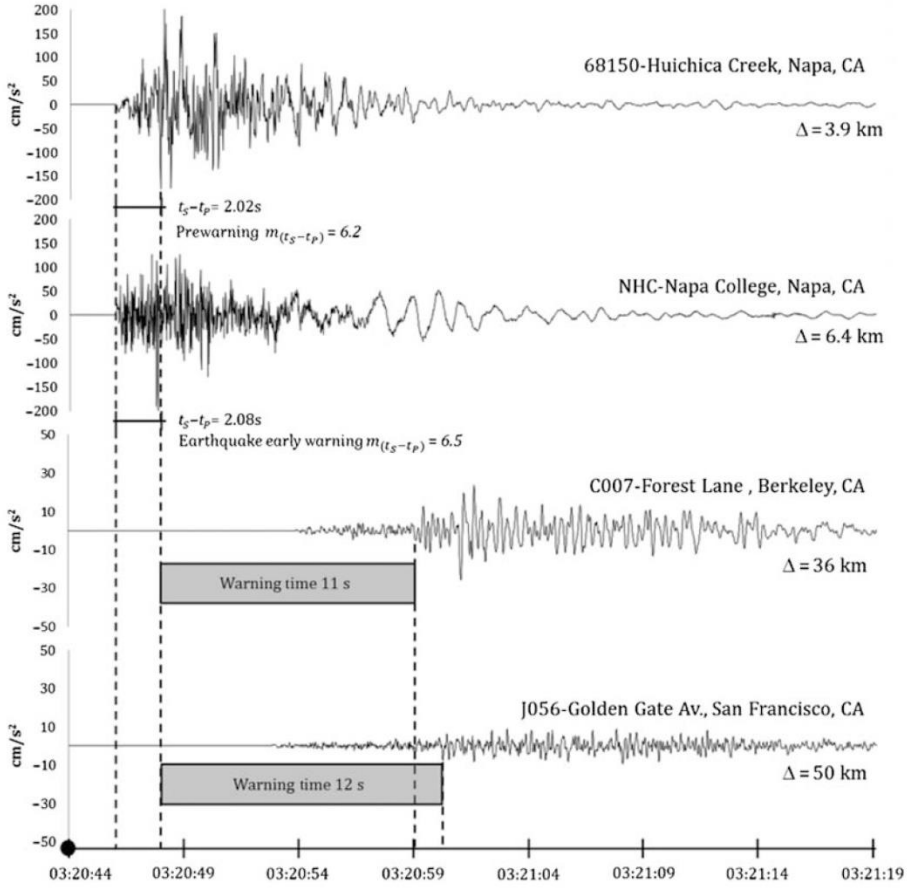

Figure 9. Graphical representation of the performance of t_S–t_P algorithm applied to the 24 August 2014 M_w 6 South Napa, California, earthquake.

record (Figs. 7 and 8). In the case of San Francisco, the warning time would have been 12 s prior to the arrival of strong shaking, based on the *S*-wave arrival at the J056-Golden Gate Avenue station (Fig. 8).

It is interesting to compare the warning times reported by ShakeAlert to those obtained by the t_S–t_P algorithm. The warning time reported for the Napa earthquake based on ShakeAlert was 5 s prior to the arrival of the *S* waves in Berkeley (Allen *et al.*, 2014; Grapenthin *et al.*, 2014a,b). As a result of this process, the t_S–t_P algorithm would almost double the early warning time. A similar result is obtained in San Francisco, where a warning time of 12 s would allow the implementation of basic civil protection procedures.

Summary and Conclusions

The recent expansion of SASMEX created the demand for possible early earthquake warnings for cities that lie close to the seismic zones. In these cases, the 2(t_S–t_P) algorithm, traditionally used by the Mexican seismic early warning system, would shorten the warning time. The purpose of deriving a fast algorithm is to rapidly issue early warnings to cities that lie at distances of a few tens of kilometers from the epicenter. Although the warning time may be of only a few seconds, it may help in establishing rapid and automated civil protection measures.

The proposed t_S–t_P algorithm reduces the time needed to estimate the magnitude in half, making use of two parameters measured from the vertical component: the logarithm of the maximum acceleration max($a(t_S$–$t_P)$) and the logarithmic cumulative quadratic acceleration SA(t_S–t_P). Based on a linear regression model that maps SA(t_S–t_P) and max($a(t_S$–$t_P)$) to M_w, a magnitude $m_{(t_S-t_P)}$ is estimated. The construction of the algorithm makes use of a supervised machine learning process that linearizes piecewise the relation between maximum and cumulative acceleration and the magnitude.

The algorithm was derived using a training dataset composed of 324 accelerograms that correspond to 101 earthquakes occurring between 1985 and 2013 (Ⓔ Table S1).

The mean absolute error is $m_{\text{error}} = 0.32$, within the accepted error tolerance of ± 0.5. In other words, considering an error tolerance of ± 0.5 and ± 1.0 in the magnitude estimation, the success rate was 85% and 96%, respectively.

The test dataset was based on 28 earthquakes occurring in the subduction zone from 2014 to 2017. The results of this test on 76 accelerograms results in the absolute mean error of 0.5. The test dataset had never been seen by the algorithm. Assuming error tolerances of ± 0.5 and ± 1.0 in the magnitude estimation, the success rate was 70% and 93%, respectively.

A test on the performance of t_S–t_P algorithm as a warning tool was conducted using 89 earthquakes in the Mexican subduction zone that met the criteria of having two strong-motion records of nearby stations to issue a seismic warning to avoid false alerts. The results show that 79 earthquakes, out of the 89 tested, were correctly classified as being above or below the magnitude threshold M_w 5.8. The magnitude of six events was overestimated and four were underestimated. This represents a success rate of 89%.

Admittedly, if the detection of the S phase is late, the value of $\max(a(t_S–t_P))$ would increase and, as a result, the magnitude would be overestimated. However, $\max(a(t_S–t_P))$ is measured on the vertical channel, where normally the amplitude of the S waves is smaller relative to the horizontal components, which are not incorporated in the algorithm. Nevertheless, using two stations to issue the alert would help avoid this situation, as shown in Ⓔ Table S2.

Clearly, now that the seismic coverage is substantially better along the subduction zone (Fig. 1), the magnitude estimations will tend to improve. It is important to underline that in the implementation of this algorithm in the earthquake early warning system, new relevant data will be systematically incorporated as part of the process of an effective learning machine.

The t_S–t_P algorithm was also tested on the 24 August 2014 Napa earthquake. The results for a hypothetical earthquake early warning for the Napa earthquake show that the t_S–t_P algorithm would have identified the event as having $M_w > 5.8$ at both stations within 2 s after the arrival of the P phase. This would have given a warning time of ~10 s in the city of Berkeley prior to the arrival of the S waves. In the case of San Francisco, the warning time would have been 12 s.

Early seismic warning algorithms face the challenge of reducing the processing time needed to identify earthquakes and discriminating a magnitude threshold with a high degree of confidence to make a decision on issuing a seismic alert. In this respect, the results of the t_S–t_P algorithm proposed here are encouraging for regions with large population centers close to seismic zones. Although the warning time would be only a few seconds, well-designed protocols could activate a civil protection response designed to mitigate damage and loss of life.

Data and Resources

Accelerograms from the Mexican Seismic Alert System (SASMEX) stations were provided by the Centro de Instrumentación y Registro Sísmico (CIRES) with the authorization of the Institutopara la Seguridad en las Construcciones del Distrito Federal in Mexico City and the Coordinación Estatal de Protección Civil de Oaxaca, Oaxaca state. Strong-motion data for the Mexican subduction earthquakes are from the webpage of the Instituto de Ingeniería of the Universidad Nacional Autónoma de México (UNAM) https://aplicaciones.iingen.unam.mx/AcelerogramasRSM/ (last accessed September 2017). Data from the Global Centroid Moment Tensor Project are from http://www.globalcmt.org/CMTsearch.html (last accessed September 2017).

Acknowledgments

The authors express their gratitude to the institutions that provided the strong-motion data. The governments of Mexico City and of the state of Oaxaca allowed us use the waveform database of Mexican Seismic Alert System (SASMEX). Thanks are also due to the Instituto de Ingeniería of the National University in Mexico (UNAM) for accelerograms in Mexico, and to the Center for Engineering Strong Motion Data for the Napa earthquake records. G. S. acknowledges support of the Consejo Nacional de Ciencia y Tecnología (CONACYT) under Grant 082821. Special thanks are due to Guadalupe Rico, Sandra Ramos, Marisela Palomino, and Cecilia Hernández for their invaluable support in collecting and organizing the data presented in this article. The article was substantially improved by the valuable and constructive comments and corrections made by three anonymous reviewers and by Associate Editor D. Melgar.

References

Allen, R. V. (1978). Automatic earthquake recognition and timing from single traces, *Bull. Seismol. Soc. Am.* **68,** no. 5, 1521–1532.

Allen, R. V., D. Given, T. H. Heaton, and J. Vidale (2014). Successful ShakeAlert performance for the Napa quake, *2014 AGU Fall Meeting*, San Francisco, California, S44D-01.

Anderson, J., R. Quaas, S. K. Singh, J. M. Espinosa, A. Jimenez, J. Lermoand, and S. Alcocer (1995). The Copala, Guerrero, Mexico earthquake of September 14, 1995 ($M_w = 7.4$): A preliminary report, *Seismol. Res. Lett.* **66,** no. 6, 11–39.

Cuéllar, A., J. M. Espinosa-Aranda, G. Suárez, G. Ibarrola, A. Uribe, F. H. Rodríguez, and B. Frontana (2014). The Mexican Seismic Alert System (SASMEX): Its alert signals, broadcast results and performance during the M 7.4 Punta Maldonado earthquake of March 20th, 2012, in *Early Warning for Geological Disasters*, Springer, Berlin, Germany, 71–87.

Cuéllar, A., G. Suárez, and J. M. Espinosa-Aranda (2017). Performance evaluation of the earthquake detection and classification algorithm $2(t_S–t_P)$ of the Seismic Alert System of Mexico (SASMEX), *Bull. Seismol. Soc. Am.* **107,** no. 3, 1451, doi: 10.1785/0120150330.

Dziewonski, A. M., T. A. Chou, and J. H. Woodhouse (1981). Determination of earthquake source parameters from waveform data for studies of global and regional seismicity, *J. Geophys. Res.* **86,** 2825–2852, doi: 10.1029/JB086iB04p02825.

Dziewonski, A. M., G. Ekström, and N. N. Maternovskaya (1999). Centroid-moment tensor solutions for April–June, 1998, *Phys. Earth Planet. In.* **112,** no. 1, 11–19.

Ekström, G., M. Nettles, and A. M. Dziewonski (2012). The global CMT project 2004–2010: Centroid-moment tensors for 13,017

earthquakes, *Phys. Earth Planet. In.* **200/201,** 1–9, doi: 10.1016/j.pepi.2012.04.002.

Espinosa-Aranda, J. M., A. Jimenez, G. Ibarrola, F. Alcantara, A. Aguilar, M. Inostroza, and S. Maldonado (1995). Mexico City seismic alert system, *Seismol. Res. Lett.* **66,** no. 6, 42–53.

Esteva, L. (1988). The Mexico earthquake of September 19, 1985—Consequences, lessons, and impact on research and practice, *Earthq. Spectra* **4,** no. 3, 413–426.

Grapenthin, R., I. Johanson, and R. M. Allen (2014a). Operational real-time GPS-enhanced earthquake early warning, *J. Geophys. Res.* **119,** no. 10, 7944–7965.

Grapenthin, R., I. Johanson, and R. M. Allen (2014b). The 2014 M_w 6.0 Napa earthquake, California: Observations from real-time GPS-enhanced earthquake early warning, *Geophys. Res. Lett.* **41,** no. 23, 8269–8276.

Hoshiba, M., O. Kamigaichi, M. Saito, S. Y. Tsukada, and N. Hamada (2008). Earthquake early warning starts nationwide in Japan, *Eos Trans. AGU* **89,** no. 8, 73–74.

Iglesias, A., S. K. Singh, M. Ordaz, M. A. Santoyo, and J. Pacheco (2007). The seismic alert system for Mexico City: An evaluation of its performance and a strategy for its improvement, *Bull. Seismol. Soc. Am.* **97,** no. 5, 1718–1729.

McCann, W. R., S. P. Nishenko, L. R. Sykes, and J. Krause (1979). Seismic gaps and plate tectonics: Seismic potential for major boundaries, in *Earthquake Prediction and Seismicity Patterns*, Birkhäuser, Basel, Switzerland, 1082–1147.

Mendez, A. J., and J. G. Anderson (1991). The temporal and spatial evolution of the 19 September 1985 Michoacan earthquake as inferred from near-source ground-motion records, *Bull. Seismol. Soc. Am.* **81,** no. 3, 844–861.

Nakamura, Y. (1996). Real-time information systems for seismic hazards mitigation UrEDAS, *Q. Rep. Railway Tech. Res. Inst.* **37,** 112–127.

Perez-Yañez, C., L. Ramirez-Guzman, G. A. L. Ruiz, D. R. Delgado, A. Macias C Marco, G. H. Sandoval, N. L. Alcantara, and R. A. Quiroz (2014). Strong ground motion database system for the Mexican seismic network, *AGU Fall Meeting*, San Francisco, California, 14–19 December.

Rosenblueth, E. (1986). The 1985 earthquake: Causes and effects in Mexico City, *J. Am. Concr. Inst.* **8,** no. 5, 23–24.

Singh, S. K., L. Astiz, and J. Havskov (1981). Seismic gaps and recurrence periods of large earthquakes along the Mexican subduction zone: A reexamination, *Bull. Seismol. Soc. Am.* **71,** no. 3, 827–843.

Suárez, G., D. Novelo, and E. Mansilla (2009). Performance evaluation of the seismic alert system (SAS) in Mexico City: A seismological and a social perspective, *Seismol. Res. Lett.* **80,** no. 5, 707–716.

Centro de Instrumentación y Registro Sísmico (CIRES)
Anaxagoras 814
Colonia Narvarte
Mexico City, Mexico 03020
cuellara@cires.org.mx
espinosajm@cires.org.mx
(A.C., J.M.E.-A.)

Instituto de Geofísica
Universidad Nacional Autónoma de México
Mexico City, Mexico 04510
gerardo@geofisica.unam.mx
(G.S.)

Manuscript received 6 April 2017;
Published Online 19 December 2017

Electronic Supplement

The supplemental material contains two Tables. **Table S1** shows the hypocentral data of the catalog of 116 earthquakes selected from the Moment Tensor Catalog (CMT) and from the catalog of the Mexican Seismological Service (SSN). **Table S2** shows the results of the performance evaluation of the t_S-t_P algorithm on 116 Mexican subduction earthquakes. **Table S2** also shows the magnitude $m(t_S$-$t_P)$ obtained from parameters $Av(t_S$-$t_P)$ and $Max(v(t_S$-$t_P))$. The last two columns indicate whether an alert would have been issued.

List of the Table Captions

Table S1. Catalog of Mexican Earthquakes in the subduction zone from 1985 to 2015 M_w≥4.8 recorded by strong motion instruments at distances < 70 km from the epicenter, acceleration records > 4 cm/s^2 and t_S-t_P times < 7 s.

Table S2. Performance evaluation of the t_S-t_P algorithm on 359 acceleration records from the selected 116 Mexican subduction earthquakes

Table S1. Catalog of Mexican Earthquakes in the subduction zone from 1985 to 2015 M_w≥4.8 recorded by strong motion instruments at distances < 70 km from the epicenter, acceleration records > 4 cm/s^2 and t_S-t_P times < 7 s.

Global Centroid Moment Tensor Catalog (CMT Catalog)						Mexican Seismological Service (SSN)		
Date	Centroid Time	Latitude °	Longitude °	Depth km	M_w	Latitude °	Longitude °	Depth km
19/09/1985	13:18:25	17.91	-101.99	21.3	8.1	18.081	-102.94	15
29/05/1986	20:31:15	16.4	-98.12	57.2	5.2	16.851	-98.93	35.6
08/02/1988	13:51:32	17.03	-100.35	47.8	5.8	17.494	-101.16	19.2
10/03/1989	05:19:49	16.91	-100.44	46.8	5.4	17.446	-101.09	17.6
25/04/1989	14:29:06	16.83	-99.12	15.0	6.9	16.603	-99.40	19
02/05/1989	09:30:18	16.82	-99.35	47.9	5.5	16.637	-99.51	13.4
08/10/1989	22:32:41	17.12	-99.93	35	5.1	17.189	-100.21	36
13/01/1990	02:07:32	16.33	-99.67	34.2	5.3	16.82	-99.63	12.2
11/05/1990	23:43:52	17.24	-100.56	15	5.5	17.046	-100.84	11.7
31/05/1990	07:35:24	16.77	-100.12	26	5.8	17.106	-100.89	15.8
14/01/1991	21:11:15	18.39	-101.37	67.8	5.5	17.838	-101.85	24.7
12/02/1992	11:57:00	17.78	-101.14	33.9	5.2	17.733	-101.06	1.7
31/03/1992	20:56:41	16.99	-100.65	15	5.4	17.233	-101.3	11
31/03/1993	10:18:19	17.29	-100.89	26.2	5.5	17.18	-101.02	8
24/10/1993	07:52:23	16.77	-98.61	21.8	6.6	16.54	-98.98	19
14/09/1995	14:04:41	16.73	-98.54	21.8	7.3	16.31	-98.88	22
09/10/1995	15:36:29	19.34	-104.80	15.0	8.0	18.74	-104.67	5
30/10/1995	14:47:59	16.55	-98.13	15.8	5.6	16.35	-98.51	27

25/02/1996	09:18:03	16.1	-97.74	15	5.9	15.86	-98.13	17
13/03/1996	21:04:23	16.93	-98.86	29.4	5.1	16.52	-99.08	18
27/03/1996	12:34:53	16.44	-97.95	21	5.5	16.21	-98.25	7
15/07/1996	21:23:42	17.50	-101.12	22.4	6.6	17.45	-101.16	20
18/07/1996	08:16:47	17.35	-101.02	26.2	5.4	17.54	-101.2	20
11/01/1997	20:28:40	18.34	-102.58	40.0	7.1	17.91	-103.04	16
16/01/1997	21:41:17	18.23	-102.55	47.2	5.5	17.94	-102.76	25
21/01/1997	21:20:02	16.49	-97.99	39.7	5.5	16.44	-98.15	18
03/03/1998	07:38:29	16.26	-96.12	44.2	5.2	15.71	-96.47	12
09/05/1998	17:03:16	17.31	-101	36.2	5.2	17.34	-101.41	18
16/05/1998	17:41:59	17.56	-101.54	33	5.2	17.25	-101.35	14
05/07/1998	19:55:10	16.92	-99.73	37.6	5.3	16.83	-100.12	5
30/09/1999	16:31:23	16.20	-96.96	46.8	7.4	15.95	-97.03	16
11/04/2000	18:35:44	18.19	-102.51	51.9	5.2	18.06	-102.64	10
09/08/2000	11:41:53	18.13	-102.39	33.0	6.5	17.99	-102.66	16
01/12/2000	14:07:46	17.98	-102.31	52.2	5.4	17.94	-102.58	14
08/10/2001	03:39:26	17.32	-99.89	15	5.8	16.94	-100.14	4
29/10/2001	05:23:18	17.49	-99.44	15	5	17	-100.19	4
07/06/2002	16:03:02	16.25	-96.65	40	5.2	15.98	-96.88	14
19/06/2002	21:50:11	16.74	-97.95	24.2	5.3	16.24	-98.09	8
25/09/2002	18:14:50	16.86	-99.79	19	5.3	16.86	-100.12	5
27/09/2002	07:05:00	17.44	-100.1	36.4	5.1	17.16	-100.59	37
08/11/2002	23:20:47	16.34	-97.99	17.3	5.2	16.21	-98.14	4
10/12/2002	03:09:33	17.17	-101.66	66.7	5.4	17.41	-101.26	29
10/01/2003	02:08:03	16.88	-99.85	44.7	5.2	16.97	-100.3	30
22/01/2003	02:06:49	18.86	-103.90	26.0	7.5	18.6	-104.22	9
27/03/2003	07:44:24	18.28	-101.8	30.9	5.2	18.01	-101.78	25
01/01/2004	23:31:53	17.45	-101.40	15.0	6.0	17.34	-101.42	6
01/01/2004	23:58:06	17.39	-101.32	20.4	5.6	17.3	-101.36	14
13/01/2004	19:50:27	16.45	-96.83	32.5	5.1	16.01	-97.3	20
13/01/2004	21:29:00	16.26	-96.94	30.3	5.4	15.99	-97.15	16
06/02/2004	19:11:36	18.36	-102.8	35.2	5.1	18.16	-102.83	12
14/06/2004	22:54:28	16.46	-97.92	18	5.9	16.22	-98.16	10
14/08/2005	02:52:04	16.3	-98.07	12	5.4	15.99	-98.4	15
31/07/2006	18:25:23	18.62	-104.08	24.1	5.3	18.83	-104.11	10
13/08/2006	15:14:28	18.45	-103.63	23.5	5.3	18.23	-103.62	13
19/08/2006	05:41:31	16.26	-97.27	26.6	5.6	15.91	-97.3	52
08/11/2006	17:18:49	16.27	-96.43	37.9	5.1	16.05	-96.54	45
15/03/2007	13:13:02	16.21	-97	12	5.3	16.08	-97.26	15
13/04/2007	05:42:27	17.37	-100.14	42.7	6.0	17.09	-100.44	41
13/04/2007	08:43:50	17.4	-100.23	66.8	5.3	17.27	-100.27	51
19/04/2007	10:02:14	17.26	-101.03	23.6	5.3	17.21	-101.37	24
28/04/2007	13:56:39	17.04	-99.64	29.9	5.1	16.94	-99.82	9
31/05/2007	10:11:14	18.94	-103.94	22.2	5.1	18.66	-104.14	11
06/11/2007	06:35:46	17.14	-99.91	18.4	5.4	17.08	-100.14	9
30/07/2008	10:23:35	16.3	-96.04	35.5	5.3	15.98	-96.1	49
20/10/2008	05:01:10	17.43	-100.95	29.3	5.2	17.25	-101.3	25
27/03/2009	08:48:20	17.42	-100.6	38.7	5.3	17.35	-100.82	30
27/04/2009	16:46:32	17.06	-99.41	32.2	5.8	16.9	-99.58	7
09/02/2010	00:47:45	16.12	-96.66	30.3	5.7	15.9	-96.86	37
19/03/2010	20:48:51	17.38	-100.91	24.3	5	17.22	-100.97	15
16/04/2010	10:01:13	16.52	-98.22	15.2	5.2	16.14	-98.41	10
20/04/2010	02:28:59	16.28	-98.4	23	5	16.07	-98.34	5
25/05/2010	23:36:22	17.39	-100.96	23.6	5.1	17.11	-101.2	15
30/06/2010	07:22:33	16.47	-97.77	17.8	6.3	16.22	-98.03	8
26/04/2011	11:07:33	16.91	-99.45	22.9	5.4	16.71	-99.69	7
05/05/2011	13:24:09	16.85	-98.72	30.7	5.7	16.61	-98.91	11
09/07/2011	12:42:30	16.01	-96.32	18.6	5.1	15.87	-96.42	22
20/03/2012	18:02:55	16.60	-98.39	15.4	7.5	16.251	-98.52	16
21/03/2012	11:36:18	16.76	-98.27	29.7	5	16.51	-98.5	20
24/03/2012	01:58:42	16.46	-98.05	30.7	4.9	16.26	-98.29	10
01/04/2012	22:23:52	16.58	-98.52	39.3	5.3	16.46	-98.54	20
02/04/2012	17:36:46	16.58	-98.35	12.0	6.1	16.27	-98.47	10
11/04/2012	22:55:17	18.10	-102.97	20.5	6.7	17.9	-103.06	16
13/04/2012	10:10:06	16.35	-98.23	13.9	5.3	16.11	-98.34	14
13/04/2012	13:06:30	16.38	-98.17	12.2	5	16.22	-98.15	16
24/07/2012	05:25:33	16.57	-98.07	18.5	5.1	16.27	-98.31	5

22/09/2012	12:30:02	16.55	-98.1	19.5	5.5	16.23	-98.3	2
18/12/2012	01:38:26	16.31	-95.7	25.9	5.3	16.1	-95.87	20
20/02/2013	21:23:13	18.5	-103.91	18.3	5.6	18.6	-104.04	5
26/03/2013	13:04:53	16.28	-98.22	12.3	5.4	15.78	-98.61	10
26/03/2013	13:12:23	16.27	-98.21	15.5	5.2	15.94	-98.45	10
05/04/2013	01:58:49	17.26	-100.7	26.2	5.5	17.08	-100.82	17
12/04/2013	03:45:10	17.95	-101.47	35.8	5.3	17.78	-101.58	35
22/04/2013	01:16:35	18.05	-102.19	26.6	6.1	17.87	-102.19	10
06/08/2013	20:17:34	16.73	-98.4	32	5	16.49	-98.58	16
16/08/2013	15:33:03	16.77	-98.43	27	5.3	16.54	-98.59	20
21/08/2013	12:38:36	17.00	-99.54	23.3	6.2	16.79	-99.56	20
21/08/2013	13:02:22	17	-99.51	29	5.3	16.73	-99.7	11
06/10/2013	14:27:58	17.05	-99.84	22.3	5	16.83	-100.1	10
06/10/2013	15:11:01	17.05	-99.97	20.6	5.1	16.81	-100.11	10
02/01/2014	23:54:01	16.31	-97.85	23.2	4.8	16.08	-97.96	1
18/04/2014	14:27:36	17.55	-101.25	18.9	7.3	17.18	-101.19	10
08/05/2014	17:00:20	17.36	-100.74	21.3	6.5	17.11	-100.87	17
10/05/2014	07:36:05	17.31	-100.82	20.7	6.1	17.06	-100.95	12
10/05/2014	17:26:40	17.23	-100.71	22.2	5	16.91	-100.95	20
24/05/2014	08:24:50	16.52	-98.28	16.2	5.7	16.21	-98.42	18
04/08/2014	00:21:54	17.35	-100.67	32.8	5.1	17.09	-100.84	10
11/08/2014	01:09:40	16.38	-98.29	21.6	4.8	16.38	-98.19	10
13/08/2014	06:48:13	16.36	-98.28	12	5.4	16.13	-98.35	10
08/09/2014	20:30:41	16.43	-98.16	18	4.9	16.33	-98.32	15
11/10/2014	16:46:05	16.35	-95.68	24	5.5	15.97	-95.61	10
12/01/2015	00:59:21	16.45	-97.63	29	4.9	16.19	-98.09	2
05/04/2015	06:55:06	16.19	-98.37	21.4	4.8	15.975	-98.664	16
25/06/2015	10:31:51	16.26	-98.16	69.5	4.8	16.15	-98.08	16
14/07/2015	01:25:35	18.29	-103.33	22.8	4.9	18.18	-103.49	2
30/09/2015	17:25:59	17.95	-101.27	64.7	5.4	17.83	-101.52	30
23/11/2015	20:41:25	17.1	-98.74	32.8	5.6	16.86	-98.94	10

Table S2. Performance evaluation of the t_S-t_P algorithm on 359 acceleration records from the selected 116 Mexican subduction earthquakes.

CMT Catalogue			Seismic Field Sensor Information			Performance of $m(t_S\text{-}t_P)$ algorithm						Hypothetical Performance of SASMEX		
Date	Centroid Time	M_w	Sensor within a radius of 70 Km since the Hypo-center	Epi-central Distance [km]	Hypo-central Distance [km]	t_S-t_P [s]	$Av(t_S\text{-}t_P)$	$Max(v(t_S\text{-}t_P))$	$m(t_S\text{-}t_P)$	tol = 0.5	tol = 1.0	Trigger Warning Range	EEW Issue	Evaluation According with M_w
19/09/1985	13:18:25	8.1	CALE	20.7	25.5	3.31	4.14	2.81	5.6			<5.8	No Apply	---
29/05/1986	20:31:15	5.2	VIGA	34.5	49.6	6.21	3.99	2.55	5.5	OK	OK	<5.8	No Apply	---
08/02/1988	13:51:32	5.8	PAPN	21.9	29.1	4.06	5.50	4.04	6.2	OK	OK	≥5.8	Earthquake Warning	OK
			LLAV	43.4	47.5	5.81	4.92	3.38	6.0	OK	OK	≥5.8		
10/03/1989	05:19:49	5.4	PAPN	13.6	22.2	3.45	4.83	3.51	5.5	OK	OK	<5.8		
			PETA	22.3	28.4	3.80	4.40	2.63	5.4	OK	OK	<5.8	No Alert	OK
			LLAV	34.4	38.8	5.17	4.63	2.99	5.8	OK	OK	≥5.8		
25/04/1989	14:29:06	6.9	VIGA	24.6	31.1	5.22	5.29	3.61	6.3		OK	≥5.8	No Apply	---
02/05/1989	09:30:18	5.5	CPDR	19.4	23.6	3.00	3.46	2.15	5.0	OK	OK	<5.8		
			SMR2	16.4	21.2	3.01	4.68	3.57	5.7	OK	OK	<5.8	No Alert	OK
			VIGA	33.0	35.6	4.35	3.87	2.54	5.4	OK	OK	<5.8		
08/10/1989	22:32:41	5.1	PARS	16.3	40.2	4.71	4.73	3.06	5.8		OK	≥5.8		
			CAYA	16.3	39.5	5.03	4.19	2.70	5.4	OK	OK	<5.8	No Alert	OK
			ATYC	24.6	43.6	5.29	4.04	2.77	5.5	OK	OK	<5.8		
			COYC	24.0	43.3	5.34	3.97	2.74	5.3	OK	OK	<5.8		

13/01/1990	02:07:32	5.3	CPDR	5.4	13.3	2.41	4.40	2.99	5.2	OK	OK	<5.8	Earthquake Warning	**Over-estimation**
			ACAZ	17.9	21.7	3.44	5.26	4.23	5.9		OK	≥5.8		
			ACAD	26.9	29.6	3.90	3.91	2.51	5.3	OK	OK	<5.8		
			ACAR	23.7	26.7	4.02	4.41	3.09	5.2	OK	OK	<5.8		
			ACAP	31.3	33.6	4.26	4.18	2.48	5.4	OK	OK	<5.8		
			MSAS	27.4	30.2	4.46	4.25	3.02	5.5	OK	OK	<5.8		
			XALT	30.5	33.1	5.00	4.02	2.38	5.8	OK	OK	≥5.8		
11/05/1990	23:43:52	5.5	SLUI	24.4	27.1	3.35	3.71	2.56	5.1	OK	OK	<5.8	No Alert	OK
			LLAV	31.9	34.1	4.41	4.25	2.64	5.6	OK	OK	<5.8		
31/05/1990	07:35:24	5.8	SLUI	17.4	23.5	3.14	4.80	3.60	5.3	OK	OK	<5.8	No Alert	**Under-estimation**
			LLAV	27.4	31.7	4.21	5.67	4.07	6.5		OK	≥5.8		
			PAPN	28.6	32.7	4.45	4.64	3.34	5.7	OK	OK	<5.8		
			MAGY	44.7	47.5	5.53	4.02	2.79	5.4	OK	OK	<5.8		
14/01/1991	21:11:15	5.5	UNIO	16.3	29.6	4.00	4.44	3.19	5.3	OK	OK	<5.8	No Apply	---
12/02/1992	11:57:00	5.2	PETA	30.7	30.7	6.32	4.10	2.50	5.2	OK	OK	<5.8	No Apply	---
31/03/1992	20:56:41	5.4	PAPN	30.3	32.2	4.06	4.00	2.63	5.5	OK	OK	<5.8	No Alert	OK
			PETA	32.6	34.4	4.51	3.49	1.94	5.2	OK	OK	<5.8		
			LLAV	57.1	58.2	6.07	3.69	1.83	5.9	OK	OK	≥5.8		
31/03/1993	10:18:19	5.5	PAPN	15.7	17.6	3.00	4.45	2.97	5.4	OK	OK	<5.8	No Alert	OK
			SLUI	17.2	18.9	3.25	3.70	2.20	5.1	OK	OK	<5.8		
			GR02	25.8	27.1	3.93	3.97	2.42	5.6	OK	OK	<5.8		
24/10/1993	07:52:23	6.6	GR11	19.0	26.9	3.32	5.41	4.03	6.0		OK	≥5.8	Earthquake Warning	OK
			GR10	11.8	22.4	3.86	5.44	4.37	6.3	OK	OK	≥5.8		
			COPL	7.4	20.4	4.00	5.74	4.19	6.7	OK	OK	≥5.8		
			GR09	36.1	40.8	5.16	4.94	3.44	5.9		OK	≥5.8		
			VIGA	36.1	40.8	5.48	5.05	3.51	6.2	OK	OK	≥5.8		
14/09/1995	14:04:41	7.3	GR11	30.8	37.8	2.00	4.26	3.30	5.8			≥5.8	Earthquake Warning	OK
			COPL	33.6	40.2	3.45	4.01	2.57	5.6			<5.8		
			GR10	38.3	44.2	3.50	4.01	2.59	5.6			<5.8		
			GR09	61.1	64.9	5.78	4.07	2.43	5.9			≥5.8		
09/10/1995	15:36:29	8.0	MZ01	50.2	50.4	6.68	6.14	4.60	7.5	OK	OK	≥5.8	No Apply	---
30/10/1995	14:47:59	5.6	PNTP	50.2	57.1	6.65	3.87	2.45	5.5	OK	OK	<5.8	No Apply	---
25/02/1996	09:18:03	5.9	PNTP	51.1	54.0	6.71	3.43	1.73	5.2		OK	<5.8	No Apply	---
13/03/1996	21:04:23	5.1	COPL	14.2	23.0	3.66	3.77	2.47	5.2	OK	OK	<5.8	No Alert	OK
			VIGA	30.2	35.2	3.73	5.12	4.03	5.7		OK	<5.8		
27/03/1996	12:34:53	5.5	PNTP	25.6	26.6	3.77	4.46	3.17	5.3	OK	OK	<5.8	No Apply	---
15/07/1996	21:23:42	6.6	PAPN	18.4	27.2	3.67	4.88	3.49	5.7		OK	<5.8	Earthquake Warning	OK
			PETA	15.6	25.4	4.50	4.89	3.35	5.9		OK	≥5.8		
			AZIH	37.4	42.4	5.62	4.38	2.90	5.8		OK	≥5.8		
			GR02	47.7	51.7	6.94	4.01	2.31	5.8		OK	≥5.8		
18/07/1996	08:16:47	5.4	PETA	7.8	21.5	3.37	4.38	2.90	5.3	OK	OK	<5.8	No Alert	OK
			PAPN	28.4	34.7	3.81	4.16	2.71	5.4	OK	OK	<5.8		
11/01/1997	20:28:40	7.1	CALE	35.8	39.2	4.79	6.28	5.23	7.0	OK	OK	≥5.8	No Apply	---
16/01/1997	21:41:17	5.5	CALE	14.0	28.6	4.08	4.53	3.31	5.4	OK	OK	<5.8	No Apply	---
21/01/1997	21:20:02	5.5	JAMI	39.7	43.8	5.61	4.16	2.70	5.4	OK	OK	<5.8	No Apply	---
03/03/1998	07:38:29	5.2	PANG	5.1	13.0	4.06	4.41	2.97	5.3	OK	OK	<5.8	No Apply	---
09/05/1998	17:03:16	5.2	PET2	26.2	31.8	3.11	4.29	2.80	5.6	OK	OK	<5.8	No Alert	OK
			COYQ	39.1	43.1	4.11	3.96	2.52	5.5	OK	OK	<5.8		
			GR01	40.6	44.5	4.28	3.80	2.66	5.2	OK	OK	<5.8		
16/05/1998	17:41:59	5.2	COYQ	35.1	37.8	4.46	3.83	2.57	5.3	OK	OK	<5.8	No Apply	---
05/07/1998	19:55:10	5.3	GR06	20.0	20.7	2.94	3.76	2.55	5.2	OK	OK	<5.8	No Alert	OK
			COYC	17.9	18.6	3.22	3.79	2.49	5.3	OK	OK	<5.8		
			GR05	19.3	20.0	3.34	3.71	2.19	5.1	OK	OK	<5.8		
			ACAC	29.8	30.2	4.70	4.41	2.95	5.3	OK	OK	<5.8		

30/09/1999	16:31:23	7.4	LANE	17.3	23.6	5.38	6.25	4.57	7.9	OK	OK	≥5.8	No Apply	---
11/04/2000	18:35:44	5.2	CALE	12.7	16.1	4.18	3.64	2.17	5.5	OK	OK	<5.8	No Apply	---
09/08/2000	11:41:53	6.5	CALE	13.5	21.0	4.00	5.33	4.11	6.2	OK	OK	≥5.8	No Apply	---
01/12/2000	14:07:46	5.4	CALE	23.7	27.5	4.11	4.01	2.45	5.7	OK	OK	<5.8	No Apply	---
08/10/2001	03:39:26	5.8	COYC	8.2	9.1	1.44	5.26	4.27	5.9	OK	OK	≥5.8	Earthquake Warning	OK
			CAYR	18.1	18.5	2.50	3.90	2.66	5.5	OK	OK	<5.8		
			GR06	22.3	22.7	3.20	4.77	3.44	5.5	OK	OK	<5.8		
			GR04	30.3	30.5	3.74	4.16	2.66	5.3	OK	OK	<5.8		
			ACAD	30.6	30.9	4.42	5.00	3.34	6.2	OK	OK	≥5.8		
			ACAC	33.3	33.6	4.60	4.59	2.86	5.7	OK	OK	<5.8		
			ACAR	34.0	34.2	4.79	5.58	3.90	6.2	OK	OK	≥5.8		
			GR03	58.8	58.9	5.65	3.37	1.71	5.1		OK	<5.8		
			ACAZ	41.6	41.8	5.91	4.77	2.95	6.1	OK	OK	≥5.8		
29/10/2001	05:23:18	5	GR04	22.0	22.4	3.11	3.38	2.10	4.9	OK	OK	<5.8	No Apply	---
07/06/2002	16:03:02	5.2	LANE	34.0	36.7	4.37	3.25	1.90	4.6		OK	<5.8	No Apply	---
19/06/2002	21:50:11	5.3	JAMI	30.0	31.2	3.37	3.69	2.27	5.6	OK	OK	<5.8	No Apply	---
25/09/2002	18:14:50	5.3	COYC	14.8	15.7	3.19	3.66	2.30	5.5	OK	OK	<5.8	No Alert	OK
			ACAD	27.3	27.8	3.90	4.21	2.92	5.4	OK	OK	<5.8		
			ACAR	31.5	31.9	4.16	3.79	2.27	5.3	OK	OK	<5.8		
			ACAC	29.7	30.1	4.46	4.19	2.73	5.4	OK	OK	<5.8		
			ACAZ	37.1	37.4	5.01	3.79	2.02	5.4	OK	OK	<5.8		
27/09/2002	07:05:00	5.1	ATYC	18.2	41.3	4.06	4.87	3.71	5.4	OK	OK	<5.8	No Alert	OK
			SUCH	8.7	38.1	4.18	4.02	2.62	5.6	OK	OK	<5.8		
			GR04	26.6	45.6	4.38	4.26	2.56	5.6	OK	OK	<5.8		
08/11/2002	23:20:47	5.2	JAMI	36.0	36.3	4.41	3.58	2.14	5.4	OK	OK	<5.8	No Alert	OK
			OMTP	57.7	57.9	6.60	3.48	1.99	5.2	OK	OK	<5.8		
10/12/2002	03:09:33	5.4	COYQ	22.6	36.8	5.08	4.67	3.14	5.8	OK	OK	≥5.8	No Alert	OK
			AZIH	30.6	42.2	5.68	4.43	2.90	5.3	OK	OK	<5.8		
			SLUI	43.1	52.0	6.77	3.77	2.34	5.2	OK	OK	<5.8		
10/01/2003	02:08:03	5.2	GR04	17.3	34.6	3.27	4.57	3.13	5.6	OK	OK	<5.8	No Alert	OK
			ATYC	29.4	42.0	4.06	4.29	2.85	5.6	OK	OK	<5.8		
			GR05	20.6	36.4	4.46	4.65	3.36	5.7	OK	OK	<5.8		
			GR03	41.6	51.3	5.43	3.89	2.51	5.5	OK	OK	<5.8		
			OCLL	46.9	56.0	6.49	3.49	2.01	5.2	OK	OK	<5.8		
			ACAD	48.5	57.0	6.97	3.53	1.76	5.5	OK	OK	<5.8		
22/01/2003	02:06:49	7.5	MZ02	50.3	51.1	4.70	5.47	4.23	6.3			≥5.8	No Apply	---
27/03/2003	07:44:24	5.2	UNIO	4.1	25.4	4.66	3.66	2.05	5.7	OK	OK	<5.8	No Apply	---
01/01/2004	23:31:53	6.0	COYQ	40.2	40.7	6.42	3.87	2.14	5.5	OK	OK	<5.8	No Alert	**Under-estimation**
			GR01	41.7	42.2	6.80	3.92	2.85	5.1		OK	<5.8		
01/01/2004	23:58:06	5.6	PET2	26.9	30.4	5.08	3.45	1.79	5.2	OK	OK	<5.8	No Alert	OK
			COYQ	34.4	37.2	6.01	3.56	1.86	5.5	OK	OK	<5.8		
13/01/2004	19:50:27	5.1	LANE	14.0	24.4	4.34	3.40	2.12	4.9	OK	OK	<5.8	No Alert	OK
			OX17	61.0	64.7	5.70	3.83	2.60	5.3	OK	OK	<5.8		
13/01/2004	21:29:00	5.4	OX07	9.0	18.6	3.97	3.51	2.07	5.2	OK	OK	<5.8	No Alert	OK
			LANE	6.0	17.1	4.00	4.29	2.87	5.6	OK	OK	<5.8		
			RIOG	31.9	35.7	5.30	3.88	2.34	5.5	OK	OK	<5.8		
			OX17	55.4	58.1	6.21	4.30	2.83	5.7	OK	OK	<5.8		
06/02/2004	19:11:36	5.1	CALE	12.4	17.2	4.38	3.39	2.03	4.9	OK	OK	<5.8	No Apply	---
14/06/2004	22:54:28	5.9	PNTP	17.2	20.0	2.96	5.38	4.18	6.3	OK	OK	≥5.8	No Alert	**Under-estimation**
			OX04	28.6	30.3	3.10	4.22	2.73	5.5	OK	OK	<5.8		
			JAMI	37.9	39.4	3.69	4.53	3.15	5.5	OK	OK	<5.8		
			OX02	35.0	36.4	5.82	3.86	2.61	5.4	OK	OK	<5.8		
			OX01	32.4	33.9	6.13	3.48	1.88	5.3		OK	<5.8		
14/08/2005	02:52:04	5.4	OX01	33.6	36.8	4.32	3.80	2.29	5.3	OK	OK	<5.8	No Apply	---

31/07/2006	18:25:23	5.3	COJU	21.8	24.0	5.52	3.37	1.97	4.9	OK	OK	<5.8	No Apply	---
13/08/2006	15:14:28	5.3	SJAL	37.7	39.9	4.34	4.46	3.28	5.3	OK	OK	<5.8	No Alert	OK
			MARU	30.2	32.9	4.39	4.29	2.86	5.6	OK	OK	<5.8		
19/08/2006	05:41:31	5.6	RIOG	18.8	55.3	3.41	3.86	2.69	5.4	OK	OK	<5.8	No Apply	---
08/11/2006	17:18:49	5.1	TAMA	22.5	51.9	4.47	3.68	2.36	5.5	OK	OK	<5.8	No Alert	OK
			GALE	9.4	47.2	4.83	4.42	3.23	5.2	OK	OK	<5.8		
15/03/2007	13:13:02	5.3	OX07	23.6	28.1	4.54	3.34	1.97	4.8	OK	OK	<5.8	No Alert	OK
			LANE	16.0	22.0	4.67	3.78	2.52	5.2	OK	OK	<5.8		
			RIOG	20.8	25.7	4.94	3.47	1.96	5.2	OK	OK	<5.8		
			OX05	37.8	40.8	6.28	3.58	1.81	5.6	OK	OK	<5.8		
13/04/2007	05:42:27	6.0	ATYC	13.0	43.1	3.83	5.64	4.19	6.5	OK	OK	≥5.8	Earthquake Warning	OK
			GR04	10.5	42.4	4.72	5.63	4.30	6.6		OK	≥5.8		
			GR03	22.3	46.7	5.83	4.89	3.21	6.1	OK	OK	≥5.8		
			COYC	39.7	57.1	6.58	4.45	2.76	5.5	OK	OK	<5.8		
			GR05	36.4	54.8	6.65	4.96	3.29	6.2	OK	OK	≥5.8		
13/04/2007	08:43:50	5.3	GR04	17.6	54.0	4.07	4.72	3.28	5.5	OK	OK	<5.8	No Alert	OK
			ATYC	18.8	54.4	4.28	4.63	3.40	5.6	OK	OK	<5.8		
			COYC	34.8	61.7	5.45	3.78	1.99	5.4	OK	OK	<5.8		
			GR05	31.7	60.1	5.52	4.38	2.91	5.2	OK	OK	<5.8		
			GR03	41.2	65.6	6.21	3.75	2.37	5.2	OK	OK	<5.8		
19/04/2007	10:02:14	5.3	GR01	37.1	44.3	2.93	3.79	2.33	5.3	OK	OK	<5.8	No Alert	OK
			COYQ	38.8	45.7	3.12	3.85	2.74	5.4	OK	OK	<5.8		
			SLU2	48.4	54.0	3.97	3.29	1.69	4.9	OK	OK	<5.8		
28/04/2007	13:56:39	5.1	ACAR	5.6	10.6	4.00	4.70	3.54	5.1	OK	OK	<5.8	No Alert	OK
			GR06	15.0	17.6	4.03	4.59	3.66	5.4	OK	OK	<5.8		
			OCLL	12.0	15.4	4.08	4.85	3.66	5.4	OK	OK	<5.8		
			VNTA	2.7	9.4	4.13	4.03	2.85	5.4	OK	OK	<5.8		
			ACP2	10.1	13.6	4.53	4.71	3.42	5.3	OK	OK	<5.8		
			ACAC	10.2	13.6	4.72	5.14	4.03	5.7		OK	<5.8		
			AGCA	22.0	23.8	4.98	4.16	2.77	5.3	OK	OK	<5.8		
			POZU	29.1	30.6	5.07	3.87	2.74	5.4	OK	OK	<5.8		
			ACAZ	16.2	18.6	5.26	4.82	3.55	5.4	OK	OK	<5.8		
			GR08	38.9	39.9	6.00	3.45	2.09	5.0	OK	OK	<5.8		
31/05/2007	10:11:14	5.1	COJU	37.1	38.7	2.24	5.40	4.10	6.3			≥5.8	No Alert	OK
			SJAL	52.3	53.4	5.21	3.68	2.17	5.6	OK	OK	<5.8		
06/11/2007	06:35:46	5.4	GR05	7.4	11.7	2.28	5.09	3.62	5.8	OK	OK	≥5.8	No Alert	OK
			OCLL	29.1	30.7	3.04	4.24	2.92	5.5	OK	OK	<5.8		
			GR06	29.8	31.2	3.25	4.69	3.46	5.7	OK	OK	<5.8		
			ACP2	35.3	36.4	3.87	4.04	2.52	5.7	OK	OK	<5.8		
			ACAD	37.4	38.4	4.05	4.59	3.09	5.7	OK	OK	<5.8		
			ACAR	39.1	40.1	4.16	4.41	2.88	5.3	OK	OK	<5.8		
			ATYC	35.1	36.2	5.20	3.91	2.42	5.4	OK	OK	<5.8		
30/07/2008	10:23:35	5.3	OX10	21.3	53.5	5.68	3.51	1.97	5.3	OK	OK	<5.8	No Alert	OK
			HUAM	47.6	68.4	6.27	3.48	1.87	5.3	OK	OK	<5.8		
20/10/2008	05:01:10	5.2	GR01	28.7	38.2	2.92	4.07	2.89	5.1	OK	OK	<5.8	No Alert	OK
			PET2	30.2	39.3	3.89	3.25	1.62	4.8	OK	OK	<5.8		
			SLU2	40.2	47.4	4.43	3.94	2.65	5.3	OK	OK	<5.8		
27/03/2009	08:48:20	5.3	NUX2	14.3	33.3	4.50	4.29	2.83	5.6	OK	OK	<5.8	No Alert	OK
			GR02	14.4	33.3	4.55	3.74	2.40	5.2	OK	OK	<5.8		
			SLU2	14.6	33.4	4.55	4.57	3.18	5.6	OK	OK	<5.8		
			COYQ	26.2	39.9	5.10	3.93	2.41	5.5	OK	OK	<5.8		
27/04/2009	16:46:32	5.8	POZU	20.1	21.4	4.15	5.33	3.94	6.3	OK	OK	≥5.8	Earthquake Warning	OK
			VNTA	26.3	27.2	4.68	4.66	3.09	5.8	OK	OK	≥5.8		
			GR08	15.3	16.8	4.96	4.79	3.25	5.7	OK	OK	<5.8		

			OCLL	35.8	36.7	5.56	4.78	3.13	5.9	OK	OK	≥5.8		
			ACAZ	25.9	26.8	5.60	5.12	3.36	6.1	OK	OK	≥5.8		
			ACAR	28.1	28.9	5.64	5.19	3.82	6.0	OK	OK	≥5.8		
			OCTT	37.9	38.7	5.74	4.88	3.33	5.9	OK	OK	≥5.8		
			ACAC	30.2	31.0	5.84	5.83	4.23	6.9			≥5.8		
			ACP2	33.8	34.6	5.90	4.58	2.97	5.7	OK	OK	<5.8		
			GR06	40.2	40.8	6.09	4.50	2.84	5.5	OK	OK	<5.8		
			VIGA	40.9	41.5	6.32	4.44	2.85	5.4	OK	OK	<5.8		
			OX07	24.4	44.5	4.62	4.11	2.64	5.3	OK	OK	<5.8		
			OX08	18.9	41.7	4.90	4.05	2.99	5.3	OK	OK	<5.8		
09/02/2010	00:47:45	5.7	LANE	36.3	51.9	5.67	4.19	2.84	5.4	OK	OK	<5.8	No Alert	OK
			GALE	41.4	56.4	5.82	4.47	2.94	5.4	OK	OK	<5.8		
			TAMA	49.2	62.6	6.26	3.82	2.10	5.4	OK	OK	<5.8		
19/03/2010	20:48:51	5	GR01	11.4	19.0	2.74	3.87	2.50	5.5	OK	OK	<5.8	No Apply	---
			OX01	17.8	20.5	2.48	4.81	3.57	5.4	OK	OK	<5.8		
16/04/2010	10:01:13	5.2	PNTP	44.5	45.6	5.70	3.50	1.76	5.4	OK	OK	<5.8	No Alert	OK
			SJLL	55.2	56.1	6.87	4.11	2.52	5.3	OK	OK	<5.8		
20/04/2010	02:28:59	5	OX01	27.3	27.7	2.44	4.60	3.20	5.6		OK	<5.8	No Alert	OK
			SJLL	64.1	64.3	5.55	3.60	2.02	5.5	OK	OK	<5.8		
			GR01	26.2	30.3	2.60	3.95	2.48	5.5	OK	OK	<5.8		
25/05/2010	23:36:22	5.1	SLU2	34.2	37.3	3.17	4.36	3.15	5.8		OK	≥5.8	No Alert	OK
			COYQ	32.5	35.8	3.37	3.70	2.17	5.1	OK	OK	<5.8		
			OX04	15.4	17.5	2.65	5.55	4.18	6.4	OK	OK	≥5.8		
			PNTP	12.9	15.3	3.17	5.68	4.31	6.7	OK	OK	≥5.8		
30/06/2010	07:22:33	6.3	JAMI	24.0	25.4	4.06	5.52	4.00	6.2	OK	OK	≥5.8	Earthquake Warning	OK
			OX02	41.5	42.3	5.04	3.93	2.36	5.5		OK	<5.8		
			OX03	47.6	48.3	5.99	5.17	4.14	5.8	OK	OK	≥5.8		
			GR08	22.1	23.2	3.27	3.99	2.37	5.7	OK	OK	<5.8		
			ACAZ	13.8	15.4	3.36	4.78	3.41	5.5	OK	OK	<5.8		
26/04/2011	11:07:33	5.4	ACP2	27.7	28.6	4.32	3.36	1.83	5.0	OK	OK	<5.8	No Alert	OK
			POZU	41.2	41.8	5.13	3.97	2.77	5.3	OK	OK	<5.8		
			VIGA	50.5	51.0	5.68	3.50	1.79	5.4	OK	OK	<5.8		
			GR09	50.5	51.0	5.81	3.97	2.42	5.6	OK	OK	<5.8		
			GR11	10.5	15.2	3.49	4.89	3.42	5.8	OK	OK	≥5.8		
			GR10	13.5	17.4	3.81	4.60	3.00	5.7	OK	OK	<5.8		
05/05/2011	13:24:09	5.7	COPL	8.1	13.7	3.82	4.70	3.31	5.4	OK	OK	<5.8	Earthquake Warning	**Over-estimation**
			VIGA	38.8	40.4	5.64	4.33	2.62	5.8	OK	OK	≥5.8		
			SJLL	45.5	46.9	6.33	5.01	3.38	6.2	OK	OK	≥5.8		
09/07/2011	12:42:30	5.1	GALE	13.7	25.9	3.29	4.45	3.23	5.3	OK	OK	<5.8	No Alert	OK
			PANG	22.7	31.6	4.98	4.16	2.67	5.4	OK	OK	<5.8		
			OX01	10.4	19.1	2.83	5.39	3.99	6.4			≥5.8		
20/03/2012	18:02:55	7.5	OX02	42.3	45.3	6.08	6.42	5.08	7.7	OK	OK	≥5.8	Earthquake Warning	OK
			SJLL	42.8	45.7	6.09	6.03	4.41	7.4	OK	OK	≥5.8		
			COPL	63.4	65.4	6.87	3.46	2.11	5.1			<5.8		
21/03/2012	11:36:18	5	OX01	22.3	29.9	5.24	3.86	2.30	5.5	OK	OK	<5.8	No Apply	---
			OX01	17.5	20.2	3.38	4.96	3.70	5.7		OK	<5.8		
24/03/2012	01:58:42	4.9	OX02	29.6	31.3	3.72	4.01	2.70	5.5		OK	<5.8	No Alert	OK
			OX04	42.0	43.2	5.37	3.34	1.59	5.1	OK	OK	<5.8		
			OX03	50.8	51.9	6.19	3.55	2.50	5.1	OK	OK	<5.8		
01/04/2012	22:23:52	5.3	SJLL	21.3	29.2	2.94	4.24	2.92	5.5	OK	OK	<5.8	No Alert	OK
			OX03	58.5	61.8	6.69	3.51	1.79	5.4	OK	OK	<5.8		
			OX01	4.8	11.1	2.01	5.19	4.12	5.8	OK	OK	≥5.8		
02/04/2012	17:36:46	6.1	OX02	37.1	38.4	4.57	4.37	2.90	5.8	OK	OK	≥5.8	Earthquake Warning	OK
			SJLL	40.8	42.1	5.52	5.41	3.77	5.8	OK	OK	≥5.8		

			COPL	66.9	67.7	6.67	3.70	2.40	5.1		OK	<5.8		
11/04/2012	22:55:17	6.7	CALE	38.2	41.4	3.70	4.10	2.41	5.3			<5.8	Earthquake Warning	OK
			MC03	39.0	42.2	4.15	4.28	2.57	5.8		OK	≥5.8		
			MC02	63.1	65.1	6.94	4.05	2.27	6.0		OK	≥5.8		
13/04/2012	10:10:06	5.3	OX01	23.5	27.4	3.07	4.53	3.15	5.5	OK	OK	<5.8	No Alert	OK
			OX02	46.1	48.2	5.78	4.26	2.96	5.6	OK	OK	<5.8		
			OX04	51.2	53.1	6.69	4.10	2.42	5.3	OK	OK	<5.8		
13/04/2012	13:06:30	5	OX01	33.5	37.1	3.46	4.21	3.03	5.4	OK	OK	<5.8	No Alert	OK
			OX02	35.4	38.8	5.64	3.49	2.16	5.1	OK	OK	<5.8		
			OX04	27.6	31.9	6.52	3.74	1.95	5.3	OK	OK	<5.8		
			SJLL	59.9	62.0	6.91	3.69	1.96	5.8		OK	≥5.8		
24/07/2012	05:25:33	5.1	OX02	29.0	29.4	3.59	4.12	2.78	5.3	OK	OK	<5.8	No Alert	OK
			OX01	15.1	15.9	3.78	4.24	2.84	5.5	OK	OK	<5.8		
			OX04	44.1	44.4	5.13	3.82	2.28	5.4	OK	OK	<5.8		
			OX03	51.1	51.4	5.79	4.14	2.59	5.3	OK	OK	<5.8		
22/09/2012	12:30:02	5.5	OX02	32.9	33.0	3.74	4.78	3.47	5.4	OK	OK	<5.8	Earthquake Warning	**Over-estimation**
			OX01	17.7	17.8	3.85	4.85	3.36	5.8	OK	OK	≥5.8		
			OX04	43.5	43.5	5.04	4.37	2.88	5.8	OK	OK	≥5.8		
			OX03	54.1	54.1	5.29	4.57	2.91	5.7	OK	OK	<5.8		
18/12/2012	01:38:26	5.3	OX11	23.8	31.1	4.26	4.58	2.99	5.7	OK	OK	<5.8	No Alert	OK
			HUAM	23.1	30.6	4.30	3.96	2.38	5.6	OK	OK	<5.8		
			OX13	35.2	40.5	5.01	4.25	2.67	5.6	OK	OK	<5.8		
			OX14	33.7	39.2	5.39	4.11	2.61	5.3	OK	OK	<5.8		
			OX12	49.3	53.2	5.70	4.48	2.67	5.6	OK	OK	<5.8		
20/02/2013	21:23:13	5.6	SJAL	40.7	41.0	4.59	3.72	2.16	5.2	OK	OK	<5.8	No Alert	OK
			MC07	41.1	41.4	5.22	3.80	2.18	5.3	OK	OK	<5.8		
			CL01	44.1	44.4	6.14	3.88	2.33	5.5	OK	OK	<5.8		
			CL02	38.7	39.0	6.94	3.66	2.32	5.5	OK	OK	<5.8		
26/03/2013	13:04:53	5.4	OX01	58.2	59.1	4.23	4.45	2.99	5.4	OK	OK	<5.8	No Apply	---
26/03/2013	13:12:23	5.2	OX01	38.5	39.8	4.42	4.07	2.58	5.2	OK	OK	<5.8	No Apply	---
05/04/2013	01:58:49	5.5	GR02	14.8	22.6	3.78	5.70	4.54	6.9			≥5.8	Earthquake Warning	**Over-estimation**
			NUX2	14.7	22.5	3.85	5.69	4.56	6.9			≥5.8		
			GR01	33.5	37.6	5.44	3.91	2.38	5.5	OK	OK	<5.8		
			ATYC	44.9	48.0	5.78	4.15	2.64	5.3	OK	OK	<5.8		
			GR04	51.9	54.6	6.42	3.66	2.05	5.7	OK	OK	<5.8		
12/04/2013	03:45:10	5.3	GR16	15.4	38.3	4.84	4.05	2.59	5.7	OK	OK	<5.8	No Alert	OK
			GR14	22.2	41.5	5.43	3.86	2.21	5.5	OK	OK	<5.8		
			GR17	29.7	46.0	5.73	4.28	2.53	5.7	OK	OK	<5.8		
			AZIH	22.2	41.4	5.74	3.63	1.94	5.7	OK	OK	<5.8		
			GR28	45.5	57.4	6.18	3.83	2.16	5.4	OK	OK	<5.8		
			GR18	43.8	56.1	6.47	4.20	2.46	5.5	OK	OK	<5.8		
22/04/2013	01:16:35	6.1	MC02	37.6	38.9	5.22	5.47	4.34	6.4	OK	OK	≥5.8	Earthquake Warning	OK
			GR18	32.1	33.6	6.06	5.11	3.65	5.9	OK	OK	≥5.8		
			GR17	42.8	44.0	6.83	4.99	3.23	6.4	OK	OK	≥5.8		
06/08/2013	20:17:34	5	GR11	28.2	32.4	4.06	3.45	1.81	5.2	OK	OK	<5.8	No Alert	OK
			OX02	36.4	39.8	4.83	3.62	2.19	5.5	OK	OK	<5.8		
16/08/2013	15:33:03	5.3	GR11	25.5	32.4	4.01	3.88	2.50	5.5	OK	OK	<5.8	No Alert	OK
			GR32	33.0	38.6	4.52	3.44	1.85	5.2	OK	OK	<5.8		
			OX02	37.2	42.2	4.72	3.53	2.07	5.3	OK	OK	<5.8		
21/08/2013	12:38:36	6.2	GR08	6.6	21.1	3.27	4.76	3.25	5.6		OK	<5.8	Earthquake Warning	OK
			POZU	31.8	37.7	4.59	4.66	3.16	5.8	OK	OK	≥5.8		
			ACAZ	25.3	32.3	4.79	5.84	4.36	6.8		OK	≥5.8		
			ACAC	32.5	38.2	4.86	5.59	3.96	6.3	OK	OK	≥5.8		

			ACAR	32.0	37.7	5.13	5.26	3.73	6.2	OK	OK	≥5.8	
			VNTA	31.3	37.2	5.28	4.85	3.17	6.0	OK	OK	≥5.8	
			ACAD	35.1	40.4	6.27	4.97	3.38	6.1	OK	OK	≥5.8	
			ACP2	37.0	42.1	6.55	4.86	3.46	5.7	OK	OK	<5.8	
			GR06	43.5	47.9	6.97	4.38	2.99	5.2		OK	<5.8	
21/08/2013	13:02:22	5.3	GR08	22.5	25.1	3.20	3.41	2.08	5.0	OK	OK	<5.8	No Alert	OK
			ACAZ	11.7	16.0	3.38	5.03	4.09	5.4	OK	OK	<5.8	
			VNTA	23.4	25.8	3.49	4.10	2.67	5.2	OK	OK	<5.8	
			ACAR	22.3	24.9	3.56	4.58	3.34	5.5	OK	OK	<5.8	
			ACAC	20.7	23.4	3.72	4.62	3.14	5.7	OK	OK	<5.8	
			ACAD	23.4	25.9	3.82	4.12	2.64	5.3	OK	OK	<5.8	
			ACP2	25.5	27.8	3.94	3.84	2.31	5.4	OK	OK	<5.8	
			GR30	39.2	40.7	4.34	4.34	3.15	5.7	OK	OK	<5.8	
			POZU	39.5	41.1	4.56	3.81	2.54	5.3	OK	OK	<5.8	
			OCLL	37.7	39.5	4.83	4.24	3.42	5.4	OK	OK	<5.8	
			GR09	51.4	52.6	6.09	3.61	1.90	5.6	OK	OK	<5.8	
06/10/2013	14:27:58	5	GR06	17.9	20.6	2.79	3.94	2.41	5.5	OK	OK	<5.8	No Alert	OK
			GR05	19.4	21.8	3.27	3.72	2.24	5.2	OK	OK	<5.8		
			GR29	42.8	43.9	5.10	3.43	1.96	5.1	OK	OK	<5.8		
06/10/2013	15:11:01	5.1	GR05	21.4	23.7	3.01	3.92	2.45	5.4	OK	OK	<5.8	No Alert	OK
			ACP2	25.5	27.4	3.07	3.43	1.97	5.1	OK	OK	<5.8		
			GR06	19.7	22.1	3.12	3.99	2.87	5.3	OK	OK	<5.8		
			ACAR	31.4	32.9	3.38	3.45	2.03	5.1	OK	OK	<5.8		
			ACAC	28.9	30.6	3.42	3.58	2.00	5.5	OK	OK	<5.8		
			COYC	19.8	22.2	3.53	3.62	2.16	5.5	OK	OK	<5.8		
			ACAD	26.8	28.6	3.89	3.84	2.42	5.4	OK	OK	<5.8		
			ACAZ	35.3	36.6	4.93	3.37	1.70	5.1	OK	OK	<5.8		
02/01/2014	23:54:01	4.8	OX04	23.3	23.3	3.85	4.41	2.87	5.3	OK	OK	<5.8	No Apply	---
18/04/2014	14:27:36	7.3	GR01	20.3	22.7	2.74	6.00	4.52	7.1	OK	OK	≥5.8	Earthquake Warning	OK
			GR13	33.8	35.3	4.63	5.07	3.52	6.2			≥5.8		
			SLU2	29.9	31.6	5.07	5.75	4.22	6.7		OK	≥5.8		
			GR14	54.0	54.9	5.20	4.49	3.23	5.4			<5.8		
			NUX2	44.0	45.2	5.99	4.99	3.42	6.1			≥5.8		
			PET2	38.2	39.5	6.11	5.33	3.92	6.3		OK	≥5.8		
			GR02	44.4	45.5	6.92	5.51	3.88	6.1			≥5.8		
08/05/2014	17:00:20	6.5	GR02	14.4	22.3	3.16	5.21	3.90	6.0	OK	OK	≥5.8	Earthquake Warning	OK
			NUX2	14.2	22.1	3.72	5.08	3.81	5.8		OK	≥5.8		
			SLU2	19.3	25.8	3.96	4.81	3.35	5.7		OK	<5.8		
			GR01	27.3	32.2	4.74	4.25	2.80	5.5		OK	<5.8		
			SUCH	28.3	33.0	5.97	4.31	2.90	5.7		OK	<5.8		
10/05/2014	07:36:05	6.1	NUX2	24.0	26.8	3.02	4.65	3.33	5.8	OK	OK	≥5.8	Earthquake Warning	OK
			GR02	24.3	27.1	3.05	5.08	3.65	5.8	OK	OK	≥5.8		
			SLU2	23.2	26.2	3.69	4.76	3.29	5.6	OK	OK	<5.8		
			SUCH	38.5	40.3	4.35	3.38	1.82	5.0			<5.8		
			GR01	26.9	29.5	4.77	4.65	3.59	5.6	OK	OK	<5.8		
10/05/2014	17:26:40	5	NUX2	36.6	41.7	4.15	3.53	2.14	5.2	OK	OK	<5.8	No Alert	OK
			SLU2	39.0	43.8	4.68	3.57	2.15	5.3	OK	OK	<5.8		
24/05/2014	08:24:50	5.7	SJLL	47.8	51.1	5.76	4.39	2.75	5.3	OK	OK	<5.8	No Alert	OK
			OX04	56.8	59.6	6.32	4.15	2.54	5.3	OK	OK	<5.8		
04/08/2014	00:21:54	5.1	NUX2	14.3	17.5	2.86	4.58	3.19	5.6	OK	OK	<5.8	No Alert	OK
			SLU2	22.6	24.7	3.58	3.90	2.69	5.5	OK	OK	<5.8		
11/08/2014	01:09:40	4.8	OX01	28.9	30.6	2.71	4.70	3.65	5.0	OK	OK	<5.8	No Apply	---
13/08/2014	06:48:13	5.4	OX01	21.2	23.4	2.72	5.16	3.91	5.9	OK	OK	≥5.8	No Alert	OK

			OX02	44.3	45.4	3.33	3.47	1.94	5.2	OK	OK	<5.8		
			OX04	51.4	52.4	5.87	3.89	2.23	5.6	OK	OK	<5.8		
08/09/2014	20:30:41	4.9	OX01	13.8	20.4	2.95	4.03	2.69	5.5		OK	<5.8	No Apply	---
11/10/2014	16:46:05	5.5	OX12	26.1	28.0	5.29	5.00	3.44	6.1		OK	≥5.8	Earthquake Warning	**Over-estimation**
			OX14	48.2	49.3	5.63	4.74	3.13	5.7	OK	OK	<5.8		
			OX35	56.4	57.3	6.80	3.94	2.03	5.9	OK	OK	≥5.8		
12/01/2015	00:59:21	4.9	OX04	22.7	22.8	3.15	4.14	2.92	5.3	OK	OK	<5.8	No Alert	OK
			OX03	50.9	50.9	5.73	3.59	2.34	5.3	OK	OK	<5.8		
			OX05	54.2	54.2	6.46	3.63	1.90	5.7		OK	<5.8		
05/04/2015	06:55:06	4.8	OX01	42.4	45.4	4.77	4.16	2.74	5.3	OK	OK	<5.8	No Apply	---
25/06/2015	10:31:51	4.8	OX03	55.0	57.4	3.48	4.23	2.72	5.5		OK	<5.8	No Alert	OK
			OX02	45.1	47.9	5.70	3.39	1.69	5.1	OK	OK	<5.8		
14/07/2015	01:25:35	4.9	MC05	19.5	19.6	2.57	3.77	2.46	5.2	OK	OK	<5.8	No Apply	---
30/09/2015	17:25:59	5.4	GR15	15.3	33.7	6.15	4.74	3.19	5.7	OK	OK	<5.8	No Alert	OK
			GR14	24.3	38.6	6.19	4.28	2.75	5.6	OK	OK	<5.8		
			GR16	22.5	37.5	6.22	4.62	3.25	5.7	OK	OK	<5.8		
			GR28	37.2	49.2	6.52	4.40	2.92	5.3	OK	OK	<5.8		
			GR17	33.3	44.9	6.77	4.62	2.95	5.8	OK	OK	≥5.8		
23/11/2015	20:41:25	5.6	GR31	19.6	22.0	4.99	5.35	3.52	6.5		OK	≥5.8	Earthquake Warning	**Over-estimation**
			GR32	22.4	24.5	5.57	4.87	3.27	6.0	OK	OK	≥5.8		
			GR10	25.1	27.1	6.40	4.49	3.31	5.3	OK	OK	<5.8		
			GR09	33.9	35.4	6.74	5.05	3.55	6.1	OK	OK	≥5.8		

Capítulo IV

A fast earthquake early warning algorithm based on the first 3 seconds of the P wave coda

(Submitted to *Bulletin of the Seismological Society of America on march 13, 2018*)

A FAST EARTHQUAKE EARLY WARNING ALGORITHM BASED ON THE FIRST 3 SECONDS OF THE *P* WAVE CODA

Armando Cuéllar[1,2], Gerardo Suárez[2] and J. M. Espinosa-Aranda[1]

[1] Centro de Instrumentación y Registro Sísmico (*CIRES)*, Mexico City, Mexico

[2] Instituto de Geofísica, UNAM, Mexico City, Mexico

ABSTRACT

A new seismic early warning algorithm is presented that estimates a magnitude threshold using the first three seconds after the onset of the *P* phase on the vertical component. This new algorithm considerably reduces the processing time compared to previous algorithms used by the Mexican earthquake early warning system (*SASMEX*). It was designed to alert in-slab earthquakes within the subducted Cocos plate. The t_P+3 algorithm was based on a training dataset of 76 accelerograms of 25 Mexican in-slab earthquakes, with focal depths > 40 km. The algorithm uses two parameters measured in the vertical component of the *P* waves: the sum of the cumulative quadratic acceleration, $a_{v(T)}$ and θ_P, a parameter that represents the slope of the curve of the cumulative acceleration. The model is based on a learning machine that linearizes piecewise the empirical relation between these two parameters and M_w. The resulting algorithm was tested on 9 recent earthquakes that took place from 2014 to 2017, recorded in 37 strong motion records. In addition, the algorithm was evaluated in the context of the Mexican earthquake early warning, applying it to 24 in-slab earthquakes occurring from 1995 to 2017 ($5.0< M_w <7.1$). The results show that the magnitude of 19 earthquakes was properly estimated, for four of them it was overestimated and in one case the magnitude was underestimated. Three earthquakes $M_w>6.5$ that affected Mexico City were included in the dataset: the M_w 6.5 event on 11 December 2011 and the destructive in-slab Tehuacán and Morelos earthquakes on 15 June 1999 (M_w 7.0) and 19 September 2017 (M_w 7.1). The retrospective application of the t_P+3 algorithm shows that these earthquakes are correctly identified as $M_w > 6$ and would activate a seismic alert. The

t_P+3 algorithm would have given 34 and 25 seconds respectively, before the arrival of strong motion in Mexico City.

INTRODUCTION

Early warning systems are in a constant race to discriminate as rapidly as possible the magnitude of earthquakes that may prove damaging to cities with a high seismic vulnerability. The challenge is to provide a warning time, as long as possible, that enables the authorities and the population to carry out preventive actions before the arrival of the damaging seismic waves (*e.g.*, Wu and Kanamori, 2005).

The Seismic Alert System of Mexico (*SASMEX*) uses the $2(t_S-t_P)$ and (t_S-t_P) algorithms (Cuéllar *et al*., 2017a; b). The (t_S-t_P) procedure requires the arrival of the *S waves* and the $2(t_S-t_P)$ needs twice this time in order to determine whether an alert is emitted (Espinosa-Aranda *et al*. 1992; Cuéllar *et al*., 2017a; b). These algorithms allow warning times in Mexico City for earthquakes originating along the subduction zone of the Cocos Plate of between 60 and 120 seconds. Therefore, waiting for the arrival of the *S* wave is not an issue considering the large lead-time available. In the case of cities located near the subduction zone, which now have a seismic alerting system, the (t_S-t_P) algorithm reduces in half the time needed to process the data and make a decision on the emission of an alert, increasing the warning time in those cities.

The situation is different, however, for earthquakes beneath Central Mexico that take place within the subducted Cocos plate. Hereon, we refer to these events as in-slab earthquakes. Due to the contorted nature of the subducting Cocos plate (Suárez *et al*., 1990; Pardo and Suárez, 1994; 1995), in-slab earthquakes range in depth from 50 km in central Mexico to 180 km, beneath the Isthmus of Tehuantepec. Although in-slab events are

generally smaller and less frequent than subduction earthquakes, they occur beneath the more highly populated areas of Mexico, frequently causing damage and loss of life. In these cases, algorithms that require the arrival of the *S* waves to issue an alert are of little use because the arrival of the *S* waves coincides with the strong ground motion.

The need of seismic early warning systems in cities located above in-slab earthquakes stimulated the development of a fast algorithm based only on the *P* wave coda. We present here an algorithm that uses the first three seconds after the *P* phase, as measured on the vertical component. The algorithm is designed for earthquakes with hypocentral depths > 40 km, where strong motion instruments are located at distances of a few tens of kilometers from the epicenter. The algorithm, called t_P*+3*, is correlated to M_w and makes use of two parameters to determine a magnitude threshold to issue a seismic early warning: $a_{v(T)}$, the cumulative quadratic acceleration in the t_P+3 s period, and a parameter called θ_P that parameterizes the shape of the cumulative quadratic acceleration in the first three seconds of *P* wave coda.

A magnitude model, m_{t_P+3}, is constructed using an active and supervised learning machine method. The algorithm was developed using a training dataset of 76 strong motion records recorded from 25 earthquakes from 1997 to 2013, with a magnitude range of 5.0 < M_w < 7.1. The resulting algorithm was tested on 9 recent earthquakes that took place between 2014 and 2017, recorded in 37 strong motion records. These earthquakes are all in-slab events with hypocentral depths > 40 km. In addition to the test earthquakes, three of the largest in-slab events are used to analyze the retrospective performance of the proposed algorithm. These are the M_w 7.0 Tehuacán earthquake on June 15, 1999, the M_w 6.5 Zumpango del Río earthquake on December 11, 2011, and the destructive earthquake that occurred near Mexico City on September 19, 2017 (M_w 7.1). The results on these test earthquakes indicate that the t_P*+3* algorithm is a robust and reliable early warning algorithm that offers a substantial time advantage for preparedness purposes, compared with algorithms that wait for the arrival of the *S* phase.

BACKGROUND ON THE DEVELOPMENT OF THE t_P+3 ALGORITHM

On December 11, 2011, an earthquake M_w 6.5 occurred near the town of Zumpango, Guerrero at a depth of 65 km. This earthquake was felt strongly in Mexico City, located at an epicentral distance of 200 km (Figure 1). The Mexico City strong motion network (*RACM*) recorded peak ground accelerations > 20 $cm/s^{2.}$ (*http://cires.org.mx/racm_historico_es.php*). Although the earthquake caused no substantial damage, there were power outages in approximately thirty districts in Mexico City and the temporary suspension of telephone and mobile communications. At that time, *SASMEX* had no coverage in this inland region of Mexico. The monitoring stations were concentrated on the Pacific coast, covering only the subduction zone. Therefore, *SASMEX* was unable to issue an early warning in Mexico City.

This experience showed that the coverage of *SASMEX* monitoring stations needed to be expanded to cover the inland regions of the country affected by in-slab earthquakes. Furthermore, it became clear that a faster algorithm was necessary, that need not wait for the arrival of the *S* waves, as the other algorithms traditionally used by *SASMEX* (Cuéllar *et al*., 2017a, b). This becomes clear when the (t_S-t_P) and the $2(t_S-t_P)$ algorithms are used in a *post facto* analysis based on the two closest strong motion stations that recorded the 2011 Zumpango earthquake: *TNLP-Tonalapa* and *COMD-La Comunidad* (Figure 1). These strong motion stations, operated by the Instituto de Ingeniería of the National Autonomous University of Mexico (II-UNAM), are located at epicentral distances of 52 and 65 km. The application of the (t_S-t_P) and $2(t_S-t_P)$ algorithms on these two seismic records would have resulted in a warning times of 27 and 16 s, prior to the arrival of the *S* waves observed at station *SCT2-Secretaría de Comunicaciones* in Mexico City (Figure 1). However, the population would have probably felt the ground motion produced by the coda of the *P* waves prior to the alert signal.

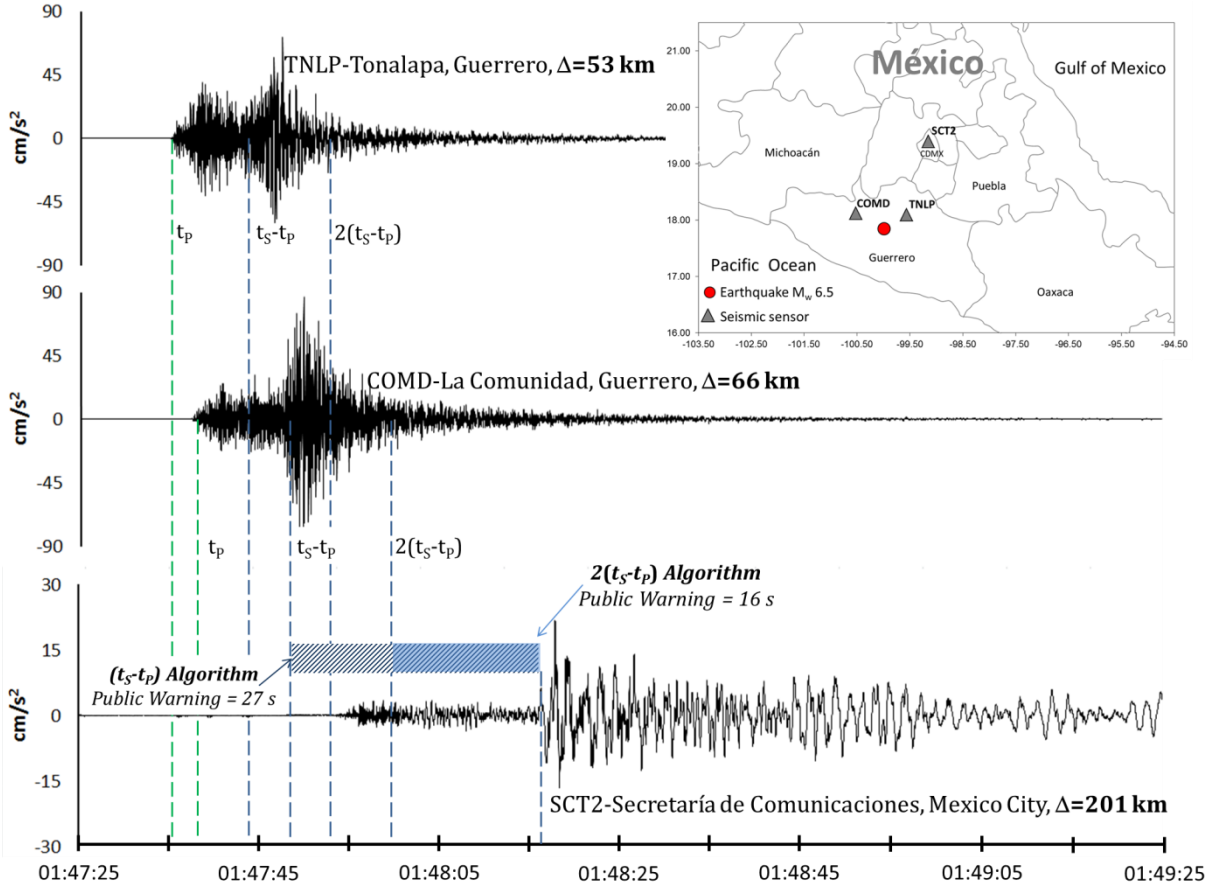

Figure 1. *Post facto* analysis of the 11 December 2011 Zumpango earthquake (M_w6.5) with a focal depth of 65 km. The $(t_S\text{-}t_P)$ and the $2(t_S\text{-}t_P)$ algorithm would have issued an alert in Mexico City approximately 27 and 16 s before the arrival of the *S* waves.

The experience of the Zumpango earthquake demonstrated that for seismic foci within the subducted Cocos plate that take place close to major cities in central Mexico, it is possible to issue a seismic early warning that provides a useful warning time. Moreover an algorithm that substantially reduces the time needed to discriminate the magnitude threshold, would offer a much longer warning time to take civil protection measures prior to the arrival of strong shaking ground.

ESTIMATION OF PARAMETERS $a_{v(T)}$ AND θ_P OF THE t_P+3 ALGORITHM

Cumulative Quadratic Acceleration, $a_{v(T)}$

The acceleration records of free field seismic stations located above the hypocenter of in-slab earthquakes normally exhibit high vertical accelerations of the *P* waves, compared to the horizontal components. This facilitates the identification of the *P* phase on the vertical channel of triaxial accelerometers. Parameter $a_{v(T)}$ measures the cumulative growth of seismic energy in the vertical component during the interval t_P+3 s. The cumulative quadratic acceleration is calculated beginning at the initial detection of the *P* wave, as in Equation 1:

$$a_{v(T)} = \sum_{i=t_P}^{t_P+T} x_{UD}(i)^2 \qquad (1)$$

where:

x_{UD} is the acceleration on the vertical channel

t_P is the arrival time of the *P* phase

T is the 3 s processing window

As an example, parameter $a_{v(T)}$ is calculated on stations *GR04-Cacalutla*, *GR18-Joluta* and *GR13-Petatlán*, of the *SASMEX* network, for three earthquakes: October 6, 2013 (M_w 5.1; focal depth = 21 km); the April 21, 2013 (M_w 6.1; depth=27 km); and the April 18, 2014 (M_w 7.2; depth=21 km). The recording strong motion stations lie at similar epicentral distances to these three earthquakes. Although these earthquakes are not in slab events, the exercise highlights the difference in the cumulative quadratic acceleration $a_{v(T)}$ of the *P* wave during the first seconds for earthquakes with different magnitudes. The cumulative growth of energy, measured by parameter $a_{v(T)}$, shows values of 10^2, 10^4 and 10^5 cm^2/s^4 for earthquakes with magnitudes 5.1, 6.1 and to 7.2 respectively (Figure 2).

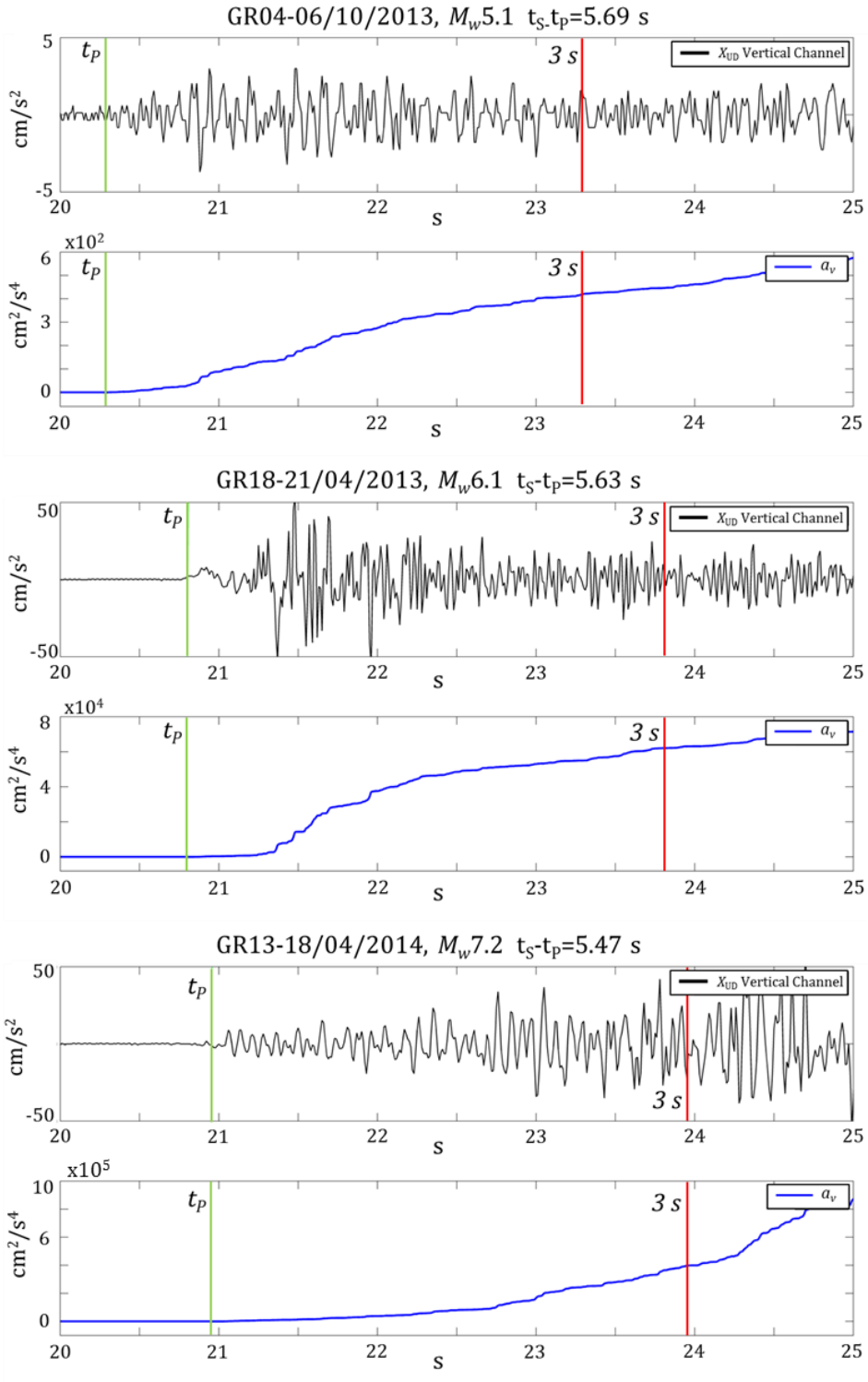

Figure 2. Cumulative quadratic acceleration observed in the first three seconds of the *P* wave coda for three earthquakes at similar epicentral distances; but with different magnitudes M_w.

The Shape of the Seismic Acceleration Curve: Parameter θ_P

The growth of the cumulative acceleration in the period t_P+3 s shows three very different growth shapes, depending on the magnitude of the earthquake: linear, sigmoidal and exponential (Figure 2). Thus the shape of the growth rate of the quadratic acceleration appears to be a good indicator to estimate magnitude.

Based on equations 2 and 3, the slope of the growth of the *P* wave quadratic acceleration is divided into two segments:

$$m_{v(T1)} = \frac{a_{v(T1)} - a_{v(T0)}}{a_{v(T1)}} \qquad (2)$$

$$m_{v(T2)} = \frac{a_{v(T2)} - a_{v(T1)}}{a_{v(T2)}} \qquad (3)$$

Where:

$a_{v(T0)}$ is the cumulative sum of the acceleration from t_P to t_P+0.5 s

$a_{v(T1)}$ is the cumulative sum of the quadratic acceleration from t_P +0.5 s to t_P+1.75 s

$a_{v(T2)}$ is the cumulative sum of the quadratic acceleration from t_P +1.75 s to t_P+3 s.

In the case of intermediate-depth earthquakes, *P* waves arrive almost vertically at seismic stations near the epicenter, producing large vertical accelerations. Thus we propose a 0.5 s waiting period to stabilize subsequent measurements. The normalized rates $m_{v(T1)}$

and $m_{v(T2)}$ define the growth rate with duration of 1.25 seconds, in the interval between 0.5 seconds and 3 s, after the arrival of the *P* wave. Thus the parameter expressing the shape of the cumulative energy growth may be expressed as:

$$\theta_P = \arctan\left(\frac{m_{v(T2)}}{m_{v(T1)}}\right) \quad (4)$$

The parameter θ_P is an angular measurement of the rate of change of the quadratic acceleration on the vertical component, $a_{v(T)}$, in the first three seconds after the *P* arrival. When $\theta_P \approx \pi/4$, the rate $m_{v(T2)}$ does not have a significant change with respect to $m_{v(T1)}$. In this case, the growth rate is constant and the *P* wave growth is linear. When $\theta_P < \pi/4$, $m_{v(T1)}$ is larger than $m_{v(T2)}$ and the *P* wave growth is sigmoidal. Finally, when $\theta_P > \pi/4$, $m_{v(T2)}$ is larger than $m_{v(T1)}$ and the *P* wave growth is exponential.

SELECTION CRITERIA OF STRONG MOTION RECORDS

Data from 349 strong seismic records from 57 earthquakes were selected to assess the usefulness of parameters $\log_{10} a_{v(T)}$ and θ_P to estimate M_w in an earthquake early warning system. The networks of the II-UNAM (Pérez-Yáñez *et al*., 2014) and *SASMEX* recorded these accelerograms. Out of this dataset, 113 acceleration records of 34 earthquakes were selected based on the following criteria (Figure 3 and Table S1 available in the electronic supplement):

1. Earthquakes M_w > 4.6, occurring from 1985 to 2017, based on the *CMT* catalogue (Ekström *et al*., 2012) (*http://www.globalcmt.org/CMTsearch.html*)

2. Focal depth > 40 km located in the intraplate region, based on the catalog of the Seismological Service of Mexico (*SSN*) (*http://www.ssn.unam.mx*)
3. Accelerograms with minimum mean accelerations of 4 cm/s^2, considered as the acceptable floor of self-noise of the strong motion instruments (Cuéllar *et al*. 2017b).
4. Strong motion stations located at epicentral distances < 110 km. This criterion is an empirical consideration. It represents twice the minimum hypocentral depth of Central Mexico of in-slab events, which is approximately 55 km.

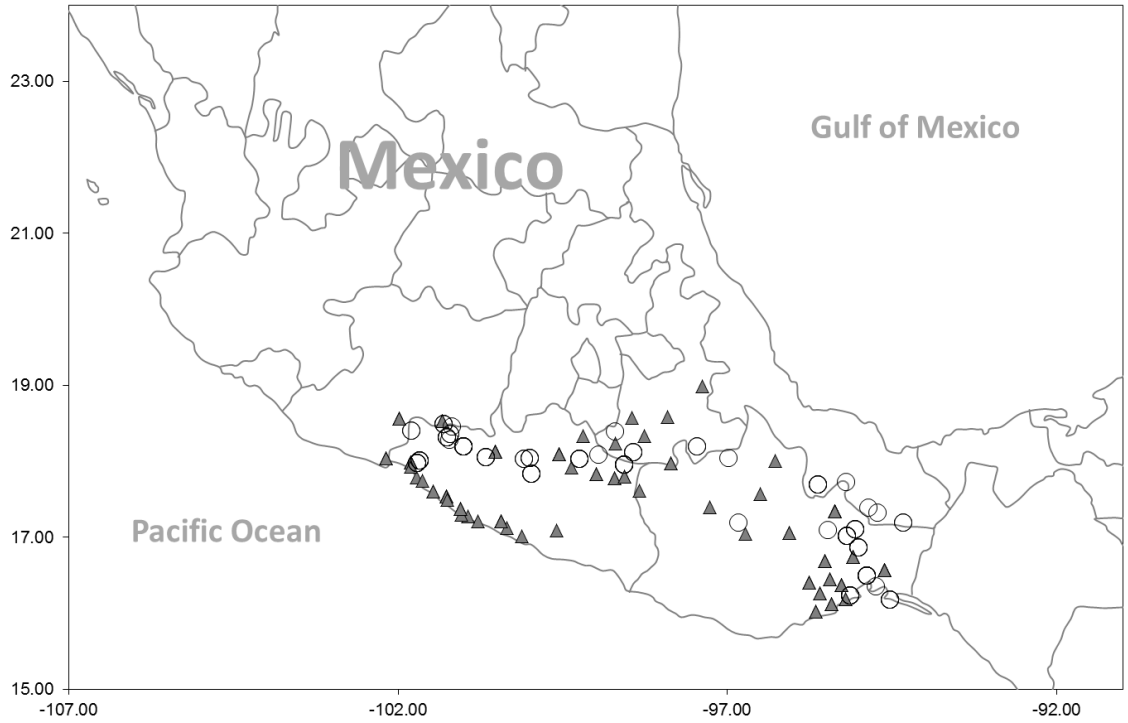

Figure 3. Location of the 34 in-slab earthquakes included in the training and testing datasets, based on the criteria described in the text. Open circles represent the epicenters of the earthquakes and closed triangles the location of the strong motion stations.

CORRELATION BETWEEN PARAMETERS $a_{v(T)}$ *and* θ_P *VERSUS* M_w

The correlation between $\log_{10} a_{v(T)}$ vs. M_w and $\theta_P$vs. M_w based on the selected 113 acceleration records is defined as (Pearson, 1895):

$$r_2 = \frac{\sum_{i=1}^{n}(\theta_{P(i)}-\overline{\theta_P})(M_{w(i)}-\overline{M_w})}{\sqrt{\sum_{i=1}^{n}(\theta_{P(i)}-\overline{\theta_P})^2}\sqrt{\sum_{i=1}^{n}(M_{w(i)}-\overline{M_w})^2}} \quad (5)$$

$$r_1 = \frac{\sum_{i=1}^{n}(\log_{10} a_{v(T)} - \overline{\log_{10} a_{v(T)}})(M_{w(i)}-\overline{M_w})}{\sqrt{\sum_{i=1}^{n}(\log_{10} a_{v(T)} - \overline{\log_{10} a_{v(T)}})^2}\sqrt{\sum_{i=1}^{n}(M_{w(i)}-\overline{M_w})^2}} \quad (6)$$

Where:

T is the time window of 3 seconds, starting at the arrival of the *P* waves

n is the number of elements; in our case 113

$\overline{\theta_P}$, $\overline{\log_{10} a_{v(T)}}$ and $\overline{M_w}$ are the average values of these parameters

The correlation between $\log_{10} a_{v(T)}$ and θ_P versus M_w of the 113 acceleration records correspond to values of r_1 = 0.42 and r_2 = 0.53, respectively (Figure 4). These correlations show that it is feasible to construct a model relating the seismic magnitude M_w with these parameters. On other hand, the correlation between $\log_{10} a_{v(T)}$ and θ_P is r =0.1, indicating that these parameters are linearly independent.

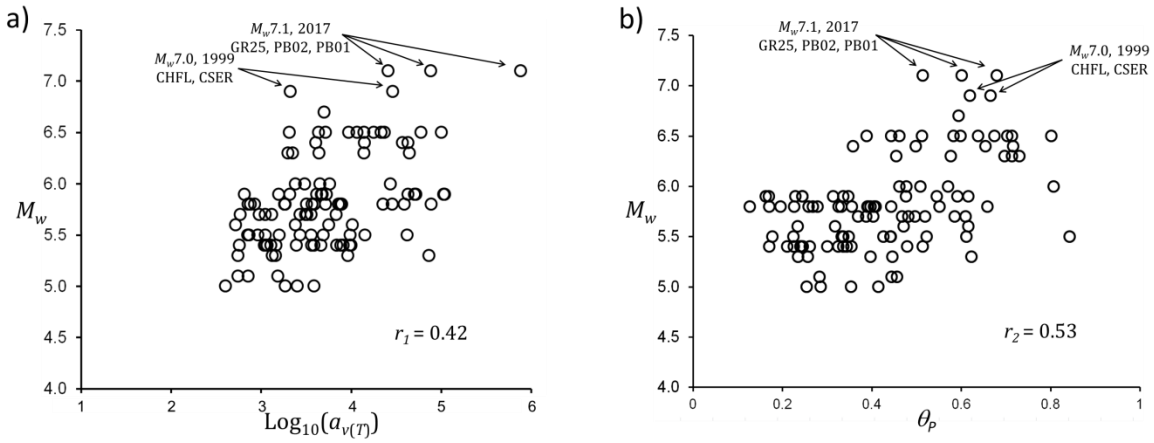

Figure 4. a) Plot of $a_{v(T)}$ versus M_w for the selected accelerograms: b) Plot of parameter θ_P versus M_w.

ESTIMATION OF MAGNITUDE BASED ON PARAMETERS $a_{v(T)}$ *and* θ_P

A procedure similar to the one used to develop the *(t_S-t_P)* algorithm (Cuéllar *et al*., 2017b) is used to calibrate the t_P*+3* algorithm. The magnitude estimation m_{t_P+3} is based on a supervised learning model that linearizes piecewise the behavior of the $a_{v(T)}$ and θ_P parameters as a function of magnitude M_w. The data used by the learning machine are $[\bar{x}_j, \bar{y}_j]$, where $\bar{x}_j = (a_{v(T)}, \theta_P)$ is the input data and $\bar{y}_j$ is the target data, $\bar{y}_j = Mw_j$. The training data used to construct the algorithm consists of 76 acceleration records corresponding to 25 earthquakes occurring from 1997 to 2013 and is expressed as the vector $[\bar{x}_j, \bar{y}_j]$. Prior to the initiating the process, the data are ordered as $a_{v(T)j} < a_{v(T)j+1}$. The flow chart of the learning machine is shown on Figure 5.

The process solves the over determined set of equations $\log_{10} Mw_j = \alpha a_{v(T)j} + \beta\theta_{Pj}$. The procedure is linearized piecewise in *m* number of sections of the curve, where for each *k*-section the system of equations is solved with the elements *(r(k)-r(k-1))*, where *r(k)* is the position of the ordered input data and its value corresponds to $[\bar{x}_j, \bar{y}_j]$. The solution of the system of equations determines the value of coefficients $[\alpha_k, \beta_k]$. $Error_k$ is the absolute mean error $|\overline{Mw}_k - \overline{Ye}_k|$; where $\overline{Mw}_k$ is the reported magnitude and $\overline{Ye}_k$ is the resulting magnitude of the inversion process in section *k*.

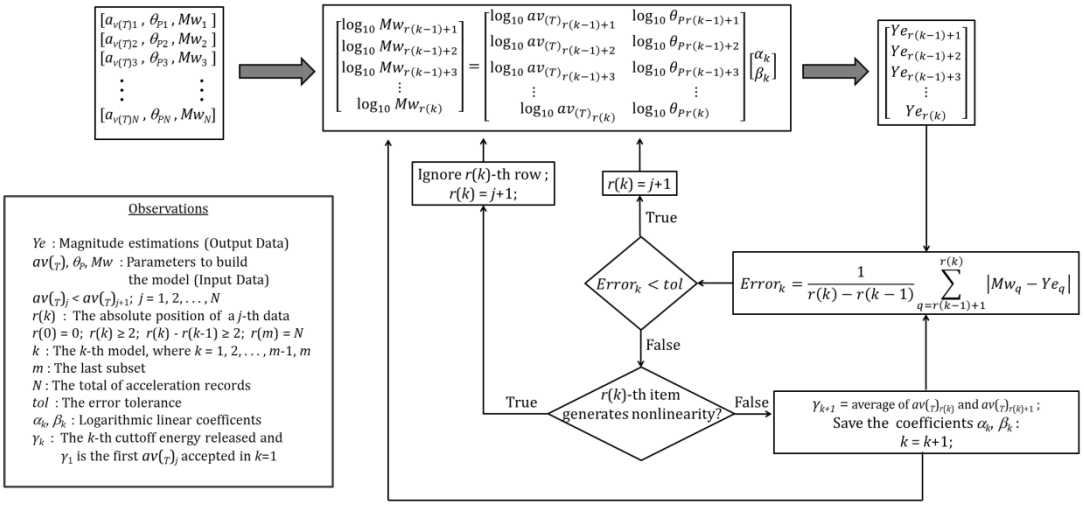

Figure 5. Schematic diagram showing the active supervised learning machine using least squares method to construct a split model to map M_w.

The process starts by estimating a solution for the first segment, *k* = 1. When the error for that segment is $Error_k$ < *tol*, the process iterates, adding the next data point $[\bar{x}_{j+1}, \bar{y}_{j+1}]$ and solves the new overdetermined set of equations (Figure 5). This iterative process is followed until $Error_k$ > *tol*. At that point, the algorithm moves on to solve for

the next section k+1 and sets the upper border γ of section k, as the value $\gamma_k = 0.5\left(a_{v(T)j} + a_{v(T)j+1}\right)$ where the j+1-th item caused the $Error_k$t > *tol*. Thus the last data point of section k is the j^{th} item $\left[\bar{x}_j, \bar{y}_j\right]$, and the first datum of section k+1 will be the j+1th pair $\left[\bar{x}_{j+1}, \bar{y}_{j+1}\right]$.

The correlation between $a_{v(T)}$ and M_w shows that in some cases, the accelerograms of large magnitude earthquakes exhibit relatively low acceleration values (Figure 4a). These outliers increase the value of $Error_k$, introducing a nonlinear behavior. Thus the inversion process is supervised at every iteration. If a data point $\left[\bar{x}_j, \bar{y}_j\right]$ is identified as a clear outlier in the k-model, the data point is manually eliminated by an active supervision of the learning algorithm (Figure 5).

Using the training set of 76 acceleration records from 25 earthquakes the resulting model relating the magnitude m_{t_P+3} to parameters $a_{v(T)}$ and θ_P is defined by seven linear equations (Equation 7):

$$m_{t_P+3} = \begin{cases} {a_{v(T)}}^{\alpha_1} \times {\theta_P}^{\beta_1} \;\; if\; \gamma_1 \geq 0.4 \times 10^3 \;\; cm^2/s^4 \\ {a_{v(T)}}^{\alpha_2} \times {\theta_P}^{\beta_2} \; if\; \gamma_2 \geq 1.0 \times 10^3 \;\; cm^2/s^4 \\ {a_{v(T)}}^{\alpha_3} \times {\theta_P}^{\beta_3} \; if\; \gamma_3 \geq 2.3 \times 10^3 \;\; cm^2/s^4 \\ {a_{v(T)}}^{\alpha_4} \times {\theta_P}^{\beta_4} \;\; if\; \gamma_4 \geq 4.6 \times 10^3 \;\; cm^2/s^4 \\ {a_{v(T)}}^{\alpha_5} \times {\theta_P}^{\beta_5} \;\; if\; \gamma_5 \geq 6.3 \times 10^3 \;\; cm^2/s^4 \\ {a_{v(T)}}^{\alpha_6} \times {\theta_P}^{\beta_6} \;\; if\; \gamma_6 \geq 9.8 \times 10^3 \;\; cm^2/s^4 \\ {a_{v(T)}}^{\alpha_7} \times {\theta_P}^{\beta_7} \;\; if\; \gamma_7 > 3.8 \times 10^4 \;\; cm^2/s^4 \end{cases} \quad (7)$$

Where:

$$\alpha_1 = 253.30 \times 10^{-3}; \quad \beta_1 = -48.18 \times 10^{-3}$$

$$\alpha_2 = 241.32 \times 10^{-3}; \quad \beta_2 = 30.42 \times 10^{-3}$$

$$\alpha_3 = 223.08 \times 10^{-3}; \quad \beta_3 = 79.81 \times 10^{-3}$$

$$\alpha_4 = 219.70 \times 10^{-3}; \quad \beta_4 = 109.14 \times 10^{-3}$$

$$\alpha_5 = 199.21 \times 10^{-3}; \quad \beta_5 = 61.87 \times 10^{-3}$$

$$\alpha_6 = 189.50 \times 10^{-3}; \quad \beta_6 = 56.48 \times 10^{-3}$$

$$\alpha_7 = 171.69 \times 10^{-3}; \quad \beta_7 = 89.83 \times 10^{-3}$$

Additionally, in the construction of the algorithm, it is necessary to establish two criteria in the model to eliminate the data inputs of the smallest and the greatest parameter values used to calibrate the algorithm. In this case based with the small number of training data set, we propose these empirical ranges:

$$m_{t_P+3} \begin{cases} < 5.0 \; if \; if \; a_{v(T)} < 0.4 \times 10^3 \; \; cm^2/s^4 \\ > 7.0 \; if \; if \; a_{v(T)} > 1.0 \times 10^5 \; \; cm^2/s^4 \end{cases} \qquad (8)$$

As the number of training data grows, the criteria expressed in equations 7 and 8 must be modified in a new calibration process.

Based on the expressions 9 and 10, the mean absolute error and its standard deviation are estimated as:

$$m_{error} = \frac{1}{N} \sum_{j=1}^{N} \left| Mw_j - m_{t_P+3\ j} \right| \qquad (9)$$

$$\sigma_{error} = \left(\frac{1}{N} \sum_{j=1}^{N} \left(m_{t_P+3\ j} - m_{error} \right)^2 \right)^{1/2} \qquad (10)$$

The mean absolute error of the estimated magnitude based on the 76 accelerograms of the training set was m_{error} = 0.30 and a standard deviation of σ_{error} = 0.22. The resulting

error lies within the tolerance in magnitude of ±0.5 and ±1.0, this last tolerance error, is accepted by the earthquake early warning system in Japan (Hoshiba M., *et al*. 2008). Based on these tolerance criteria, the algorithm accurately predicts the magnitude with a success rate of 82% and 100% respectively. A comparison between the estimated magnitude m_{t_P+3} and the catalog M_w shows a good correlation (Figure 6 and Table S2 available in the electronic supplement).

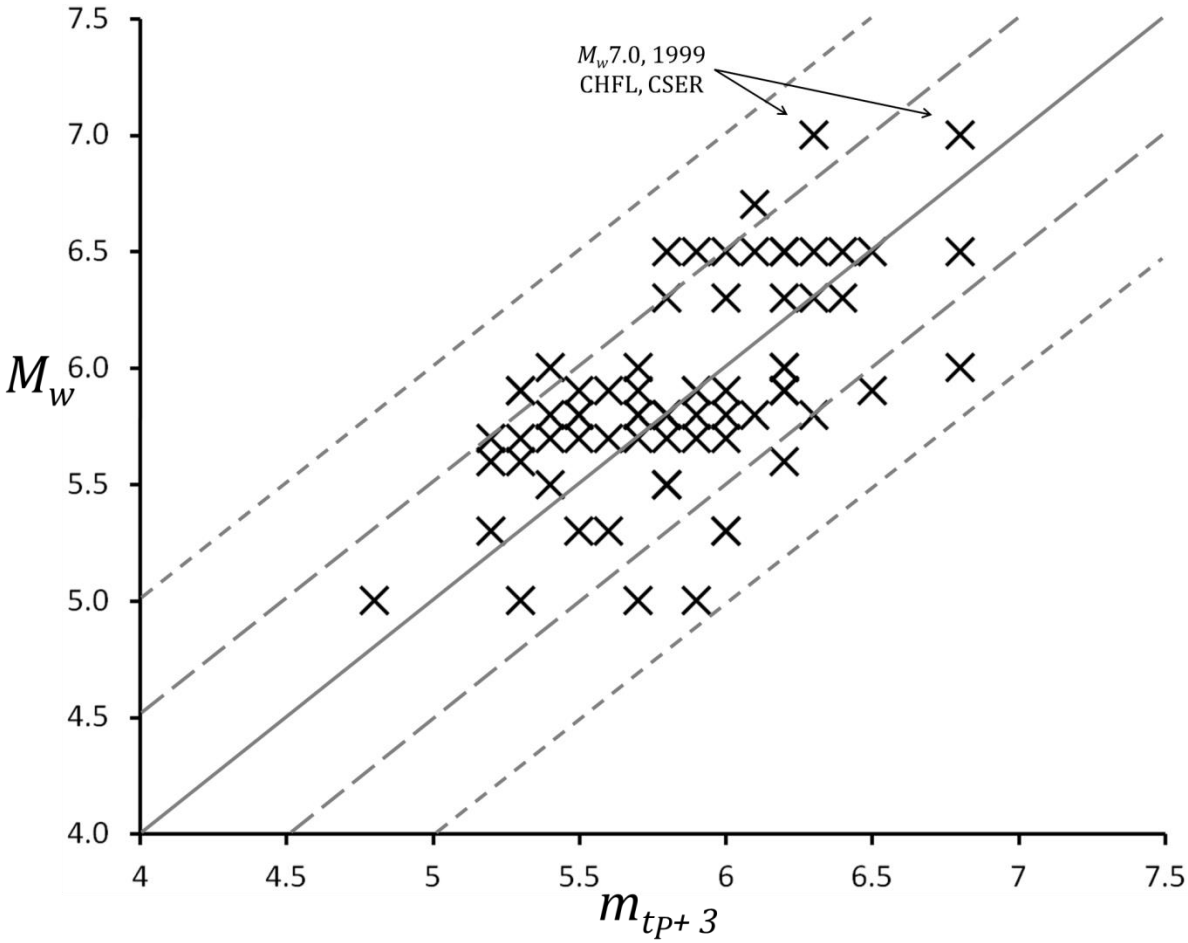

Figure 6. The magnitude estimation m_{t_P+3} is plotted versus the catalog magnitude M_w for the training dataset composed of 76 accelerograms of 25 Mexican in-slab earthquakes recorded from 1997 to 2013.

MAGNITUDE ESTIMATION m_{t_p+3} ON INDEPENDENT TESTING DATA

In order to verify the robustness of the algorithm, a testing dataset was used based on 37 acceleration records, stemming from 9 in-slab earthquakes occurring from 2014 to 2017 ($5.0 \leq M_w \leq 7.1$). This more recent dataset was used to test the resulting algorithm considering that the seismic coverage in this period had a substantial improvement and is similar to the current conditions. The test data includes the M_w 7.1 Morelos earthquake that occurred on September 19, 2017. It is worth emphasizing that these data were not used in the construction of the algorithm.

Based on expressions 9 and 10, the mean absolute error of the estimated magnitude was m_{error} = 0.5, with a standard deviation σ_{error} = 0.20. Considering an error tolerance of ±0.5 and ±1.0 in the magnitude estimation, the success rate was 89% and 97% respectively. Thus the estimated magnitude m_{t_p+3} resulting from the test accelerograms compares favorably with the catalog magnitude M_w (Figure 7).

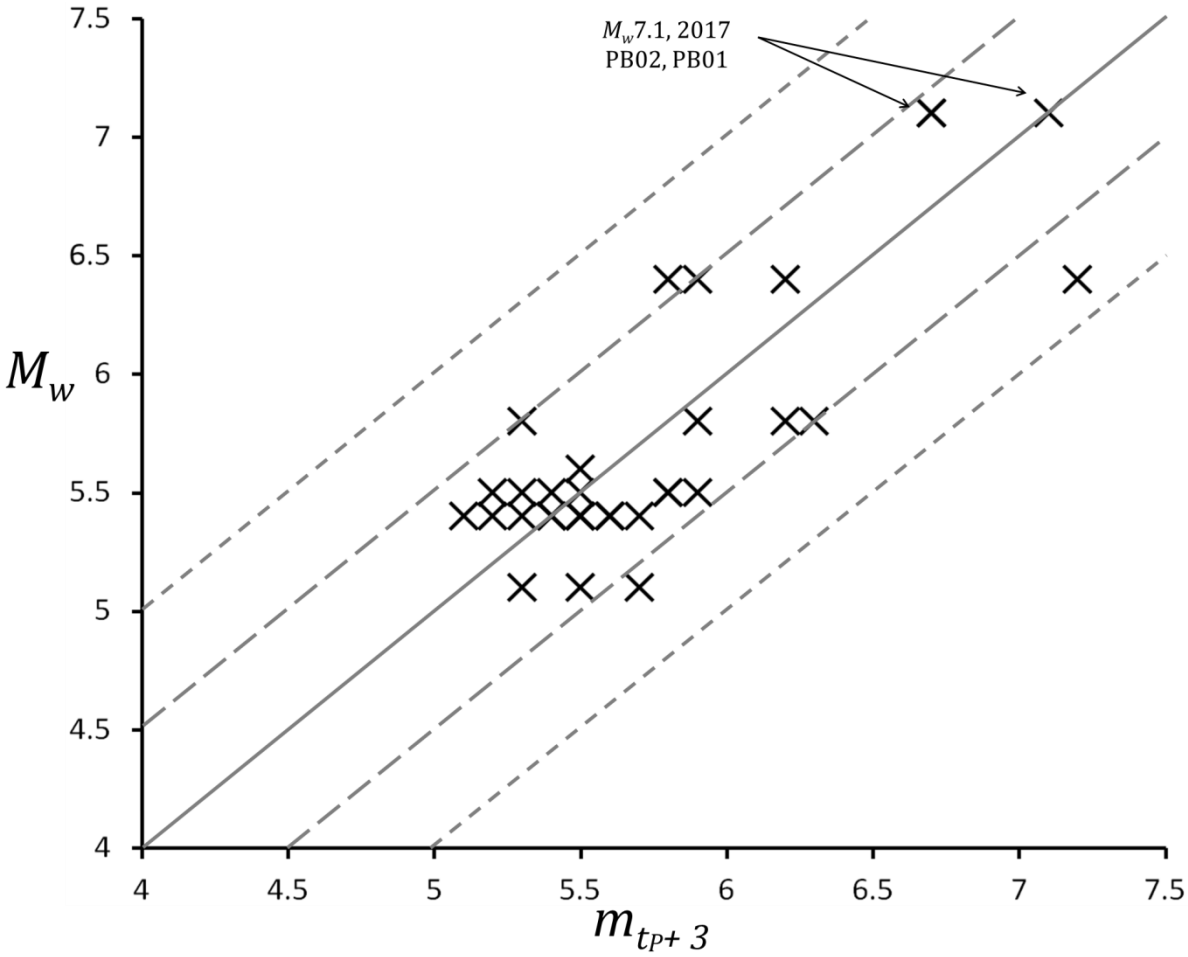

Figure 7. Magnitude estimation m_{t_P+3} compared to the catalog magnitude M_w of the test data consisting of 37 accelerograms of 9 Mexican in-slab earthquakes occurring from 2014-2017. The estimated magnitude for the M_w 7.1 Morelos earthquake was M_w > 7.0.

EARTHQUAKE EARLY WARNING PERFORMANCE EVALUATION OF THE t_P+3 ALGORITHM ON MEXICAN IN-SLAB EARTHQUAKES FROM 1997 TO 2017

The warning criterion used by *SASMEX* requires that two neighboring seismic sensors confirm the magnitude threshold in order to issue an alert. Thus to test the performance of the t_P+3 algorithm as an actual warning tool, it was tested on 24 earthquakes with magnitudes ranging from $5 \leq M_w \leq 7.1$. These 24 earthquakes met the criteria of having at least two strong motion stations that meet the specifications described above. Iglesias *et al*. (2007) and Suárez *et al*. (2009) pointed out the difficulties of the $2(t_S-t_P)$ algorithm of correctly identifying the magnitude in the narrow bins prescribed by the Mexico City authorities to issue preventive alerts ($5.5 < M_w < 6$). In order to avoid this problem of estimating magnitude within very narrow bins, we propose a single earthquake early warning criterion: $M_w \geq 5.8$.

Of the 24 earthquakes analyzed, 19 were correctly classified considering the magnitude threshold $M_w \geq 5.8$. In four cases, the magnitude was overestimated and in only one case it was underestimated. The only earthquake for which the algorithm underestimated the magnitude was the M_w 5.8 earthquake on April 28, 2008 (Table S2 available in the electronic supplement). The strong motion stations *COMD*, *TNLP* and *ATYC* estimated magnitudes m_{t_P+3} of 5.8, 5.5 and 5.7 respectively. *TNLP* estimated a lower magnitude due to the low acceleration recorded. Because of the large hypocentral distance to *ATYC* (112 km), the magnitude estimated was slightly below the threshold and did not confirm the

seismic alert. A more densely distributed network of monitoring stations probably would have estimated the correct magnitude threshold.

The four earthquakes that were overestimated have relatively small magnitudes 5.5, 5.7, 5.3 and 5.5. In all cases, the epicentral distance was greater than 110 km. The algorithm is not designed for these large epicentral distances. As discussed before, a denser coverage of strong motion station, as exists today in central Mexico, probably would yield better results.

PERFORMANCE OF THE t_P+3 ALGORITHM ON LARGE MEXICAN IN-SLAB EARTHQUAKES (M_w > 6.5)

To further evaluate the performance of the t_P+3 algorithm as an earthquake early warning tool, three large magnitude in-slab earthquakes M_w > 6.5 that occurred relatively close to Mexico City are analyzed in detail.

M_w 7.0 *Tehuacán* Earthquake on June 15, 1999

The M_w 7.0 Tehuacán earthquake on June 15, 1999 had a focal depth of 61 km. It is one of the more damaging in-slab, recent earthquakes in Mexico (Singh *et al.*, 1999; Garcia *et al.*, 2005). Forty people lost their lives and the earthquake caused damage to many private and public buildings in more than 600 localities in central México, including Mexico City. The earthquake was well recorded by strong motion stations of Instituto de Ingeniería,

UNAM: the closest stations were *CHFL-Chila de las Flores* and *CSER-Ciudad Serdán*, which are located 50 km and 83 from the epicenter respectively. The estimated magnitudes m_{t_P+3} were 6.3 and 6.8 respectively (Table S2, available in the electronic supplement). Therefore, a warning would have issued based on these two accelerograms. The resulting warning time in Mexico City based on the t_P *+3* algorithm would have been 34 s (Figure 8). In contrast, the $2(t_S\text{-}t_P)$ and $(t_S\text{-}t_P)$ algorithms would have given a warning time of only 11 and 24 seconds respectively.

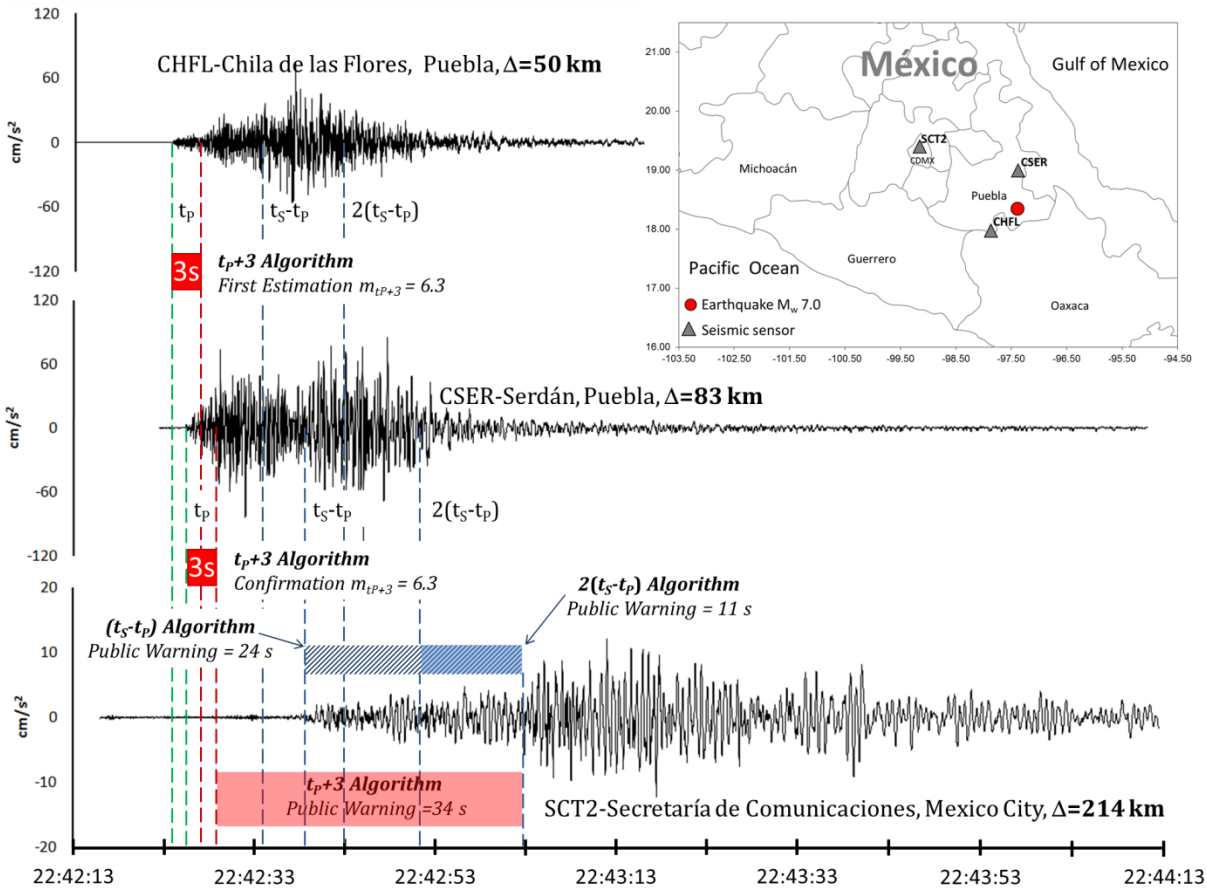

Figure 8. *Post facto* analysis of the M_w 7.0 Tehuacán earthquake comparing an earthquake early warning system using the t_P*+3* algorithm and the $(t_S\text{-}t_P)$ and $2(t_S\text{-}t_P)$ algorithms. The horizontal axis corresponds to GMT time beginning at the origin time of the earthquake. The red dot on the map shows the location of the Tehuacán earthquake.

M_w 6.5 *Zumpango del Río* earthquake on December 11, 2011

The Zumpango del Río, Guerrero earthquake occurred on December 11, 2011, at a depth of 53 km. The distance from the epicenter to Mexico City was 200 km. In Mexico City some high-rise buildings swayed for more than one minute, causing damage in the electrical system that affected nearly 82,000 people and the disruption of the phone service. Landslides blocked a toll road between Acapulco and Mexico City in several places.

At the time, the strong motion stations closest to the epicenter were *TNLP-Tonalapa* and *COMD-La Comunidad*, at epicentral distances of 52 km and 65 km respectively. The magnitude estimation m_{t_P+3} in both strong motion records was 6.2. Here again, the t_P+3 algorithm would have issued a public alert in Mexico City with a lead warning time of 35 seconds, prior to the beginning of the strong shaking (Figure 9). In contrast, the $2(t_S-t_P)$ and (t_S-t_P) algorithms would have provided a warning time of 16 and 27 seconds respectively.

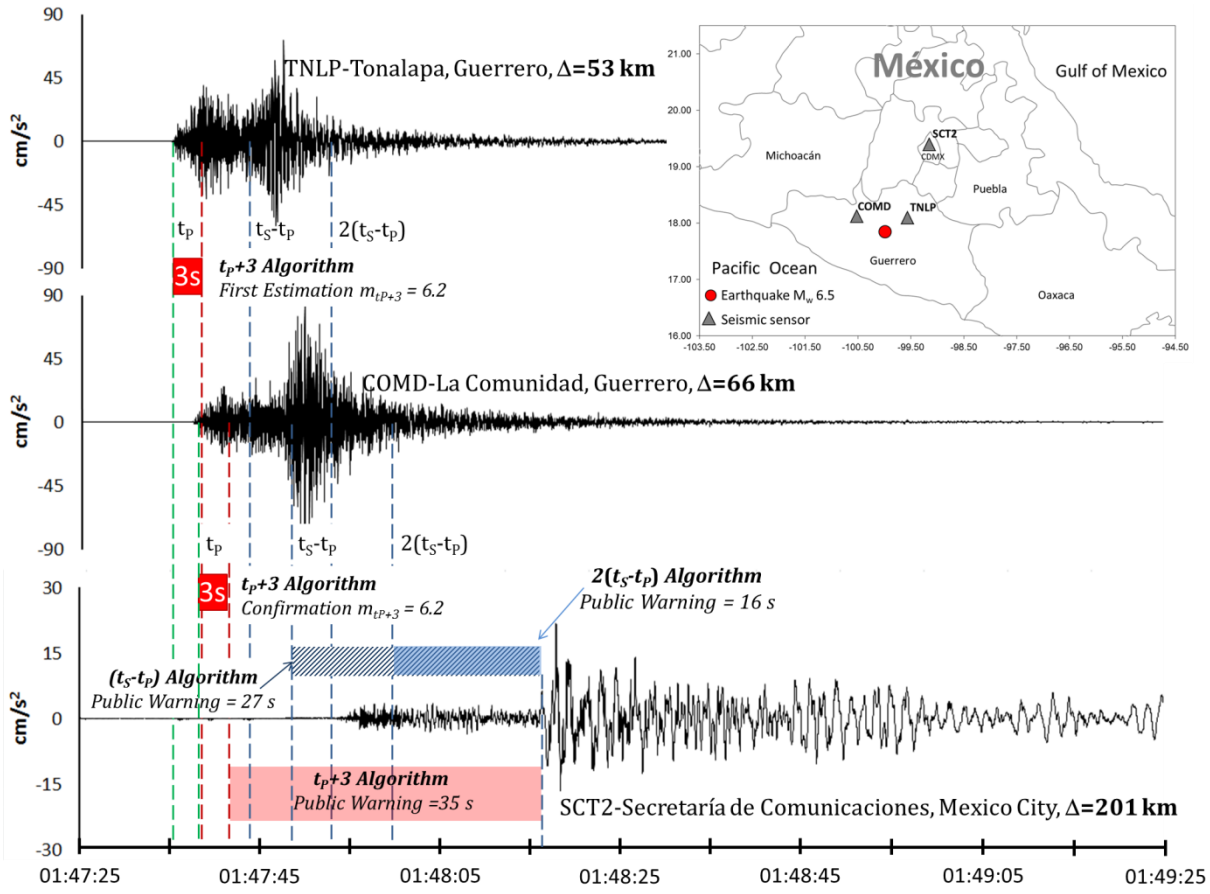

Figure 9. *Post facto* analysis of Zumpango del Río earthquake of December 11, 2011 (M_w 6.5) (CMT catalog), comparing an earthquake early warning system using the t_P+3 algorithm with the $2(t_S-t_P)$ and (t_S-t_P) algorithms. The horizontal axis corresponds to GMT time beginning at the origin time of the earthquake. The red dot on the map shows the location of the Zumpango earthquake.

M_w 7.1 Morelos, Earthquake on September 19, 2017

The 19 September 2017 (M_w 7.1) took place a couple of hours after the annual national drill, which annually sounds the seismic early warning alert to commemorate the destructive earthquakes of September 1985 and to remind the population of the existing seismic hazard. The 2017 earthquake caused 380 casualties and major damage in Mexico

City and in surrounding locations. More than 11,500 buildings were damaged and 36 collapsed. Thanks to the expanded coverage of the *SASMEX* network, the nearest strong motion instrument was located just 17 km from the epicenter. Based on the $(t_S\text{-}t_P)$ algorithm, an alert was issued in Mexico City. Although the alert was heard ~12 seconds prior to the arrival of the *S* waves, most people felt strongly the incoming *P* waves, almost simultaneously with the sound of the seismic early warning alert (Figure 10).

At the time, the $t_P{+}3$ algorithm was still under testing and calibration and had not been operationally implemented by *SASMEX*. However, it is interesting to compare the theoretical performance of this new method, designed specifically for these types of earthquakes, with the $(t_S\text{-}t_P)$ algorithm that was operational at the time. The two strong motion stations closest to the epicenter were: *PB01-San Juan Pilcaya* and *PB02-Tehuitzingo*, at epicentral distances of 17 km and 51 km respectively. The magnitude estimation for *PB01* was saturated due to the very large value of $a_{v(T)}$, which is notoriously larger than those used in the training data. By default, the magnitude at this station would have been fixed to $m_{t_P+3} > 7.5$. *PB02* estimated a magnitude m_{t_P+3} 6.7. Under these conditions, the $t_P{+}3$ algorithm would have issued a public alert ~25 s prior to the *S* wave arrival and ~12 s prior to the *P* waves (Figure 10).

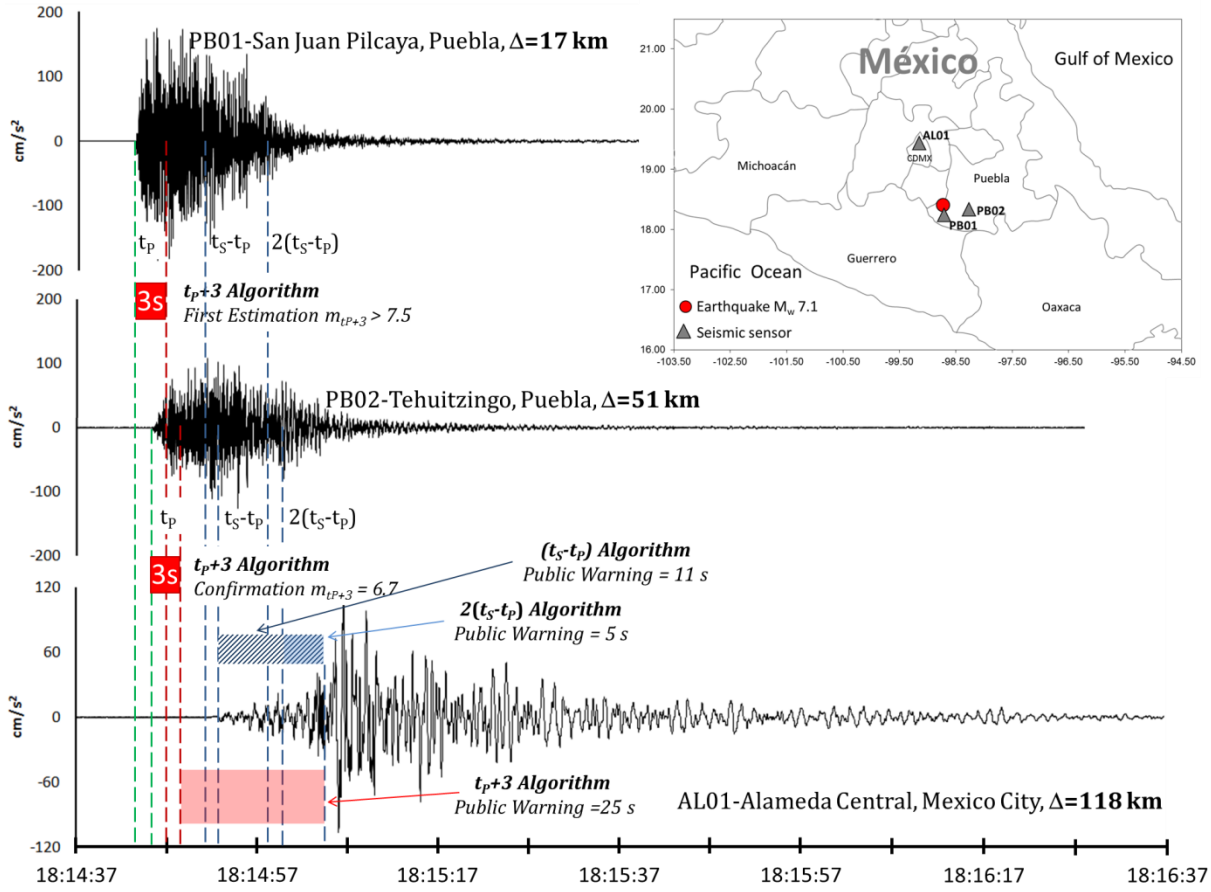

Figure 10. *Post facto* comparison of the performance of the t_P+*3* algorithms with the *2*(t_S-t_P) and (t_S-t_P) algorithms for the M_w 7.1 Morelos earthquake on September 19, 2017. The horizontal axis corresponds to GMT time starting ten seconds before the origin earthquake time. The red dot on the map shows the location of the Morelos earthquake.

SUMMARY AND CONCLUSIONS

The t_P+*3* algorithm developed here, makes use of the first three seconds of the *P* wave acceleration observed on the vertical component to estimate the magnitude threshold of earthquakes and to make a decision whether an alert should be issued. The algorithm was

constructed using a learning machine based on training data of 76 strong motion records produced by 25 earthquakes, occurring between 1997 and 2013.

The t_P+3 algorithm was tested *post facto* as a seismic early warning tool on 24 earthquakes with magnitudes $5 \leq M_w \leq 7.1$. We propose a simple confirmation criterion as a warning trigger of $M_w \geq 5.8$. Nineteen events were correctly classified, in four cases, the magnitude was overestimated and in only one case was underestimated. The performance of the t_P+3 algorithm was also analyzed on the three largest and more recent earthquakes in central Mexico. Thus the magnitude m_{t_P+3} would have correctly screened the M_w 7.0 Tehuacán, M_w 6.5 Zumpango and M_w 7.1 Morelos earthquakes. An early warning alert would have been activated with warning times substantially longer than the algorithms that require the arrival of the *S* waves. These results show that the t_P+3 algorithm is a robust and reliable method to rapidly estimate the magnitude threshold of earthquakes within the subducted in-slab in central Mexico.

ACKNOWLEDGEMENTS

The authors express their gratitude to the institutions that provided strong motion data. The Mexico City and Oaxaca governments allowed us use the waveform database of *SASMEX* stations and the Instituto de Ingeniería of the National Autonomous University of Mexico (UNAM) provided data from the Center for Engineering Strong Motion Data. AC acknowledges support of Centro de Instrumentación y Registro Sísmico (CIRES) Special thanks are due to Guadalupe Rico Zetina for her invaluable support in collecting and organizing the data presented in this article.

DATA AND RESOURCES

Accelerograms from the SASMEX stations were provided by the Centro de Instrumentación y Registro Sísmico (*CIRES*) with the authorization of the Instituto para la Seguridad en las Construcciones del Distrito Federal in Mexico City and the Coordinación Estatal de Protección Civil de Oaxaca. Data from the Instituto de Ingeniería of the

Universidad Nacional Autónoma de México (UNAM) is in the strong motion database (https://aplicaciones.iingen.unam.mx/AcelerogramasRSM/Default.aspx); last opened on 11 March 2018). Data from the Global Centroid Moment Tensor Project are from http://www.globalcmt.org/CMTsearch.html (last opened on 11 March 2018).

REFERENCES

Cuéllar, A., Suárez, G., and Espinosa-Aranda, J. M. (2017a). Performance Evaluation of the Earthquake Detection and Classification Algorithm $2(t_S–t_P)$ of the Seismic Alert System of Mexico (SASMEX), *Bulletin of the Seismological Society of America*, doi: 10.1785/0120150330.

Cuéllar, A., Suárez, G., and Espinosa-Aranda, J. M. (2017b). An Earthquake Early Warning Algorithm based on the P-wave Energy Released in the t_S-t_P Interval, *Bulletin of the Seismological Society of America*, doi: 10.1785/0120170115.

Ekström, G., M. Nettles, and A. M. Dziewonski (2012). The global CMT project 2004-2010: Centroid-moment tensors for 13,017 earthquakes, *Phys. Earth Planet. Inter*., 200-201, 1-9, doi:10.1016/j.pepi.2012.04.002

Espinosa-Aranda, J. M., Jimenez A., Contreras O., Ibarrola G., and Ortega R. (1992) Mexico City Seismic Alert System, International Symposium on Earthquake Disaster Prevention 18-21 may 1992, Mexico, Proceedings Centro Nacional de Prevención de Desastres and Japan International Cooperation Agency CENAPRED-JICA. Mexico I: 1992. p. 315–24,

García, D., Singh, S. K., Herráiz, M., Ordaz, M., & Pacheco, J. F. (2005). In-slab earthquakes of central Mexico: peak ground-motion parameters and response spectra. *Bulletin of the Seismological Society of America*, 95(6), 2272-2282.

Hoshiba, M., Kamigaichi, O., Saito, M., Tsukada, S. Y., & Hamada, N. (2008). Earthquake early warning starts nationwide in Japan. *EOS, Transactions American Geophysical Union*, 89(8), 73-74.

Iglesias, A., Singh, S. K., Ordaz, M., Santoyo, M. A., and Pacheco, J. (2007). The seismic alert system for Mexico City: an evaluation of its performance and a strategy for its improvement, *Bulletin of the Seismological Society of America*, 97(5), 1718-1729.

Pearson, K. (1895). Note on regression and inheritance in the case of two parents. *Proceedings of the Royal Society of London*, *58*, 240-242.

Pérez-Yáñez C., Ramirez-Guzman L., Ruiz G A. L., Delgado D. R., Macias C Marco A, Sandoval G. H., Alcantara N. L. and Quiroz R A., (2014). Strong Ground Motion Database System for the Mexican Seismic Network, AGU Fall Meeting, San Francisco, CA, December 14-19.

Suárez, G., Monfret, T., Wittlinger, G., and David, C. (1990). Geometry of subduction and depth of the seismogenic zone in the Guerrero gap, Mexico. *Nature*, *345*(6273), 336-338.

Suárez, G., Novelo, D. and Mansilla, E. (2009). Performance evaluation of the seismic alert system (SAS) in Mexico City: a seismological and a social perspective. *Seismol. Res. Lett.*, 80(5), 707-716.

Pardo, M., & Suárez, G. (1993). Steep subduction geometry of the Rivera plate beneath the Jalisco block in western Mexico. *Geophysical Research Letters*, 20(21), 2391-2394.

Pardo, M. and Suárez, G. (1995). Shape of the subducted Rivera and Cocos plates in southern Mexico: Seismic and tectonic implications. *J. Geophys. Res*, *100*(12), 357-12.

Singh, S. K., Ordaz, M., Pacheco, J. F., Quaas, R., Alcántara, L., Alcocer, S. and Ovando, E. (1999). A preliminary report on the Tehuacan, Mexico earthquake of June 15, 1999 (*Mw* 7.0). *Seismological Research Letters*, *70*(5), 489-504.

Wu, Y. M., & Kanamori, H. (2005). Experiment on an onsite early warning method for the Taiwan early warning system. *Bulletin of the Seismological Society of America*, 95(1), 347-353.

Table S1. Mexican in-slab earthquakes (1997 to 2017), $M_w \geq 5$, epicentral distance < 110 km and acceleration records > 4 cm/s^2.

Global Centroid Moment Tensor Catalog (CMT Catalog)						Mexican Seismological Service (SSN)		
Date	**Centroid Time**	**Latitude N °**	**Longitude W °**	**Depth (km)**	**Mw**	**Latitude N°**	**Longitude W°**	**Depth (km)**
22/05/1997	07:51:00	18.76	-101.73	55.5	6.5	18.41	-101.81	59
20/04/1998	22:59:22	18.76	-100.94	59.6	5.9	18.37	-101.21	66
15/06/1999	20:42:13	18.44	-97.38	61.2	7.0	18.20	-97.47	92
21/06/1999	17:43:09	18.09	-101.62	48.0	6.3	17.99	-101.72	54
29/12/1999	05:19:49	18.00	-101.63	50.0	5.9	18.02	-101.68	82
21/07/2000	06:13:44	18.25	-98.46	56.0	5.8	18.09	-98.97	48
16/05/2003	09:09:25	18.32	-100.89	84.3	5.0	18.29	-101.23	67
07/08/2004	11:49:14	17.25	-95.30	104.7	5.8	17.10	-95.48	106
18/08/2004	09:03:12	16.40	-95.14	77.6	5.8	16.24	-95.15	51
24/09/2005	01:14:06	18.20	-96.85	61.0	5.0	18.05	-96.99	81
11/08/2006	14:30:44	18.50	-101.06	57.8	6.0	18.32	-101.27	51
04/05/2007	10:21:13	17.50	-96.68	59.5	5.0	17.20	-96.84	70
26/11/2007	21:56:15	18.80	-101.58	70.1	5.8	18.50	-101.31	53
12/02/2008	12:50:21	16.35	-94.51	87.1	6.5	16.19	-94.54	90
28/04/2008	00:06:30	17.89	-100.10	55.5	5.8	18.05	-100.01	52
29/04/2008	10:56:46	18.67	-101.14	63.5	5.3	18.47	-101.19	60
22/05/2009	19:24:23	18.22	-98.26	59.4	5.6	18.13	-98.44	45
15/08/2009	13:22:48	18.02	-100.53	69.0	5.5	18.06	-100.67	55
25/02/2011	13:07:29	17.98	-95.20	128.4	6.0	17.73	-95.21	135
07/04/2011	13:11:28	17.28	-94.12	153.8	6.7	17.20	-94.34	167
11/12/2011	01:47:28	17.89	-99.84	55.3	6.5	17.84	-99.98	58
01/05/2012	16:37:59	18.36	-100.95	59.7	5.7	18.20	-101.01	51
06/01/2013	18:24:46	17.22	-94.97	62.2	5.3	16.87	-95.02	55
16/06/2013	05:19:04	18.25	-99.18	49.6	5.9	18.04	-99.25	60
02/08/2013	09:29:47	16.61	-94.65	93.5	5.0	16.36	-94.76	77
02/05/2014	19:08:24	17.61	-94.51	148.1	5.1	17.33	-94.73	130
20/05/2014	01:39:15	18.27	-99.94	46.5	5.1	18.04	-100.10	53
21/05/2014	10:06:15	17.25	-95.00	125.1	5.8	17.11	-95.07	121
29/07/2014	10:46:19	17.97	-95.69	109.2	6.4	17.70	-95.63	117
04/10/2014	19:16:38	17.61	-94.72	141.3	5.6	17.40	-94.87	143
20/03/2015	22:30:11	18.12	-98.35	58.4	5.4	17.96	-98.58	61
28/04/2015	18:56:55	17.22	-95.07	116.9	5.5	17.03	-95.19	113
28/06/2015	15:54:43	16.67	-94.68	95.6	5.4	16.50	-94.89	84
19/09/2017	18:14:47	18.51	-98.62	52.7	7.1	18.40	-98.72	57

Table S2. Results of the t_P+3 algorithm of 113 acceleration records of 34 Mexican in-slab earthquakes (1997 to 2017): 5.0 ≤ M_W ≤ 7.1 and depth > 40 km, considering an alert trigger threshold of M_W >5.8.

CMT Catalogue			Seismic Field Sensor Information			Performance of t_P+3 algorithm						Hypothetical Performance of SASMEX		
Date	Centroid Time	M_w	Sensor within a radius of 110 km since the Epicenter	Epicentral Distance [km]	Hypo-central Distance [km]	t_S-t_P [s]	$av(T)$	θ_P	m_{tP+3}	tol = 0.5	tol = 1.0	Trigger Warning Range	EEW Issue	Evaluation According with M_w
22/05/1997	07:51:00	6.5	UNIO	44.35	73.85	10.75	4.25	0.714	5.8		OK	≥5.8	Earthquake Warning	OK
			VILE	56.60	81.82	11.51	4.07	0.703	6.3	OK	OK	≥5.8		
20/04/1998	22:59:22	5.9	UNIO	77.31	101.69	11.12	3.32	0.546	6.2	OK	OK	≥5.8	Earthquake Warning	OK
			PET2	87.82	109.89	12.89	3.62	0.617	6.2	OK	OK	≥5.8		
15/06/1999	20:42:13	7.0	CHFL	49.80	106.13	9.49	3.32	0.62	6.3		OK	≥5.8	Earthquake Warning	OK
			CSER	83.48	126.43	12.45	4.46	0.665	6.8	OK	OK	≥5.8		
21/06/1999	17:43:09	6.3	UNIO	9.97	54.97	7.36	4.65	0.577	6.2	OK	OK	≥5.8	Earthquake Warning	OK
			AZIH	49.05	72.96	9.02	3.30	0.731	6.4	OK	OK	≥5.8		
			VILE	51.90	74.96	9.03	4.14	0.455	6.3	OK	OK	≥5.8		
			PETA	68.21	87.01	10.43	3.64	0.713	5.8	OK	OK	≥5.8		
			COYQ	97.09	111.12	14.45	3.35	0.697	6	OK	OK	≥5.8		
29/12/1999	05:19:49	5.9	UNIO	14.76	83.37	6.09	4.70	0.229	5.7	OK	OK	<5.8	Earthquake Warning	OK
			AZIH	49.42	95.75	7.79	3.73	0.337	6	OK	OK	≥5.8		
			VILE	56.04	99.39	8.57	3.20	0.314	5.9	OK	OK	≥5.8		
			PET2	68.54	106.90	8.91	3.67	0.591	5.5	OK	OK	<5.8		
			COYQ	96.00	126.28	11.21	3.68	0.245	5.6	OK	OK	<5.8		
21/07/2000	06:13:44	5.8	TNLP	64.99	81.23	8.36	3.60	0.659	6.1	OK	OK	≥5.8	No Apply	---
16/05/2003	09:09:25	5	PET2	79.31	103.85	12.55	2.61	0.354	4.8	OK	OK	<5.8	No Apply	---
07/08/2004	11:49:14	5.8	OXJM	68.86	126.54	13.14	2.85	0.398	5.5	OK	OK	<5.8	No Apply	---
18/08/2004	09:03:12	5.8	SCRU	8.53	51.79	7.48	3.90	0.405	5.8	OK	OK	≥5.8	Earthquake Warning	OK
			OX12	32.42	60.49	7.90	2.93	0.393	5.8	OK	OK	≥5.8		
			OXJM	38.92	64.28	8.02	3.50	0.258	5.9	OK	OK	≥5.8		
			OX13	48.79	71.73	8.24	3.27	0.279	6	OK	OK	≥5.8		
			OX11	61.25	79.76	9.65	2.88	0.227	5.4	OK	OK	<5.8		
			NILT	67.85	84.92	10.78	3.26	0.409	5.7	OK	OK	<5.8		
24/09/2005	01:14:06	5	OX23	75.92	112.57	11.19	3.40	0.415	5.3	OK	OK	<5.8	No Apply	---
11/08/2006	14:30:44	6.0	CANA	82.00	96.75	10.91	3.48	0.509	5.4		OK	<5.8	Earthquake Warning	OK
			UNIO	68.95	85.80	10.98	3.38	0.477	5.7	OK	OK	<5.8		
			COMD	84.66	99.00	11.44	3.65	0.571	6.2	OK	OK	≥5.8		
			PETA	81.69	96.32	13.35	3.76	0.462	6.2	OK	OK	≥5.8		
04/05/2007	10:21:13	5	OX29	20.25	74.35	7.71	3.59	0.254	5.7		OK	<5.8	No Apply	---
26/11/2007	21:56:15	5.8	SNJE	3.98	53.33	8.30	3.71	0.356	5.8	OK	OK	≥5.8	Earthquake Warning	OK
			CANA	73.73	91.00	8.84	4.36	0.39	5.8	OK	OK	≥5.8		
			UNIO	76.99	93.50	11.88	3.26	0.17	6.3	OK	OK	≥5.8		
12/02/2008	12:50:21	6.5	NILT	40.29	98.67	11.07	5.01	0.462	6.2	OK	OK	≥5.8	Earthquake Warning	OK
			SCRU	73.62	116.34	12.17	4.78	0.388	6.4	OK	OK	≥5.8		
			OX35	82.90	122.41	12.59	4.37	0.444	6.1	OK	OK	≥5.8		
			OX12	97.36	132.63	15.85	3.31	0.599	6.8	OK	OK	≥5.8		
28/04/2008	00:06:30	5.8	COMD	57.03	77.38	8.18	3.88	0.552	5.8	OK	OK	≥5.8	No Alert	Under-estimation
			TNLP	49.64	72.42	9.69	3.56	0.444	5.5	OK	OK	<5.8		
			ATYC	99.37	112.18	10.59	3.86	0.332	5.7	OK	OK	<5.8		
29/04/2008	10:56:46	5.3	CANA	87.19	106.03	11.27	2.74	0.397	5.2	OK	OK	<5.8	No Apply	---
22/05/2009	19:24:23	5.6	HMTT	37.23	58.41	7.79	3.75	0.471	5.2	OK	OK	<5.8	No Alert	OK
			RABO	46.11	65.33	8.29	4.02	0.234	6.2		OK	≥5.8		
			CHFL	65.39	80.36	8.85	2.72	0.318	5.3	OK	OK	<5.8		
15/08/2009	13:22:48	5.5	COMD	17.36	57.97	6.33	4.62	0.426	5.8	OK	OK	≥5.8	Earthquake	Over-

			SLU2	86.87	102.83	11.92	3.20	0.612	5.4	OK	OK	<5.8	Warning	estimation
			NUX2	89.54	105.09	12.33	2.96	0.523	5.8	OK	OK	≥5.8		
			ATYC	92.66	107.78	12.55	2.87	0.843	5.8	OK	OK	≥5.8		
25/02/2011	13:07:29	6.0	OX33	44.59	142.24	15.39	4.44	0.807	6.8		OK	≥5.8	No Apply	---
07/04/2011	13:11:28	6.7	NILT	73.29	182.43	18.41	3.70	0.594	6.5	OK	OK	≥5.8	Earthquake Warning	OK
			OX33	109.68	202.64	22.94	4.33	0.661	6.1		OK	≥5.8		
11/12/2011	01:47:28	6.5	TNLP	53.35	79.35	8.72	4.33	0.802	6.2	OK	OK	≥5.8	Earthquake Warning	OK
			COMD	66.76	88.64	10.46	3.98	0.674	6.2	OK	OK	≥5.8		
			POZU	89.28	106.66	13.39	3.72	0.583	6	OK	OK	≥5.8		
			GR05	88.05	105.45	13.71	3.64	0.513	5.9		OK	≥5.8		
			GR04	85.36	103.22	14.23	4.14	0.638	6.5	OK	OK	≥5.8		
01/05/2012	16:37:59	5.7	SNJE	49.28	71.05	7.79	3.84	0.61	5.2	OK	OK	<5.8	Earthquake Warning	Over-estimation
			COMD	54.10	74.56	9.50	3.50	0.497	6	OK	OK	≥5.8		
			UNIO	90.85	104.21	11.97	2.98	0.37	5.3	OK	OK	<5.8		
			GR17	91.86	105.12	12.16	3.05	0.519	5.5	OK	OK	<5.8		
			GR13	78.44	93.60	12.19	3.51	0.586	5.7	OK	OK	<5.8		
			GR16	89.43	102.98	12.22	2.77	0.403	5.9	OK	OK	≥5.8		
			GR15	83.57	97.94	12.23	3.44	0.388	5.8	OK	OK	≥5.8		
			COYQ	86.23	100.20	12.87	3.55	0.482	5.4	OK	OK	<5.8		
			GR01	94.87	107.79	13.71	3.12	0.468	5.6	OK	OK	<5.8		
06/01/2013	18:24:46	5.3	OX36	15.78	57.82	6.57	3.96	0.623	5.6	OK	OK	<5.8	Earthquake Warning	Over-estimation
			OX35	58.95	80.67	9.68	3.12	0.446	5.5	OK	OK	<5.8		
			OX33	62.98	83.66	11.93	4.87	0.235	6		OK	≥5.8		
			OX14	95.42	110.58	11.94	3.16	0.257	6		OK	≥5.8		
16/06/2013	05:19:04	5.9	GR25	31.74	68.73	6.23	4.72	0.347	5.3		OK	<5.8	Earthquake Warning	OK
			GR24	18.10	63.39	6.84	5.04	0.245	5.9	OK	OK	≥5.8		
			TNLP	34.68	69.94	7.16	4.63	0.17	5.3		OK	<5.8		
			GR27	36.52	70.88	7.32	5.03	0.163	6.5		OK	≥5.8		
			GR26	64.62	89.10	9.15	2.81	0.477	6.2	OK	OK	≥5.8		
02/08/2013	09:29:47	5	NILT	26.68	81.55	9.68	3.27	0.286	5.9		OK	≥5.8	No Apply	---
02/05/2014	19:08:24	5.1	OX33	70.83	148.10	16.07	2.86	0.456	5.5	OK	OK	<5.8	No Apply	---
20/05/2014	01:39:15	5.1	COMD	47.41	71.34	7.84	3.19	0.445	5.3	OK	OK	<5.8	No Alert	OK
			ATYC	94.18	108.09	13.44	2.74	0.283	5.7		OK	<5.8		
21/05/2014	10:06:15	5.8	OX36	38.79	127.66	12.75	4.59	0.196	5.9	OK	OK	≥5.8	Earthquake Warning	OK
			OX33	41.32	127.93	12.95	4.89	0.326	5.3	OK	OK	<5.8		
			OX34	66.77	138.94	13.47	4.46	0.127	6.2	OK	OK	≥5.8		
			NILT	75.87	142.88	14.32	3.26	0.269	6.3	OK	OK	≥5.8		
29/07/2014	10:46:19	6.4	OX25	77.55	140.48	13.57	4.15	0.358	6.2	OK	OK	≥5.8	Earthquake Warning	OK
			OX33	47.02	126.16	14.19	4.57	0.717	5.8		OK	≥5.8		
			OX24	96.67	154.21	15.52	3.61	0.655	7.2		OK	≥5.8		
			OX32	82.55	145.08	17.38	4.63	0.498	5.9	OK	OK	≥5.8		
04/10/2014	19:16:38	5.6	OX33	55.76	153.55	13.25	3.38	0.617	5.5	OK	OK	<5.8	No Apply	---
20/03/2015	22:30:11	5.4	HMTT	17.12	64.22	6.33	3.91	0.241	5.2	OK	OK	<5.8	No Alert	OK
			PB02	52.70	81.44	6.44	3.89	0.325	5.1	OK	OK	<5.8		
			PB01	32.63	70.25	6.49	3.98	0.241	5.4	OK	OK	<5.8		
			GR26	24.92	67.14	6.64	3.04	0.344	5.5	OK	OK	<5.8		
			GR27	46.64	77.38	7.69	3.39	0.515	5.5	OK	OK	<5.8		
			OX38	44.40	76.53	8.34	4.00	0.479	5.5	OK	OK	<5.8		
			PB03	98.78	116.10	12.94	3.05	0.171	5.7	OK	OK	<5.8		
28/04/2015	18:56:55	5.5	OX36	32.06	118.06	11.49	3.99	0.336	5.3	OK	OK	<5.8	Earthquake Warning	Over-estimation
			OX33	38.45	119.43	12.37	4.15	0.443	5.5	OK	OK	<5.8		
			OX34	51.39	124.91	12.74	3.69	0.349	5.2	OK	OK	<5.8		
			OX35	69.39	132.66	13.36	3.04	0.333	5.8	OK	OK	≥5.8		
			NILT	79.72	138.35	13.68	2.85	0.442	5.4	OK	OK	<5.8		
			OX32	95.85	149.94	15.13	3.43	0.225	5.8	OK	OK	≥5.8		
			OX14	91.30	145.96	15.42	3.56	0.178	5.9	OK	OK	≥5.8		
28/06/2015	15:54:43	5.4	NILT	30.81	89.53	9.35	3.59	0.246	5.4	OK	OK	<5.8	No Alert	OK
			OX36	33.90	91.16	9.87	3.84	0.355	5.3	OK	OK	<5.8		

			OX35	44.10	94.93	10.92	3.67	0.225	5.6	OK	OK	<5.8		
			OX34	72.41	111.55	12.58	3.11	0.336	5.4	OK	OK	<5.8		
			OX12	70.72	109.86	13.22	3.56	0.24	5.6	OK	OK	<5.8		
			OX13	81.06	117.88	14.19	3.16	0.3	5.4	OK	OK	<5.8		
			OX14	96.57	128.57	14.77	3.07	0.261	5.5	OK	OK	<5.8		
			OX11	99.07	129.94	14.90	2.76	0.211	5.6	OK	OK	<5.8		
			PB01	16.75	60.58	7.19	5.89	-0.29	>7.0			≥5.8		
19/09/2017	18:14:47	7.1	PB02	50.82	77.18	7.72	4.88	-0.17	6.7	OK	OK	≥5.8	Earthquake Warning	OK
			GR25	52.18	77.98	9.21	4.41	-0.22	6.7	OK	OK	≥5.8		

CONCLUSIONES

México inició su sistema de alerta sísmica a partir de los daños que sufrió principalmente la Ciudad de México por los sismos de septiembre de 1985; al ser uno de los primeros sistemas en el mundo, ha tenido que evolucionar y adaptarse al conocimiento y gestión del riesgo sísmico entre otras recomendaciones no previstas en su diseño principalmente en el ámbito geofísico y muy en especial referente a lo social para la mejor preparación, respuesta y resiliencia; no sólo para la ciudad de México, sino en otras ciudades vulnerables, en este sentido aún falta muchos esfuerzos por hacer, por ejemplo, mejorar el conocimiento de este fenómeno natural en la sociedad y principalmente en tomadores de decisiones. Ampliar, fortalecer y asegurar las redes sísmicas diversas que existen en el país. Implementar redes de monitoreo de múltiples variables físicas y mediciones sistemáticas a largo plazo que permitan comprender aún más esta amenaza.

Este trabajo presentó una línea de investigación y desarrollo, con una ruta trazada en la lógica de proponer metodologías con el objeto de reducir el tiempo de procesamiento y márgenes de error para contribuir en la mitigación del riesgo sísmico de acuerdo al escenario sísmico del sur de México en el contexto de sistemas de alerta temprana. Hay varias líneas de investigación que continuarán y derivarán del trabajo, tales como proponer otros modelos de regresión para el algoritmo original del

SASMEX en busca de definir rangos mayores de alerta; replantear algunos modelos desde el paradigma de clasificación; proponer otros parámetros; evaluar algunos parámetros propuestos en otras partes del mundo; incluir más parámetros y criterios para determinar el activar o no una alerta, además de proponer métodos alternos al criterio de activación de alerta que en la actualidad sólo considera de manera básica, la confirmación de dos estimaciones de magnitud asociados a una distancia entre la ciudad a alertar y el epicentro.

Los sistemas de alerta temprana si bien son herramientas que pueden salvar vidas y reducir daños y aún en el caso que pudiera reducirse el tiempo de procesamiento a casi cero segundos buscando el mayor tiempo de anticipación, habrá ciudades que no dispondrán de algún lapso para responder adecuadamente. Por lo que estas herramientas no debemos enfocarlas exclusivamente en obtener una estimación de baja incertidumbre respecto al posible tamaño de un sismo ya que aún prevalece la complejidad en los modelos actuales para dimensionar el tamaño de un sismo y los efectos que podría ocasionar. Así el esfuerzo debe ser encausado en mejorar la densidad y cobertura de los sensores sísmicos para alerta sísmica, perfeccionar mapas de intensidades y desde luego, hacer énfasis en hacer del conocimiento las limitaciones e imprecisiones que ocurrirán en estos sistemas. Finalmente pero de igual importancia, realizar sistemáticamente campañas de difusión, proponer protocolos, programas y normas encaminados en aprovechar los pocos segundos de anticipación, ya que de no hacerlo, ninguna alerta servirá a la población.